C00-1569-128

ORDER PARAMETER FLUCTUATIONS

and

COLLECTIVE MODES IN SUPERCONDUCTORS

R. V. Carlson

Solid State and Low Temperature Physics Group

SCHOOL OF PHYSICS AND ASTRONOMY

JUNE 1975

UNIVERSITY OF MINNESOTA
MINNEAPOLIS, MINNESOTA

Work supported by the Energy Research and Development Administration

DISCLAIMER

ORDER PARAMETER FLUCTUATIONS
AND
COLLECTIVE MODES IN SUPERCONDUCTORS

A THESIS

SUBMITTED TO THE FACULTY OF THE GRADUATE SCHOOL

OF THE UNIVERSITY OF MINNESOTA

BY

RICHARD VERNAL CARLSON

IN PARTIAL FULFILLMENT OF THE REQUIREMENTS

FOR THE DEGREE OF

DOCTOR OF PHILOSOPHY

JUNE, 1975

ABSTRACT

ORDER PARAMETER FLUCTUATIONS

AND

COLLECTIVE MODES IN SUPERCONDUCTORS

Measurements of the frequency and wave vector dependence of the pair-field susceptibility and the dynamical structure factor of homogeneous, short mean free path aluminum films have been carried out. These measurements critically probe the dynamical nature of order parameter fluctuations in the vicinity of the superconducting phase transition.

The pair-field susceptibility of an aluminum film is obtained by using a thin film tunneling junction in which aluminum is one electrode, and lead the other. At temperatures near T_c of aluminum, an excess current which is a consequence of fluctuation induced pair tunneling is observed in the dc current-voltage characteristic of the junction. This current is a direct measure of the imaginary part of the pair-field susceptibility of the aluminum film, where the frequency and wave vector dependence of the susceptibility respectively, are determined by the dc voltage and magnetic field applied to the junction. The order parameter structure factor, related to the imaginary part of the susceptibility by the fluctuation-dissipation theorem, is determined by dividing the excess current by the voltage.

Two important results are found. The first is that at temperatures higher than the transition temperature of the aluminum film, the fluctuations of the order parameter can be described by a diffusive time-dependent generalization of the Ginzburg-Landau equation. Detailed comparison of the data to the results of theoretical calculations of Scalapino, and Shenoy and Lee are carried out. Except in the immediate vicinity of the transition, there is excellent agreement with the theories, and where deviations occur, they involve values of coefficients which are only imprecisely known for the junctions. A major discrepancy between theory and experiment does exist in the vicinity of the superconducting transition, in that the pair relaxation frequency falls well below the theoretical predictions. Possible explanations of this behavior are discussed.

Below the transition temperature measurements of the structure factor (Fourier transform of the order parameter-order parameter correlation function) provide the first clear cut demonstration of the existence of a propagating, low frequency, order parameter collective mode which appears as a finite frequency peak in the structure factor. This mode has been identified with fluctuations in the phase of the order parameter and has a linear dispersion relation over the range in which it is observed. The propagation velocity is less than either the Fermi velocity in aluminum or the velocity

of Swihart modes in the junction. The velocity is also found to be temperature dependent only over a relatively narrow region of $T \approx T_c$, with a saturation value greater than the sound velocity in aluminum. The mode is also highly damped in the range in which it is observed. Theoretical calculations are somewhat controversial and are currently in a state of flux. A detailed comparison to some of the theoretical explanations is made, with the conclusion that at this time, existing theories do not adequately explain the behavior of the mode over the range of temperature and magnetic field in which it is observed.

CONTENTS

LIST OF FIGURES

Figure

LIST OF TABLES

I. INTRODUCTION

The belief that physical effects of fluctuations of the order parameter in superconductors above T_c would not be observed over a broad enough range of temperature to be studied in the laboratory was held for a long time.[1] It was a consequence of two factors: a lack of understanding of the possible order parameter fluctuations within the Landau theory, and an erroneous identification of the condition for the breakdown of the Landau theory and the onset of critical behavior as the condition for fluctuations to be observable. The fluctuation effects discussed in this dissertation are outside the critical region[2] except possibly for some anomalous behavior in the immediate vicinity of T_c.

The investigations were directed at the study of the dynamics of order parameter fluctuations in superconductors near the transition temperature. These investigations were carried out by measuring the generalized susceptibility both above and below the transition temperature. Determination of the frequency and wave number dependence of the generalized susceptibility is the most critical probe of fluctuations of the order parameter. In most other phase transitions, the generalized susceptibility measures the response of the order parameter to an applied field which couples to it. For example, in a ferromagnetic transition the response of

the magnetization to the applied magnetic field determines the magnetic susceptibility χ. In superconductors, the analogous characteristic susceptibility also involves coupling to an order parameter, in this case the pair-field Δ, a quantity which is off-diagonal in the number representation. For this reason there is no classical field thermodynamically conjugate to the pair-field and consequently a direct determination of the susceptibility had been thought to be impossible.[3] However, recent theoretical[4,5] and experimental [6-11] work has shown that the generalized susceptibility can be measured by a simple dc tunneling experiment in which the susceptibility is proportional to an excess current, due to pair tunneling, in the I-V characteristic of a thin-film junction consisting of the superconductor of interest near its transition temperature and a second superconductor well below its transition temperature. The coupling to the order parameter of the film near its transition temperature is provided by the non-zero pair-field amplitude of the superconducting electrode.

A local, diffusive time-dependent generalization of the Ginzburg-Landau equation is believed to provide an essentially correct description of order parameter fluctuations in a superconductor above its transition temperature. Extensive measurements of the precursive electrical conductivity,[12] diamagnetic susceptibility,[13]

and density of states[14] have been carried out. However, since these quantities involve complicated convolutions of the generalized susceptibility, the experiments cannot be used as a critical test of the theory.

The first part of the experimental work described here was a continuation of the measurements of the pair-field susceptibility of Anderson and Goldman[6] and was initiated in an effort to understand some of the discrepancies between their results and theory. They found the lifetime of fluctuations above T_c to be approximately 30% smaller than predicted by theory and the magnetic field dependence of the excess current to be inconsistent with theory. In the experiments described here, extensive measurements on the excess current-voltage characteristics of Al-Al_2O_3-Pb tunneling junctions were made to determine the pair-field susceptibility of aluminum above its transition temperature. Aluminum was chosen for this investigation because of its low transition temperature relative to that of lead and the ease with which films of a known character could be made. Measurements could then be carried out at temperatures sufficiently below the transition temperature of lead that the single-particle tunneling current was not the dominant contribution to the total tunneling current. This made an accurate determination of the excess current due to pair tunneling possible. The situation in the tin-lead junctions is much less favorable because the

transition temperature of tin is much closer to that of lead, resulting in a substantially larger single particle tunneling current at the temperature required for the measurements. Except for a region in the immediate vicinity of the transition temperature, and in the high magnetic field limit, results for the generalized susceptibility were found to be in excellent quantitative agreement with the theory. Results in high magnetic fields are in qualitative agreement with an extension of the theory given by Shenoy and Lee.[15]

The second part of the dissertation contains a description of the first measurements of the pair-field susceptibility of a superconductor below its transition temperature. Using the asymmetrical Josephson junction geometry described above in an applied magnetic field large enough to quench the dc Josephson effect, a contribution to the excess current-voltage characteristic was observed to develop in a continuous manner from the generalized susceptibility above T_c, as the temperature was reduced below T_c. This excess tunneling current is also a measure of the susceptibility of the low transition temperature electrode of the junction. Extensive measurements and analysis of the data have demonstrated the existence of a propagating order parameter collective mode with a linear dispersion relation in addition to the nonpropagating diffusive mode which is also present above T_c. The mode propagates

only in the immediate vicinity of T_c becoming highly damped when $T_c - T > 30$ mK. The propagating mode has been identified with fluctuations of the phase of the order parameter and the diffusive mode with fluctuations of the amplitude.[17,18] Above the superconducting transition temperature, no such distinction can be made.

The existence of a propagating mode is inconsistent with a description of the dynamics of order parameter fluctuations by a diffusive time-dependent generalization of the Ginzburg-Landau equation.[16] The generalized susceptibility calculated from the Gor'kov-Eliashberg[19] theory of a gapless neutral superconductor is qualitatively similar to that found experimentally in that it contains a collective mode which has a phonon-like dispersion relation below T_c. Other calculations[21,22] have been carried out which predict collective modes which in some limits are qualitatively similar to the data. However, no theory adequately describes the behavior of the susceptibility over the full range of temperature and magnetic field over which it has been studied.

In Chapter II we describe the theoretical ideas on which this experimental work is based. There an outline of the calculation of the pair-field susceptibility above the transition temperature is given, along with a discussion of related experimental and theoretical work which has been carried out by other authors.

Experimental techniques are discussed in Chapter III. Chapter IV contains the data and analysis. The discussion of theoretical calculations of the susceptibility below T_c is also given after the data in the regime has been presented. Conclusions and suggestions for further experimental and theoretical work are given in Chapter V.

II. THEORY

This chapter contains a description of the theoretical ideas on which the pair susceptibility measurements are based. In order to introduce the general concepts which are important in any discussion of phase transitions, the first section contains a brief discussion of the Landau theory. In the next section we show how the dc current-voltage characteristic of an asymmetrical Josephson junction consisting of two superconductors with different transition temperatures can be used to determine the frequency and wave number dependent pair-field susceptibility of the low transition temperature superconductor. This discussion is equivalent to the original work of Scalapino. An explicit calculation of the susceptibility within the context of a diffusive time-dependent Ginzburg-Landau theory for $T > T_c$ is given. The following section contains a description of the theory of Shenoy and Lee which is an extension of the theory of Scalapino to the regime of high magnetic fields. A brief discussion of other pertinent experimental and theoretical work concludes this chapter. The discussion of theoretical calculations of the susceptibility for $T < T_c$ is deferred until after the data in that temperature range has been presented.

A. PHASE TRANSITIONS

The study of phase transitions is one of the most interesting and difficult problems in physics. A

system undergoing a phase transition changes drastically when external conditions are modified only slightly. In liquid He^4, there is a drastic change in the transport properties at the lambda point; in a superconductor the conductivity becomes infinite at the transition temperature and in a ferromagnet, a spontaneous magnetization develops below the Curie point.

The change in phase of a system usually involves a symmetry breaking. The specific symmetries which are broken are clearly viewed in the cases of crystals (translations), ferromagnets (spin rotations), and antiferromagnets (spin rotations and translations). The symmetry breaking is more subtle in the three superfluid transitions: superfluid He^3, superfluid He^4, and superconducting metals where the broken symmetry is the disappearance of gauge invariance in the ordered state.

To characterize the symmetry breaking at a phase transition, Landau[22] introduced the concept of an order parameter which is defined in such a way that in the less symmetrical (low temperature) phase, the order parameter is nonzero, whereas in the symmetrical (high temperature) phase it is zero. In a second order phase transition, the order parameter goes to zero continuously as the temperature approaches the critical temperature. In a first order transition there is a discontinuous jump in the order parameter to zero at the critical temperature.

Examples of order parameters are the spontaneous magnetization of ferromagnets, the density difference between the liquid and gaseous phases in the condensation of gasses, and the complex order parameters of superfluids.

In the Landau theory[22] of second order phase transitions, the Helmholtz free energy density near T_c is expanded as a sum of powers and gradients of the order parameter. In particular for a superconductor, the free energy is

$$f = f_N + \alpha|\psi|^2 + \frac{\beta}{2}|\psi|^4 + \frac{1}{2m}\left|(-i\hbar\vec{\nabla} - \frac{2e}{c}\vec{A})\psi\right|^2 + \frac{H^2}{8\pi}, \tag{1}$$

where f_N is the energy density in the normal state and $\vec{A}$ is the vector potential. This theory is valid both above and below T_c. The order parameter ψ, of the phenomenological theory is related in a simple way to the pair potential $\Delta(r,t)$ of the microscopic theory:[23]

$$\psi(\bar{r},t) = \left(\frac{N(0)}{\alpha(T)/\epsilon}\right)^{\frac{1}{2}} \Delta(r,t). \tag{2}$$

Here N(0) is the single spin density of states calculated at the fermi energy and $\epsilon = (T-T_c)/T_c$. Using the microscopic theory of superconductivity Gor'kov[23] determined the coefficients $\alpha(T)$ and β to be

$$\alpha(T) = \alpha_o \epsilon \text{ and } \beta = \alpha_o/(N(0)\ (3.2\ k_B T_c)^2). \tag{3}$$

The limiting forms for the constant α_o are

$$\alpha_o = \frac{24\,\pi^2 (k_B T_c)^2}{7\,m\,\zeta(3)\,v_f^2} \qquad l \gg \xi_o \tag{4}$$

and

$$\alpha_o = \frac{12\,\hbar^2 k_B T_c}{\pi\, m\, v_f l} \qquad l \ll \xi_o$$

The quantity l is the conduction electron mean free path and ξ_o is the coherence length of the BCS theory. The condition $l \gg \xi_o$ corresponds to the long mean free path or "clean" limit and $l \ll \xi_o$ corresponds to the short mean free path or "dirty" limit. The Ginzburg-Landau equations[16,24] can be obtained by minimizing the free energy with respect to the order parameter and the vector potential:

$$\alpha\psi + \beta\,|\psi|^2\,\psi + \frac{1}{2m}\left(-i\hbar\vec{\nabla} - \frac{2e\vec{A}}{c}\right)^2 \psi(\vec{r},t) = 0 \tag{5}$$

and

$$\vec{J} = \frac{-e\hbar}{im}\left(\psi^*\vec{\nabla}\psi - \psi\vec{\nabla}\psi^*\right) - \frac{4e^2}{mc}\,\psi^*\psi\vec{A}. \tag{6}$$

Neglecting fluctuations and the gradient term, the equilibrium value of the order parameter becomes

$$|\psi|^2 = 0 \qquad T > T_c$$

and

$$|\psi|^2 = -\alpha/2\beta \qquad T < T_c\ .$$

At finite temperatures, fluctuations of the order parameter about its equilibrium value can occur because of the thermal fluctuations in the system. The thermal average of the order parameter $\langle\psi(\vec{r},t)\rangle$ is the same as the average value without fluctuations, however the

mean square fluctuation, given by

$$\langle |\delta\psi|^2 \rangle = \langle (\psi(r,t))^2 - \langle \psi(r,t) \rangle^2 \rangle ,$$

is not zero.

The correlation length $\xi(T)$ represents the natural length for variations in $\psi(\vec{r},t)$. For a superconductor, $\xi(T)$ can be related to $\alpha(T)$ by

$$\xi(T) = \hbar^2/(2m\,\alpha(T)) \tag{7}$$

Combining Eq. (3), (4), and (7) the limiting values for the temperature dependent correlation length are,

$$\xi(T) = .74\,\xi_o\,|\epsilon|^{-\frac{1}{2}} \qquad l \gg \xi_o$$

and

$$\xi(T) = .85\,(\xi_o l)^{\frac{1}{2}}\,|\epsilon|^{-\frac{1}{2}} \qquad l \ll \xi_o \tag{8}$$

or

$$\xi(T) = \xi(0)\,|\epsilon|^{-\frac{1}{2}}$$

where $\xi(0)$ is taken in the appropriate limit. The BCS coherence length ξ_o is given by

$$\xi_o = 2\hbar v_f/(3.5\,\pi k_B T_c).$$

Above T_c, $\xi(T)$ is a measure of the size of the regions in which superconductivity is nucleating prematurely as a consequence of fluctuations.

The Ginzburg-Landau equations are concerned with the thermal equilibrium situation only. The extension of these equations to describe time-dependent nonequilibrium situations is still a controversial subject.[16] The existing time-dependent generalizations are valid

only in very special circumstances. Above T_c a diffusive equation for the order parameter can be derived from the microscopic theory.[25,26] In this equation the relaxation of the order parameter to its equilibrium value is determined by the functional derivative of the Ginzburg-Landau free energy,

$$\left(\frac{\partial}{\partial t} + \frac{2i\mu}{\hbar}\right)\psi\alpha - \frac{\delta F}{\delta \psi^*}\ , \tag{9}$$

where μ is the electrochemical potential. This relation defines a relaxation frequency which from the microscopic theory is

$$\Gamma_o = \frac{8}{\pi}\frac{k_B T_c}{\hbar}\left(\frac{T-T_c}{T_c}\right). \tag{10}$$

Γ_o is called the pair relaxation frequency and $1/\Gamma_o$ is a measure of the fluctuation lifetime above the transition temperature.

Below T_c the existence of the gap in the excitation spectrum makes it difficult to derive a microscopic equation for the order parameter. It is beyond the scope of this dissertation to discuss critically the derivation of a time-dependent Ginzburg-Landau equation in this regime. In Chapter IV, we will discuss two of the time-dependent equations which have been directly applied to these experiments.

To conclude this section, we define some of the important quantities involved in the study of phase transitions. In most second order phase transitions,

it is possible to couple to the order parameter with an external field. The response of the order parameter to this field determines the response function. The response function of a system in which a field couples linearly to the order parameter is given by

$$R(\vec{r}-\vec{r}',\ t-t') = -i/\hbar \left\langle \left[\psi(\vec{r}',t'),\psi(\vec{r},t)\right]\right\rangle \theta(t), \tag{11}$$

where $[\ ,\ ]$ denotes the two-time commutator and $\theta(X) = 0,(1)$ for x negative (positive). The space and time Fourier transform of $R(\vec{r}-\vec{r}',\ t-t')$ is

$$\chi(\omega,q) = \lim_{\epsilon \to 0^+} \int d(t-t')\ R(\vec{r}-\vec{r}',\ t-t') \tag{12}$$
$$\exp\left(-iq\cdot(\vec{r}-\vec{r}')-i\omega(t-t')\right) \exp\left(-\epsilon(t-t')\right),$$

which is the generalized susceptibility. The latter is related to the transform of the correlation function, called the dynamical order parameter structure factor $S(\omega,q)$ through the fluctuation-dissipation theorem:

$$S(\omega,q) = 2\hbar \left(1-\exp\left(-\frac{h\omega}{k_B T}\right)\right)^{-1} \mathrm{Im}\,\chi(\omega,q), \tag{13}$$

where

$$S(\omega,q) = \int d\vec{r}dt e^{-i\,(q\cdot\vec{r}-\omega t)} \left\langle \psi(\vec{r},t)\ \psi(0,0)\right\rangle . \tag{14}$$

Here $\mathrm{Im}\,\chi(\omega,q)$ is the imaginary part of the generalized susceptibility. In the low frequency limit $\hbar\omega \ll k_B T$ the fluctuation-dissipation theorem becomes

$$S(\omega,q) = 2k_B T_c\ \mathrm{Im}\ \chi(\omega,q)/\omega\ . \tag{15}$$

The quantity $S(\omega,q)$ is directly measured in inelastic scattering experiments provided the probe particles (photon, neutron, etc.) couple linearly to the order parameter. The advantage of studying the structure factor is that it provides more direct information than the susceptibility about propagating modes of the system that may be coupled to the experimental probe. Propagating modes appear as peaks at finite frequency in the plot of $S(\omega,q)$ at fixed q, versus ω. The width of the peak is a measure of the inverse of the lifetime. Thus the most critical way to probe the dynamical nature of a phase transition is to measure the structure factor. In the next section we show how $S(\omega,q)$ can be measured for a superconductor.

B. CALCULATION OF EXCESS CURRENT

In this section we determine the relationship of the fluctuation induced tunneling current in a Josephson junction, in which the electrodes have different transition temperatures, to the pair-field susceptibility of the low transition temperature electrode. We follow the phenomenological approach introduced by Ferrell[4] and extended by Scalapino.[5] Detailed microscopic calculations of the fluctuation induced pair current above T_c are given by Shenoy and Lee[15] and by Takayama.[27] A third method of obtaining the desired relationship between the excess current and susceptibility is a phenomenological derivation given in Refs. 7 and 8,

where the time rate of change of the internal energy due to the coupling of the two electrodes of the junction is related to the power dissipated in the pair tunneling channel. These calculations were carried out for $T > T_c$ however, as we will show, they are easily extended to the case of $T < T_c$.

Since the superconductor order parameter is off diagonal in the number representation, it was believed that the generalized susceptibility could not be measured because no classical field could couple to it. However, Ferrell[4] suggested the use of a tunneling junction as a probe of the pair field susceptibility. In the geometry he suggested, the junction is operated at temperatures at which one electrode was well below its superconducting transition temperature and the other, the metal of interest, was above its transition temperature. The order parameter in the high transition temperature superconductor provides the off diagonal coupling to the fluctuating order parameter. The fluctuations of the order parameter in the metal of interest give rise to instantaneous Josephson currents which result in an excess conductivity.

In subsequent theoretical work Scalapino[5] showed that the dc I-V characteristic of such a tunneling junction is related to the imaginary part of the generalized susceptibility and thus provides direct information on the dynamics of order parameter fluctuations

in the low transition temperature electrode. Because of the simultaneous presence of the usual quasiparticle tunneling current, the fluctuation induced pair tunneling current is called an excess current.

The geometry of a junction is shown in Fig.(1). The primes refer to the higher transition temperature superconductor. Side 1 is the superconductor of interest with transition temperature T_c. Since $T \approx T_c$ the penetration depth $\lambda(T)$ is large and a field applied in the y direction completely penetrates the film of thickness d. Side 2 is a superconductor well below its transition temperature with penetration depth λ'. The order parameter of side 2 has a well defined average value with negligible fluctuations. The effective coupling Hamiltonian used by Scalapino[5] to describe the coupling between the two electrodes follows from the usual low temperature Josephson coupling energy[28] with the assumption that the order parameter of the fluctuating side is much smaller than that of the high transition temperature superconductor. The coupling energy involves the phase difference $\phi - \phi'$ across the barrier, a function of both the magnetic field and the dc voltage applied to the junction. A field H, in the y direction produces a gradient in the phase difference in the z direction along the junction given by

$$\frac{\partial(\phi' - \phi)}{\partial z} = \frac{2e}{\hbar c} H (\lambda' + d/2), \qquad (16)$$

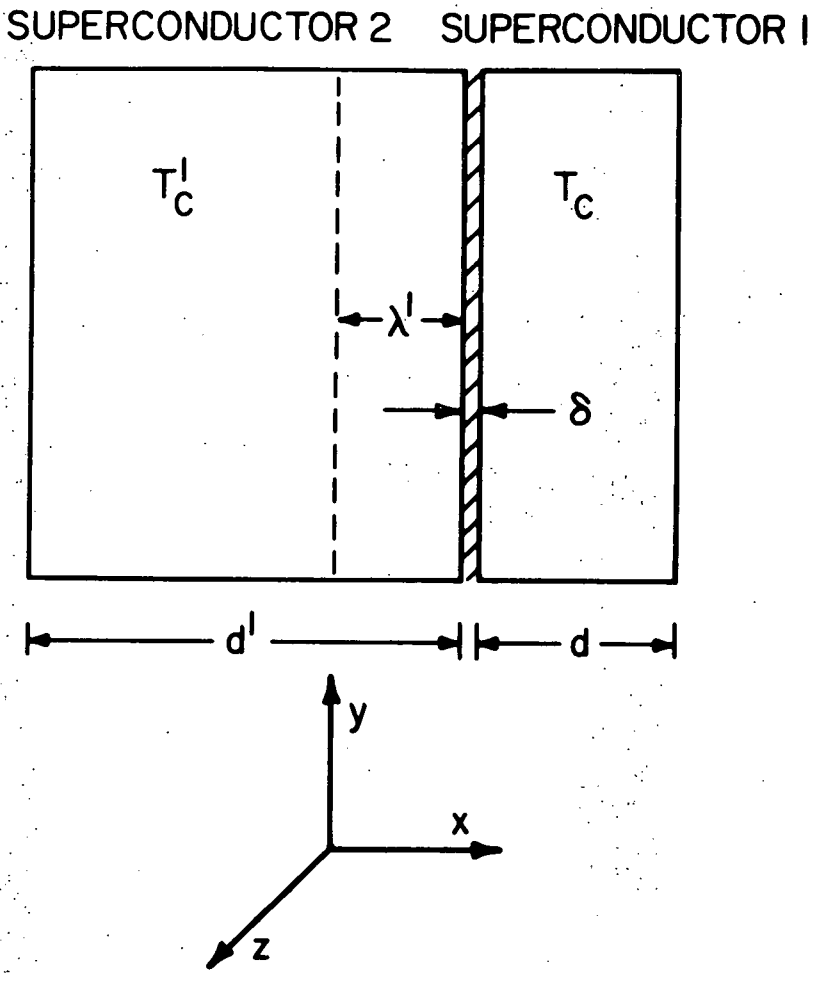

Fig. (1) Tunneling junction geometry used to determine the pair-field susceptibility of superconductor 1. δ is the thickness of the insulating layer exaggerated for clarity. Magnetic fields are applied in the y direction.

while a dc voltage V, applied to the junction produces time variation of the phase difference of the form

$$\frac{\partial(\phi'-\phi)}{\partial t} = \frac{2eV}{\hbar} \quad . \tag{17}$$

Using the above two equations to describe the space time oscillations of the phase difference across the junction, the effective coupling Hamiltonian first introduced by Scalapino[5] becomes

$$H_I = \frac{|\bar{c}|}{d} e^{-i\omega t} \int_1 d\bar{r} e^{iqz} \hat{\Delta}(\bar{r},t) + h.c., \tag{18}$$

with the frequency and wave vector set by

$$\omega = \frac{2eV}{\hbar} \quad \text{and} \quad q = \frac{2e}{\hbar c} H(\lambda' + d/2). \tag{19}$$

The coupling constant $\bar{c}$ is

$$\bar{c} = \frac{\hbar}{e^2} (R_N A)^{-1} \ln\left|\frac{4T_c'}{T_c}\right| e^{-i\phi'} , \tag{20}$$

where R_N is the normal state tunneling resistance in ohms and A is the area of the junction. The operator $\hat{\Delta}(r,t)$ is the order parameter of side 1, and may be defined in terms of electron field operators as

$$\hat{\Delta} = g \ \psi_\uparrow(\vec{r},t)\psi_\downarrow(\bar{r},t) ,$$

where g is the strength of the BCS pairing interaction. The integration in Eq. (18) extends over the volume of the fluctuating film.

If the thickness of the high transition temperature film is comparable to the penetration depth λ', the wave vector q (Eq. (19)) must be modified to:[29]

$$q = \frac{2e}{\hbar c} H \left({}^{d}/_{2} + \lambda' \tanh {}^{d'}/_{2\lambda'} \right). \qquad (21)$$

For the films used in this work Eq. (21) represents a small correction to the wave vector and can be ignored.

The pair transfer current induced by the interaction Hamiltonian is given by

$$\langle I_{ex} \rangle = \frac{4e}{\hbar d} \operatorname{Im} \bar{c} e^{i\omega t} \int d\bar{r} e^{iqz} \langle \hat{\Delta}(\bar{r},t) \rangle . \qquad (22)$$

The thermal average in the right of Eq. (22) is with respect to the statistical operator ρ, where

$$\rho = e^{-\beta H} / \operatorname{Tr} (e^{-\beta H}).$$

Here $\beta = {}^{1}/_{k_B T}$ and $H = H_o + H_I$ where H_o is the Hamiltonian for the noninteracting system.

Using the standard linear response theory[30] to calculate $\langle \hat{\Delta}(r,t) \rangle$ gives

$$\langle \hat{\Delta}(\bar{r},t) \rangle = \langle \hat{\Delta}(\bar{r},t) \rangle_o + \frac{i\bar{c}}{\hbar d} \int_{-\infty}^{t'} dt' \int d\bar{r} e^{i\omega t'} e^{iqz'} \left\langle \left[\hat{\Delta}(\bar{r},t), \hat{\Delta}^{\dagger}(\bar{r}',t') \right] \right\rangle_o , \qquad (23)$$

where $\langle \ \rangle_o$ denotes a thermal average using a statistical operator containing only the noninteracting Hamiltonian of the fluctuating film.

For $T>T_c$ the first term on the right hand side of Eq. (23), $<\hat{\Delta}(r,t)>_o$, is zero. The excess current is

$$I_{ex}(V,H) = \frac{4e|\bar{C}|^2 A}{d\hbar} \text{ Im } \chi(\omega,q), \quad (24)$$

where $\chi(\omega,q)$ is the pair-field susceptibility which from Eq. (12) is the Fourier transform of the response function for the pair potential

$$R(\bar{r},t) = -i/h < \left[\hat{\Delta}(\bar{r},t), \quad \hat{\Delta}^{\dagger}(0,0)\right] >_o \theta(t). \quad (25)$$

Here the frequency ω and wave vector q are set by the dc bias fields according to Eq. (19). Noting that $\text{Im}\chi(\omega,q)$ can be related to the structure factor through the fluctuation-dissipation theorem, the current can also be written in terms of the dynamical structure factor

$$I_{ex}(V,H) = \frac{2e|\bar{C}|^2 A\omega}{\hbar dk_B T_c} S(\omega,q) \quad (26)$$

Equations (24) and (26) give the desired relationship between the excess current and the generalized susceptibility and order parameter structure factor.

Below T_c the first term on the right of Eq. (23) is nonzero, in constrast to the case for $T>T_c$ where it vanishes. Thus two contributions to the excess current result. The first term is first order in the interaction Hamiltonian, but second order in the tunneling matrix element, since $\bar{C}$ is second order in the tunneling matrix element. This term is proportional to

the imaginary part of the average value of the pair-field on the fluctuating side of the junction and is recognized as the usual Josephson zero voltage current,[31]

$$I = Im\bar{C}\langle\Delta_o(r,t)\rangle_o \propto \langle\Delta_o(r,t)\rangle \quad \sin(\phi - \phi'),$$

where $\phi - \phi'$ is the difference between the phases of the pair-fields of the two sides of the junction.

The physical manifestations of this term are the usual ac and dc Josephson effects. Josephson[32] showed that a supercurrent density given by

$$j = j_o \sin(\phi - \phi'), \tag{27}$$

could flow across the junction. If a chemical potential difference $\Delta\mu$ exists across the junction, the time variation of the phase difference is given by

$$\frac{\partial(\phi - \phi')}{\partial t} = \frac{2\Delta\mu}{\hbar}$$

If a uniform magnetic field is applied parallel to the plane of the junction the spacial variation of the phase difference is given by

$$\frac{\partial(\phi - \phi')}{\partial x} = \frac{2e}{\hbar c}\left(\frac{d}{2} + \lambda'\right) H,$$

and the total maximum zero voltage current as a function of H is given by

$$I_o(H) = \left| \frac{\sin \frac{e}{\hbar c}(\lambda + \lambda' + \delta) HL}{\frac{e}{\hbar c}(\lambda + \lambda' + \delta) HL} \right| . \tag{28}$$

Here L is the length of the junction.

The second contribution to the excess current is proportional to the imaginary part of the pair-field susceptibility of the electrode below its transition temperature. This component is fourth order in the tunneling matrix element, and is usually obscured by the dc Josephson effect. However a magnetic field of 10 to 20 Oe is sufficient to completely quench the dc Josephson current (see Eq. (28)), making the second component of the current observable. Since $\xi(T)$, the parameter which determines the range of coherence of the fluctuating component of the order parameter, is always smaller than q^{-1}, the effective wave length of the fluctuating current, the latter would not be expected to exhibit diffraction effects analogous to those described by Eq. (28).

C. SUSCEPTIBILITY FOR $T > T_c(H)$

The calculation of the explicit dependence of the pair current on the voltage and magnetic field reduces to the determination of the pair-field susceptibility from theory. A microscopic calculation is given in Ref. 5. In this section we outline the calculation given in Refs. 7 and 8 based on the Ginzburg-Landau theory.

Two approximations are made in this calculation. It is assumed that the thickness of the film is less than the temperature dependent coherence length. Then variations of the order parameter in a direction perpendicular to the plane of the junction can be neglected.

It is also assumed that the effects of a magnetic field can be neglected in the free energy and appear only in the phase of the order parameter.

Using the fluctuation-dissipation theorem, the calculation of the susceptibility reduces to determining the structure factor. Expanding the order parameter in plane waves

$$\Delta = \sum_k \Delta_k \, e^{i\bar{k}\cdot\bar{r}}$$

thermal averages of time independent quantities such as $\langle \Delta_k^* \Delta_{k'} \rangle$ can be found by weighting the fluctuations according to the free energy associated with them.[33] Quantities like

$$\langle \Delta_k \rangle, \quad \langle \Delta_k^* \Delta_{k'}^* \rangle, \quad \langle \Delta_k \Delta_{k'} \rangle$$

vanish and the only nonvanishing product is

$$\langle \Delta_{k'}^*, \Delta_k \rangle = \delta_{kk'} \frac{\alpha(T)}{N(0)\epsilon} \frac{k_B T_c}{Ad} \frac{2m}{\hbar} \left(\frac{1}{\xi(T)} + \frac{1}{k2} \right)^{-1}. \tag{29}$$

The lifetimes of the fluctuations above T_c can be obtained from diffusive time-dependent Ginzburg-Landau equation (Eq. (9)) which describes the relaxation of the order parameter in zero field. For a fluctuation with wave vector q, the temporal correlation function decays exponentially

$$\langle \Delta^*(q,0) \, \Delta(q,t) \rangle = \langle |\Delta(q,t)|^2 \rangle e^{-\Gamma_q t}, \tag{30}$$

where

$$\Gamma_q = \Gamma_o \left(1 + \xi(T)^2 q^2\right) . \tag{31}$$

Using Eq. (29) and (30) in the fluctuation-dissipation theorem, the susceptibility for $T > T_c$ becomes

$$\mathrm{Im}\,\chi(\omega,q) = \hbar/N(0)\epsilon \; \omega/\Gamma_o \Big/ \left((1 + \xi(T)\, q^2)^2 + \left(\frac{\omega}{\Gamma_o}\right)^2\right) \tag{32}$$

Substituting this into Eq. (24) the fluctuation contribution to the current above T_c is

$$I_{ex}(V,H) = \frac{4eA\,|\tilde{c}|^2}{dN(0)\,\epsilon} \qquad \frac{\omega/\Gamma_o}{(1 + \xi^2 q^2)^2 + (\omega/\Gamma_o)^2} \tag{33}$$

Equation (33) is equivalent to the fluctuation induced pair current originally obtained by Scalapino.

An aspect of the calculation of the pair current omitted in the derivation of Eq. (33) is the role of thermal noise associated with the quasiparticle-tunneling channel. With voltage fluctuations due to quasiparticle noise, it is necessary in the above calculation of $\chi(\omega,q)$ to add an independently fluctuating component to the overall phase of the order parameter in the normal metal. The phase fluctuation is implied by quasiparticle voltage fluctuations through the Gor'kov-Josephson relation

$$\frac{\partial \Phi}{\partial t} = \frac{2e\tilde{V}}{\hbar} ,$$

where $\tilde{V}$ is the voltage fluctuation. Noise fluctuations are known to modify the I-V characteristic of symmetric junctions at low voltages.[34] Since the theoretical

calculation is difficult and has not been carried out in detail for an asymmetrical junction, the full effect of noise on the I-V characteristic is not known. However, in this experimental investigation, there is no evidence that thermal noise plays a significant role, since the excess current-voltage characteristic of junctions with high quasiparticle resistances did not differ from the characteristics of junctions with low quasiparticle resistances.

We note the experimentally interesting features of the theory of Scalapino. The quasi-Lorentzian form of the excess current-voltage characteristic predicted by Eq. (33) is shown in Fig. (2). This equation can be written in terms of the values of current and voltage at the peak as

$$I = 2I_p \frac{V/V_p}{1 + (V/V_p)^2} , \qquad (34)$$

where this result is applicable in both zero and weak magnetic fields. Equation (34) is used to compare the experimental form of the excess current to theoretical predictions. In zero field, the peak voltage is directly related to the pair relaxation frequency by the relation

$$V_p = \frac{\hbar \Gamma_o}{2e} = \frac{4k_B}{\pi e} (T - T_c) , \qquad (35)$$

A graph of V_p versus T is a direct measure of the temperature dependence of the relaxation frequency and should be a straight line with intercept at T_c and

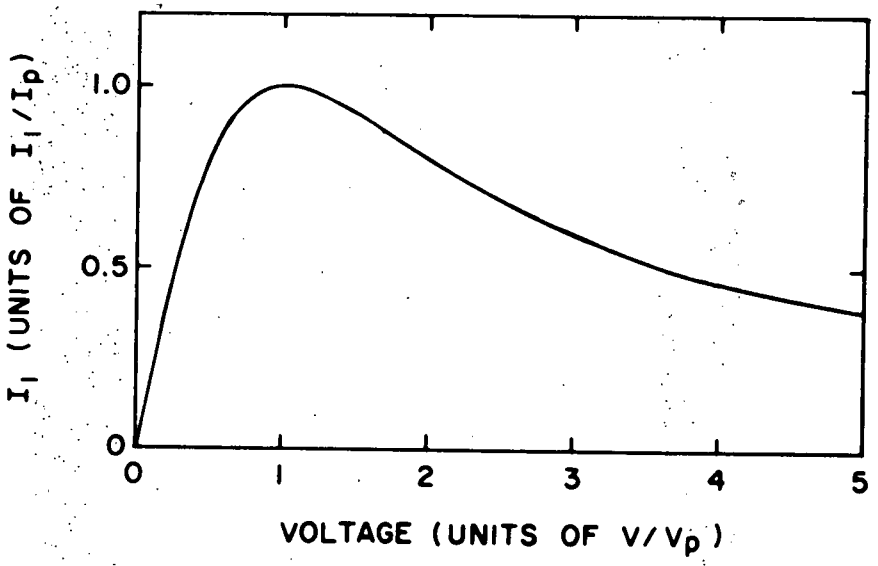

Fig. (2) Theoretical dependence of excess current on voltage predicted by Eq. (34) in terms of peak voltage and current.

slope dependent only on fundamental constants. The current at the peak is given by

$$I_p = \frac{2eA\left|\bar{C}\right|^2}{dN(0)} \left(\frac{T_c}{T - T_c}\right). \qquad (36)$$

The inverse peak current plotted as a function of temperature should also be linear with intercept at the transition temperature. One further interesting quantity in zero field is

$$\sigma(0) = \left.\frac{dI_{ex}}{dV}\right)_{V=0},$$

the static conductivity at the origin, given by

$$\sigma(0) = \frac{4eA\left|\bar{C}\right|^2}{dN(0)\epsilon} \frac{1}{\Gamma_o}. \qquad (37)$$

A plot of $(\sigma(0))^{-\frac{1}{2}}$ versus T should also be linear with intercept at T_c.

The effect of a magnetic field is to shift the peak to a higher voltage for a given temperature and at the same time to shift the transition temperature of the fluctuating film downward without changing the quasi-Lorentzian shape of the excess current-voltage characteristic. The shift in T_c was not included in the theory of Scalapino, however will be discussed in the next section. The plot of V_p versus T is still linear with the slope given from Eq. (35). Both V_p and I_p^{-1} are linear functions of H^2, given by

$$V_p = \frac{\hbar \Gamma_q}{2e} = \frac{\hbar}{2e} \Gamma_o (1 + q^2 \xi^2(T))$$

$$I_p^{-1} = \frac{dN(0)\epsilon}{2eA |\bar{C}|^2} (1 + q^2 \xi^2(T)) \quad (38)$$

D. THE CALCULATION OF SHENOY AND LEE

The result of Scalapino's calculation, Eq. (33) shows that with the application of a dc voltage V, and a magnetic field H parallel to the junction only fluctuations of frequency $\omega = 2eV/\hbar$ and wave vector $q = 2e/(\hbar c)(\lambda' + d/2)H$ contribute to the tunneling current. These results are a consequence of the form of the interaction Hamiltonian used by Scalapino, but which has not been justified explicitly using microscopic theory. In addition, possible variations of the order parameter across the film thickness and the reduction of the transition temperature of the film due to the parallel magnetic field are not taken into account.

Shenoy and Lee have presented the details of a microscopic calculation in which they show explicitly that only fluctuations of wave vector $q = 2e/(\hbar c)H(\lambda' + d/2)$ are picked out by the magnetic field. Furthermore they treat the effect of the magnetic field on the transition temperature of the fluctuating film.* Their results are

*The parallel magnetic field acts with opposite signs on the two members of a Cooper pair promoting pair breaking. The effects of the pair breaking are to lower T_c and to shift the temperature dependence of the relaxation frequency. The first effect is treated by Shenoy and Lee, while the second is neglected. The effect of depairing is discussed in Section IV-E.

also not restricted to the cases of films thinner than the coherence length and weak magnetic fields. They find as might be expected, that for high fields, non-uniform fluctuations of the order parameter across the film are important. A brief outline of their calculation follows.

The single particle tunneling Hamiltonian is given by

$$H_T = \int d\vec{r}d\vec{r}' \; M^*(r',r)\sum_\sigma \psi^\dagger_{\sigma R}(r)\psi_{\sigma L}(r') + H.C., \tag{39}$$

where $\psi_{\sigma R}$ ($\psi_{\sigma L}$) refers to an electron field on the right-hand (left-hand) side of the junction, and $M(r,r')$ is the tunneling matrix element. The tunneling current is then calculated from the equation of motion

$$I = -e\dot{N}_L = ie\left[H_T, N_L\right] . \tag{40}$$

Its average value is

$$I = 2e\,\mathrm{Im}\int d\vec{r}d\vec{r}' \; M^*(r,r')\sum_\sigma \langle \psi_{\sigma R}(\bar{r})\,\psi_{\sigma L}(\bar{r}')\rangle \tag{41}$$

A nonlinear response theory is then used to determine the fluctuation-induced Josephson current which is fourth-order in the tunneling Hamiltonian. The current is then written in terms of the Fourier transform with respect to time of the correlation function:

$$T(r_1,r_2,t) = i \left\langle \left[\hat{\Delta}(r,t) \quad \hat{\Delta}^\dagger(r,0)\right]\right\rangle \theta(t). \tag{42}$$

In the presence of a magnetic field, $T(r_1,r_2,\omega)$ is expanded in terms of the solutions to the linearized

time-dependent Ginzburg-Landau equation for an isolated film in a parallel field, a procedure more general than the earlier method of expanding the correlation function in plane waves.

The Ginzburg-Landau equation near T_c is :

$$\epsilon_o + \xi^2(0)\Pi\Pi^2 + \epsilon/\Gamma_o \left(\frac{\partial}{\partial t} + \frac{2ieV}{\hbar} \right) \Delta(r,t) = 0, \tag{43}$$

where $\Pi\Pi = \left(\frac{\nabla}{i} + \frac{2e\vec{A}}{\hbar c} \right)^2$. For an isolated film of thickness d, with x axis perpendicular to the film plane, the condition that there be no supercurrent leaving the film gives the boundary condition

$$\frac{\partial \Delta}{\partial x} \left(\pm \frac{d}{2}, y, z, t \right) = 0 \tag{44}$$

With the magnetic field in the z direction the order parameter can be written in terms of the functions

$$\psi_{\nu kq}(\bar{r}) = e^{ikz} e^{iqy} \frac{f_\nu (2b)^{\frac{1}{2}} (\bar{x} - \bar{x}_o)}{\frac{1}{2}Ad}, \tag{45}$$

which are eigenfunctions of the operator[35]

$$\xi^2(0)\Pi\Pi^2 \psi_{\nu kq}(\bar{r}) = \left(\xi^2 k^2 + (2\nu + 1)\, b\bar{\xi}^2 \right) \psi_{\nu kq}(\bar{r}) \tag{46}$$

satisfying the boundary condition given in Eq. (44). The bar denotes a length measured in units of d/2. The dimensionless field variable is given by

$$b = \frac{2e\,H}{\hbar c} \left(d/2 \right)^2, \tag{47}$$

and the centering position x_o of the functions $f_\nu(t)$ is proportional to the wave number q, and is given by

$$\bar{x}_o = q\, d/2b.$$

The function $f_\nu(t)$ is a linear combination of the Weber functions $D_\nu(t)$, $D_\nu(-t)$:

$$f_\nu(t) = D_\nu(\bar{t}) + \alpha_\nu D_\nu(-\bar{t}).$$

The eigenvalue ν is not an integer but is a function of b and q determined by the boundary condition that $f_\nu(t)$ should have zero slope at the film surfaces. This can be written as

$$\alpha_\nu = D_\nu^{(1)}(\bar{t}_+) \,/\, D_\nu^{(1)}(-\bar{t}_+) = D_\nu^{(1)}(\bar{t}_-) \,/\, D_\nu^{(1)}(-\bar{t}_-) \tag{48}$$

where $\bar{t}_\pm = (2b)^{\frac{1}{2}}(\pm 1 - \bar{x}_o)$ and $D_\nu^{(1)}(\bar{t})$ is the derivative of the Weber function with respect to the whole argument.

The correlation function is then written as

$$T(r_1, r_2, \omega) = \sum_{\nu\, kq} T_{\nu kq}\, \psi_{\nu kq}(\bar{r}_1)\, \psi^{*}_{\nu kq}(r_2) \tag{49}$$

This expansion was first used by Tan.[36] However with the film lying between $x = \pm d/2$, he chose the boundary conditions

$$\frac{\partial \Delta}{\partial x}\left(\frac{d}{2}, y, z, t\right) = 0$$

and

$$\frac{\partial \Delta}{\partial x}\left(-\frac{d}{2}, y, z, t\right) = \mu \Delta\left(\frac{d}{2}, y, z, t\right),$$

with $\mu = Td/\xi_o$, where T is the tranmission coefficient of the barrier. The boundary condition involving T would seem appropriate to the surface of the film adjacent to the oxide layer of the junction. However Shenoy and Lee have argued that since the effect itself is the result of a perturbation calculation in the tunneling matrix element, the appropriate boundary conditions are those of an isolated film. It is inconsistent to use the boundary conditions of Tan in that they are equivalent to mixing in a higher order in the tunneling Hamiltonian.

Using the expansion for the correlation function in terms of Weber functions, the current through the junction becomes (50)

$$I_{ex} = 2eIm \left| C_o^s \right|^2 \sum_{\nu} \left[\epsilon_o + (2\nu + 1) b\bar{\xi}^2 - \frac{2eiV\epsilon_o}{\Gamma_o} \right]^{-1},$$

with $C_o^s = 2\pi N(0) \Omega_L \rho_R \, d\, C_1 \left(\frac{\Delta}{2\pi kT} \right) M_s^2$

where Ω is the volume of the superconducting side and

$$C_1(x) = \sum_{n > 0} \frac{x}{n + \frac{1}{2}} \left[(n + \tfrac{1}{2})^2 + x^2 \right]^{\frac{1}{2}}$$

The sum over ν is over the ground state and the excited state solutions. $2\nu + 1$ must be determined by solving the boundary condition, Eq. (44).

For weak fields only the lowest eigenvalue in the sum over is important. The current peaks at a voltage given by

$$V_p = \frac{h\Gamma_o}{2e}\left[1 + \left(\frac{2eH}{\hbar c} \right)^2 \left(\frac{1}{3}\left(\frac{d}{2}\right)\right)^2 + \left(\frac{d}{2} + \lambda' + \delta \right)^2 \xi^2(T) \right.$$
$$\left. - 8\left(\frac{2eH}{hc}\right)^2 \left(\frac{d}{4}\right)^4 \xi^2(T) \left(\left(\frac{d}{2}\right)^2 \frac{1}{945} + \frac{1}{15}\left(\frac{d}{2} + \lambda' + \delta\right)^2 \right) \right]. \quad (51)$$

The first term on the right is the expression for the relaxation frequency in zero field. The first field dependent term is the familiar Ginzburg-Landau lowering of the transition temperature of a film in a parallel magnetic field. The second field dependent term is just the field-dependent term obtained by Scalapino. The higher order terms correspond to increasing spatial variation of the order parameter across the film, leading to deviations from the simple linear dependence of V_p on H^2 given by the first two field-dependent terms.

The quadratic dependence of V_p and H^2 is then due to both the supression of T_c by the field and the picking out of fluctuations of a particular wave-vector $q = \left[2e/\hbar c\right] (\lambda' + d/2)H$. The departure from the linear dependence of V_p on H^2 at high fields is due only to the selection of fluctuations of a particular wave-vector. For thick ($d > \xi(T)$), "dirty" films in high magnetic fields, the excited states of Eq. (50) should contribute to the current. The current will be a sum of quasi-Lorentzians and the excited states will appear as peaks in the I-V characteristic.

E. OTHER RELATED THEORETICAL AND EXPERIMENTAL WORK

We conclude this chapter with a brief discussion of other pertinent theoretical and experimental work relating to the fluctuating conductivity problem in an asymmetrical junction above T_c.

Early studies of fluctuation conductivity, magnetic susceptibility and quasiparticle tunneling involve complex convolutions of the susceptibility. They can provide only indirect information about the pair-field susceptibility and thus will not be compared to this work.

As discussed earlier, Ferrell[4] was actually the first worker to suggest that there might be a connection between fluctuation induced pair tunneling and the generalized susceptibility. He showed that the frequency dependent conductivity could be used to determine $\chi(\omega)$ and that, in principle, the pair relaxation frequency could be determined from these measurements.

After Scalapino's calculation of the relationship of the dc I-V characteristic to the pair-field susceptibility, Takayama[27] carried out microscopic calculations of the fluctuation induced current and found agreement with the frequency dependence of $\sigma(0)$ obtained by Ferrell. In his calculation of the I-V characteristic, he included the effect of the magnetic field on the transition temperature of the fluctuating film, however neglected the field dependence of the phase of the order parameter (i.e. he let $q = 0$).

The calculation of the pair tunneling current of Scalapino, and Shenoy and Lee were carried out assuming specular transmission of electrons through the barrier. Takayama[27] also calculated the fluctuation induced tunneling current for the case of diffuse transmission and found qualitatively different behavior of the excess current. For zero magnetic field the expression for the peak voltage given by Takayama is

$$V_p = \left(\frac{2e\epsilon}{\Gamma_o \hbar}\right)^{-1} \quad (\epsilon (1 + \xi^2(0)\, k_c^2)), \quad (52)$$

where k_c is a cut off wave vector which is expected to be on the order of $(\xi(T)\, l)^{\frac{1}{2}}$ when $l \ll \xi_o$ and $\xi^{-1}(T)$ when $l \gg \xi_o$. Since the films used in this work have mean free paths of the order of 20 Å and zero temperature coherence lengths of 500 Å, the difference between diffuse and specular transmission should be easily recognizable.

A calculation of the effect of pair breaking mechanisms[37] (parallel magnetic field, paramegnetic impurities, etc.) on the pair-field susceptibility of a superconductor above T_c has been carried out by Schmidt and co-workers.[17,38,39] They found that in addition to the usual shift in the transition temperature of a superconducting film characterized by a depairing parameter ρ, that: 1. the apparent lifetimes of fluctuations $1/\Gamma_o$ are increased, 2. the apparent range

of coherence of fluctuations is enhanced, and 3. the quasi-Lorentzian shape of the pair-field susceptibility is the same as in the absence of a pair breaking mechanism. The slope of dV_p/dT, being a measure of Γ_o, thus provides a direct measure of the pair breaking strength. The explicit form of the susceptibility and a discussion of depairing mechanisms is given in Chapter IV where they are used in the analysis of the data for $T<T_c$.

Other theoretical contributions have been made by Šimánek and Walker[40] who consider the effect of non-uniform coupling on the temperature dependence of the peak voltage; Tan,[37] who carried out a calculation of the magnetic field dependence of the excess current and Kulik,[41] who considered the problem of the fluctuation pair current between two identical superconductors above T_c. Ichikawa[42] has calculated the temperature dependence of the static excess conductivity for various dimensional contacts and found that

$$\sigma(0) \propto \epsilon^{-1} \quad \text{or} \quad \epsilon^{-2},$$

depending upon whether the dimensions of the junction are large or small in comparison with the temperature dependent coherence length. He interprets this as being due to diffuse transmission through the barrier.

Measurements in qualitative agreement with Ferrell's calculation of the excess static conductivity have been reported by several groups.[43,44] Yoshihiro and Kajimura[44] confirmed the $((T - T_c)/T_c)^{-2}$ temperature dependence

of the excess static conductivity in Pb-Al_2O_3-Al junctions above T_c. Yoshihiro, Yamaji and Kajimura[45] investigated the effect of an electric field on the fluctuation induced junction conductivity. This situation is physically different than the work reported in this dissertation so no comparison can be made to it.

The experiments of Anderson and Goldman[6,7] measured the full current voltage characteristics of Pb-Sn_xO_y-Sn and found qualitative agreement with the theory of Scalapino. Several qualitative differences were found however. The dependence of the peak voltage on H^2 was not linear as expected and the relaxation frequency Γ_o was 50% larger than predicted by Scalapino's theory. The latter problem was explained by later experimental work[8] as being a consequence of the limited range in temperature near T_c over which the measurements were made. The theoretical work of Shenoy and Lee, and Tan was carried out to explain the effects of large magnetic fields on the excess current. Although the theory of Shenoy and Lee predicts a fall off of the linear dependence of V_p upon H^2 at high fields, it does not seem to be enough to account for the saturation seen in the work of Anderson and Goldman. However the experimental errors in the determination of peak voltages were large in this investigation so that no quantitative statements can be made.

III. EXPERIMENTAL TECHNIQUES

In these experiments thin film Josephson tunneling junctions were fabricated and their current-voltage characteristics were precisely determined as functions of both temperature and magnetic field. As in most experiments using Josephson tunneling junctions, a major effort was required to make reliable insulating layers between the electrodes of the junctions. It was a formidable matter to obtain the right conditions in the sample preparation system that would give junctions that were strongly coupled enough to be able to see the fluctuation induced current, yet still free from filamentary shorts through the insulating layer. As evidence of this, of the 140 junctions made, only nine were suitable for measurement.

The basic sample preparation techniques and data acquisition system were designed by John Anderson and are described in detail in his thesis.[7] No attempt will be made to repeat such descriptions. Only special features pertaining to the present work along with an outline of the general procedures will be given in this chapter.

A. EVAPORATION SYSTEM

Junctions were prepared in a oil-free high vacuum system capable of maintaining the pressure in the evaporation chamber at less than 5×10^{-8} torr during most

stages of sample preparation. The system consisted of three parts: a pumping section, an evaporation and collimation section, and a sample holder and masking section. With this system it was not necessary to expose the sample to atmospheric conditions during any stage of sample fabrication.

The pumping section consisted of a titanium sublimation pump, a 100 liter per sec Ultek ion pump, and a Welch 1397B mechanical pump. During the actual preparation of the sample, only the ion pump and sublimation pump were used. The mechanical pump, separated from the evaporator by a molecular sieve trap to prevent contamination of the evaporation chamber by oil, was used only for the initial pump-down and bakeout of the system.

Films were evaporated onto a 2.54 X 2.54 cm glazed alumina substrate from resistively heated boats. The substrate was held approximately 40 cm above the evaporation source on a rotatable disk. A substrate could be positioned over any of the six sources. Masks were held on a second disk approximately 1 mm below the substrate. Any of the 12 masks could be positioned between the substrate and a source. Film thicknesses and deposition rates were measured in-situ with a Sloan quartz crystal thickness monitor.

Junction properties were very sensitive functions of the background contamination that was present in the evaporation chamber. To characterize the back-

ground, a Ultek partial pressure analyzer (PPA) was mounted on the system, enabling the residual gas background in the system to be monitored continuously during sample preparation.

Care was taken to keep the evaporation system in a clean state. Materials with high vapor pressure were not used in the system. Whenever the system was opened to atmospheric conditions, heaters on the system were turned on to reduce the absorbtion of water vapor on the surfaces. The system was baked out for at least eight hours at 375 K before any materials were evaporated.

B. SAMPLE

The structure of the tunneling junction is shown in Fig.(3). They are of the crossed film variety with the insulating layer formed by thermally oxidizing the lower electrode in an oxygen environment at room temperature. For most junctions, aluminum was used as the lower electrode and lead as the upper. Both metals had impurity levels lower than one part in 10^5.[46] All but a .271 X .271 mm area of the lower electrode was covered with at least 1000 Å of Bi_2O_3, to eliminate edge effects which tend to broaden the resistive transition producing an ambiguity in the transition temperature. The area of the tunneling junction was then defined by this small window in the center of the lower electrode. The electrical leads B, H, and F were used to make electrical measurements on the aluminum film.

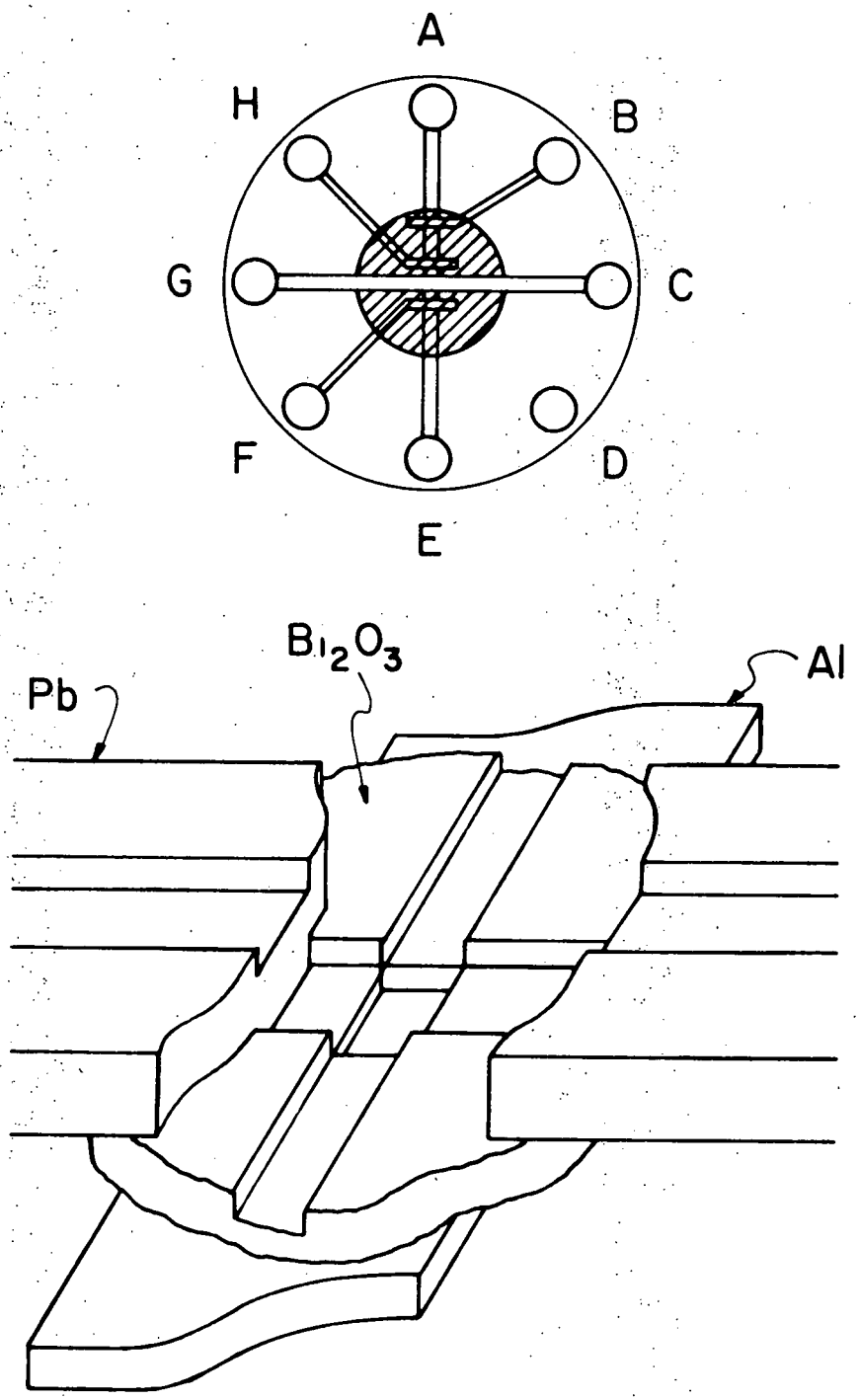

Fig. (3) Junction structure used in these experiments.

Aluminum films were all of a "dirty" character, in that they were characterized by conduction electron mean free paths short in comparison with the BCS coherence length. The usual way to produce such films is to evaporate aluminum from a tungsten filament in the presence of a partial pressure of oxygen or other gasses. In this work aluminum was evaporated from an alumina coated molybdenum boat. When heated, the alumina coating on the boat released a considerable amount of oxygen, hydrogen, nitrogen and water vapor into the system. For example, the partial pressure of water vapor at the position of the substrate was measured with the PPA to increase from less than 1×10^{-9} to 2×10^{-7} torr. Films formed in the presence of these gasses were granular with short conduction electron mean free paths. Since relatively little control could be exercised over the gas background, physical properties of the aluminum films such as the transition temperature and resistivity, varied from sample to sample.

The insulating layer was formed by allowing dry oxygen into the evaporator at a pressure of 100 microns for a period of from 1 to 5 minutes. A 10 to 20 Å layer of aluminum oxide then formed on the surface of the aluminum film. This was a most difficult step to perform since factors other than oxygen pressure and oxidation time play an important part in the growth of the oxide layer. The success of making good tunneling

junctions depended on the control of the various factors which determined the oxidization rate. Some of the parameters which were involved and which could be controlled were: residual gasses in the system such as water vapor, hydrogen and chlorine, temperature of the substrate during oxidization and film deposition, and substrate smoothness and cleanliness.

The most important factor affecting the oxide layer was the level of water vapor in the system. This could be reduced by a bakeout at 400 K for 72 hours with only the mechanical pump running, followed by a bakeout for 24 hours with the sublimation and ion pump running. After this processing, the partial pressure of water was found to be less than 1×10^{-9} torr.

A procedure which most readily resulted in usable junctions was to leave the system at a high vacuum (1×10^{-8} torr) for two to three weeks before making any evaporations. Junctions could then be made in a reproducable manner. Of course, this procedure was impractical since the same evaporation system was used to make samples for another experiment in the laboratory. In practice, when the evaporator was available, it was necessary to be very careful that conditions remained constant from sample to sample, so that one parameter, usually oxidization time, could be varied until a good oxide layer resulted.

The Bi_2O_3 evaporation which followed the oxidization step also affected the oxide layer. During this step, if the rate of evaporation was too fast, large amounts of oxygen were released into the system, because some of the bismuth trioxide was converted to bismuth metal. By keeping the deposition rate below 100 Å per minute, the oxygen pressure could be kept below 5×10^{-7} torr, a level that would not lead to further oxidization of the aluminum film.

Immediately after the junction was fabricated, it was removed from the evaporator, placed in the cryostat and cooled to liquid nitrogen temperature. No electrical checks were made on the junction until it was cooled to 77 K.

After cooling below the transition temperature of the aluminum film, several tests were performed on the junctions to determine their quality. Of primary concern was the requirement that junctions be free of filamentary shorts that might support supercurrents above T_c and thus might be confused with the excess current. Strong shorts are easily detected as they are insensitive to weak magnetic fields, and their presence makes it impossible to see the nonlinear features of the quasiparticle tunneling characteristic. A test for weak shorts is the presence of zero field steps in the I-V characteristic, which Matisoo[47] has shown can result from metallic wiskers. In unshorted junctions, steps

appear in homogeneous junctions only in the presence of a magnetic field. The magnetic field dependence of the Josephson current was examined for the Fraunhofer pattern, Eq. (28). If the junction coupling were nonuniform, secondary maxima would be reduced in magnitude.

Distortion of the current-voltage characteristic of a junction due to nonuniform current flow across the barrier is possible if the barrier resistance is the order of the resistance of the normal electrode.[48] When the resistance of the film is small in comparison with the barrier resistance, the effect is negligible. This was the case for all junctions used in this experiment.

C. LOW TEMPERATURE APPARATUS

The cryostat shown in Fig. (4), was carefully designed to give maximum isolation of the tunneling junction from electromagnetic noise and temperature fluctuations. An earlier apparatus used for measurements on samples Al-5, 6, 7, and 23 is not described here. The apparatus consisted of an outer OFHC copper vacuum can which was immersed in the 4.2 K helium bath. Suspended from the upper plate of this can by 3 stainless steel tubes was a copper helium pot which could be pumped to below 1.2 K. The sample was mounted in the holder shown in Fig. (5). The holder was attached to the base of the helium pot with a nylon screw. A 1.25 mm mica spacer was placed between the holder and

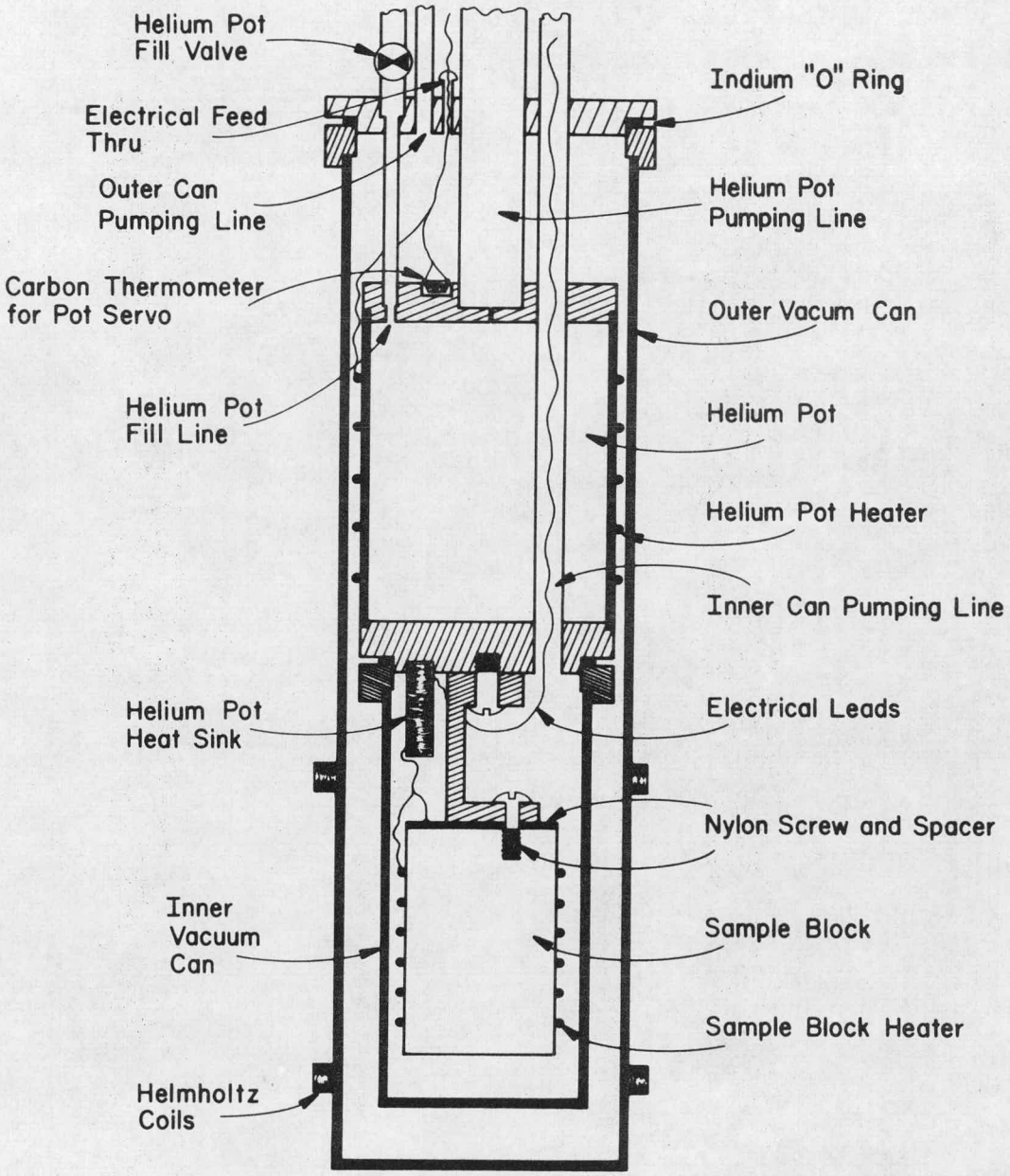

Fig. (4) Cross section of lower portion of cryostat.

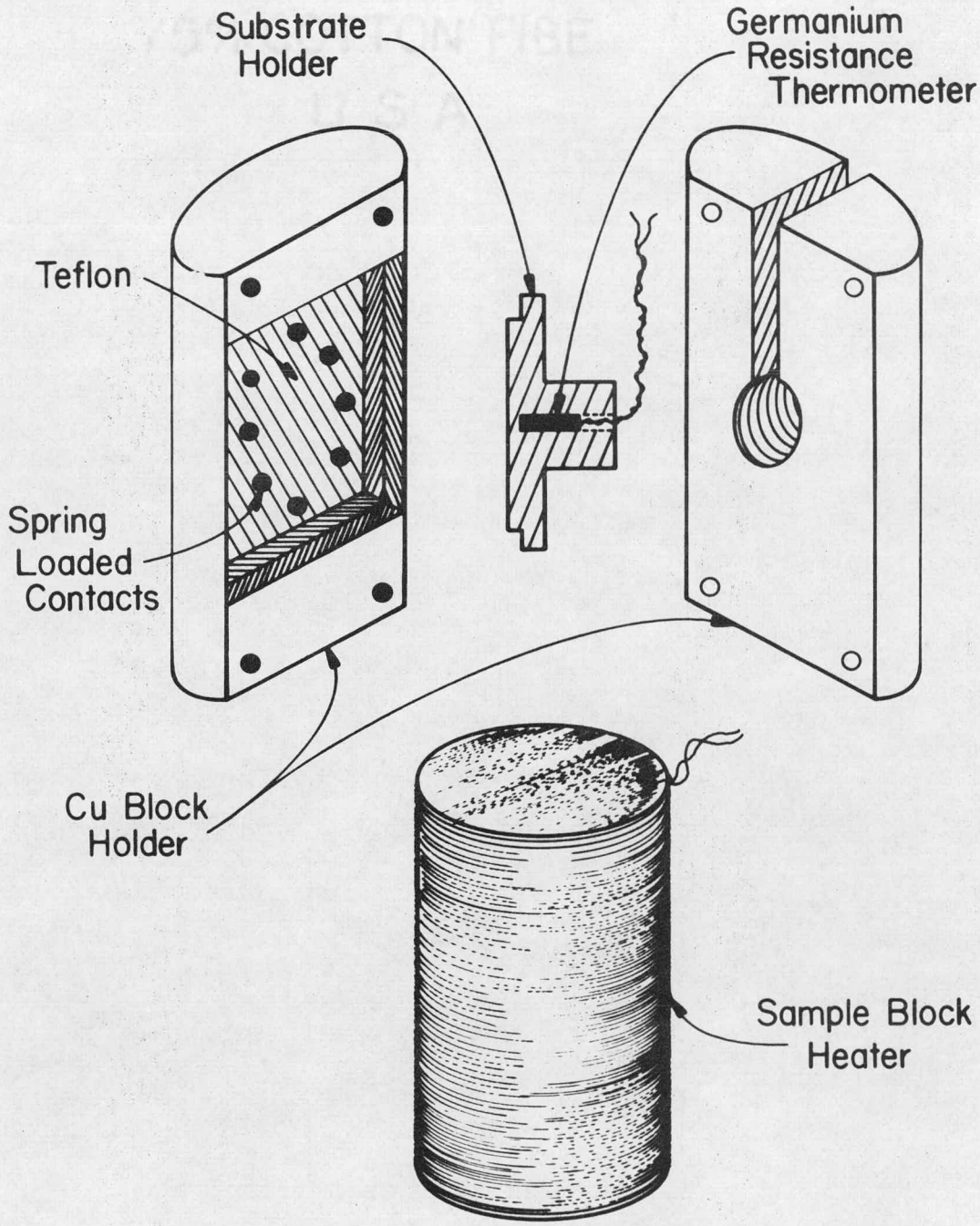

Fig. (5) Sample holder designed by J.T. Anderson. The alumina substrate was attached to a copper substrate holder with Eastman 910 contact cement. The two halves of the holder were bolted together and the copper can with the heater attached slipped over the cylindrical block.

base of the pot, to provide thermal isolation of the sample from temperature fluctuations of the pot. A second vacuum can around the sample holder allowed for the possibility of using helium exchange gas while still maintaining the isolation of the helium pot from the bath.

Electrical leads into the inner can (7 twisted pairs of #36 Cu wire) were passed through a room temperature feed-through at the top of the cryostat and down the inner can pumping line. The leads were thermally anchored to the 4.2 K bath by attaching them to a copper post in contact with the bath. Approximately two feet of the leads were wrapped around the post, covered with "N" grease and lens tissue and tied securely to the post. The same procedure was followed to heat sink the leads to the helium pot. To reduce the heat leak to the sample from the copper electrical leads, #36 manganin wire was used from the helium pot to the sample block. The manganin leads were clamped to the sample holder to insure that they were at the same temperature as the sample. Electrical contact to the sample was made by eight spring loaded berylium-copper contacts which pressed against contact pads evaporated on the substrate. Contacts were wet with a solder that was liquid at room temperature to give a more reliable electrical connection.

Several steps were taken to shield the tunneling junction from electromagnetic interference. All elec-

trical leads entering the inner can were filtered with subminiature pi-section low pass filters[49] which gave about 60 db of attenuation at frequencies above 5 MHz. The complete experimental apparatus was housed in a 10' X 10' X 8' shielded room, which attenuated signals in the range from 10 KHz to 10 GHz by better than 120 db. Magnetic shielding was provided by two cylindrical, concentric, high permeability shields enclosing the lower part of the cryostat external to the dewars. The magnetic field measured at the site of the sample was less than 5×10^{-4} Oe.

As evidence that the electromagnetic shielding of the cryostat itself was effective, electromagnetically noisy instruments such as digital voltmeters and oscilloscopes could be used near the cryostat with no effect on junction current-voltage characteristics.

A small persistent current superconducting Helmholtz coil, mounted on the outside of the outer vacuum can provided a magnetic field parallel to the plane of the junction. The coil was carefully centered on the sample and provided a field of 43 Oe per ampere. The component of the magnetic field perpendicular to the plane of the junction was estimated to be less than .7% of the applied field.

D. THERMOMETRY AND TEMPERATURE STABILIZATION

The temperature of the sample was determined by measuring the resistance of germanium thermometer,[50]

the calibration of which was based on the NBS He^4 vapor pressure scale. The absolute accuracy of temperatures determined from this thermometer were $\pm$ 2 mK. A resolution of 10×10^{-6} K was easily possible with the resistance bridges used.

Short term stability of the temperature of the sample of better than 20 μK was obtained in three stages. Coarse temperature stabilization was obtained by holding the vapor pressure of the liquid helium pot constant with the mechanical pump. In addition two servo feedback loops were used to stabilize the sample temperature. These systems worked by using the change in resistance of a resistance thermometer to control the amount of current to a heater. The first system used a 470 ohm $\frac{1}{2}$ watt Speer carbon resistor mounted with "N" grease in a slot on the top of the helium pot, and a 100 ohm noninductively wound heater made from 33 ft. of #36 manganin wire varnished with GE 7031 to the outside of the helium pot. The second system employed the germanium resistor, used to determine the sample temperature, and a second noninductively wound heater mounted on the sample block.

With the first two systems, long term stability of the sample temperature was better than .5 mK. When the third system was included, fluctuations in the temperature of the sample were less than 20 μK.

Once the system was adjusted to a selected temperature, it could be left over 6 hours with only minor adjustments necessary to keep the temperature constant.

Magnetoresistive corrections to the thermometry were experimentally insignificant for the range of magnetic fields and temperatures explored.[51]

E. CURRENT-VOLTAGE CHARACTERISTICS

The current-voltage characteristics of the junctions were obtained using four terminal ac techniques with the junctions current biased. The ac method was used to eliminate the effect of thermocouple voltages that are present in dc measurements at low voltages. Current biasing the junctions eliminated the need for a low temperature resistive shunt and low temperature noise filters that would be necessary if the junctions were voltage biased. Negative resistance regions of the I-V characteristic cannot be studied with a current biasing technique.

A block diagram of the electronics is shown in Fig. (6). Except for the minicomputer and its peripheral equipment, they are the same as described in Ref. 7. Only a brief sketch of the operation of the system is given in this section.

The ramp produced a slow, linearly increasing voltage that was chopped at 400 Hz. Since the chopping rate is large compared to the ramp rate, which is typi-

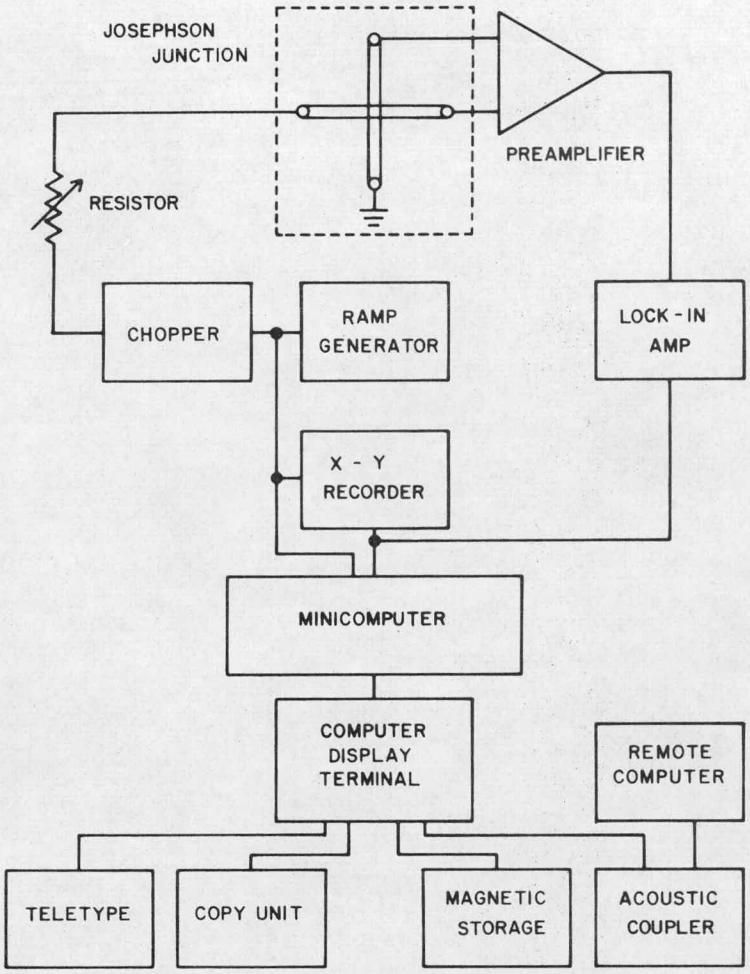

Fig. (6) Block diagram of the current-voltage characteristic acquisition system. The preamplifier, chopper and ramp generator were built by J.T. Anderson. The minicompueter was a Nova 1200 purchased with a grant from the Research Corporation. The computer diplay terminal, hard copy unit and magnetic storage unit were purchased from Textronics Company.

ically 0.25 volts per sec, the output of the chopper appears as a square wave of slowly increasing amplitude. The chopped voltage was converted to a chopped current by using a large resistance in series with the low impedence junction. The voltage drop across the junction was amplified by a broadband preamplifier mounted on top of the cryostat. The lock-in amplifier detected the 400 Hz component of the voltage. The dc output of the lock-in related to the voltage drop across the junction, and the signal from the ramp, proportional to the current through the junction, were displayed on an X-Y recorder. By changing the resistance in series with the junction and the gain of the lock-in amplifier, any position on the current-voltage characteristic could be studied. A voltage drop across the junction as low as 1 nanovolt could be detected with this system.

To eliminate pickup of electrical noise on the voltage leads, the preamplifier was mounted on top of the cryostat. The leads from the sample were soldered directly to the input of the preamplifier. Noise currents in the junction from external sources were estimated to be approximately 10^{-9} A.

Signals proportioned to the voltage across the junction and the current through the junction were transmitted to the analog-to-digital converters in the minicomputer where they were digitized. After the completion of a sweep of the I-V characteristic, the data was displayed on the CRT screen for preliminary analysis.

The raw data was then either stored on paper tape or magnetic tape for further analysis.

F. QUASIPARTICLE CURRENT SUBTRACTION

Figure (7) shows the full current-voltage characteristic of junction Al2-36. The total junction current contains contributions from both the fluctuation induced pair tunneling current and the quasiparticle or single-particle tunneling current. The latter must be subtracted to determine the pair-field susceptibility. Other tunneling channels such as conduction through the Bi_2O_3 masking were estimated at less than 0.1% of the total measured current and were ignored.

Two methods were used to determine the quasiparticle current. For junctions Al-5, 6, 7, and 23, the graphical technique described in Ref. 7 was used. In this method a linear extrapolation is made from a point on the I-V characteristic where the pair current is small to the origin. The excess current is then the portion of the current above the line. This procedure is not unreasonable because at low voltages the quasiparticle conduction is approximately ohmic.

The actual quasiparticle current across a normal-insulation-superconductor junction is given by[51]

$$I_{qp} = 2C_{NN}\frac{\Delta}{e}' \sum_{m} (-1)^{m+1} K_1\left(m\frac{\Delta'}{kT}\right) \sinh\left(\frac{meV}{T}\right) \tag{53}$$

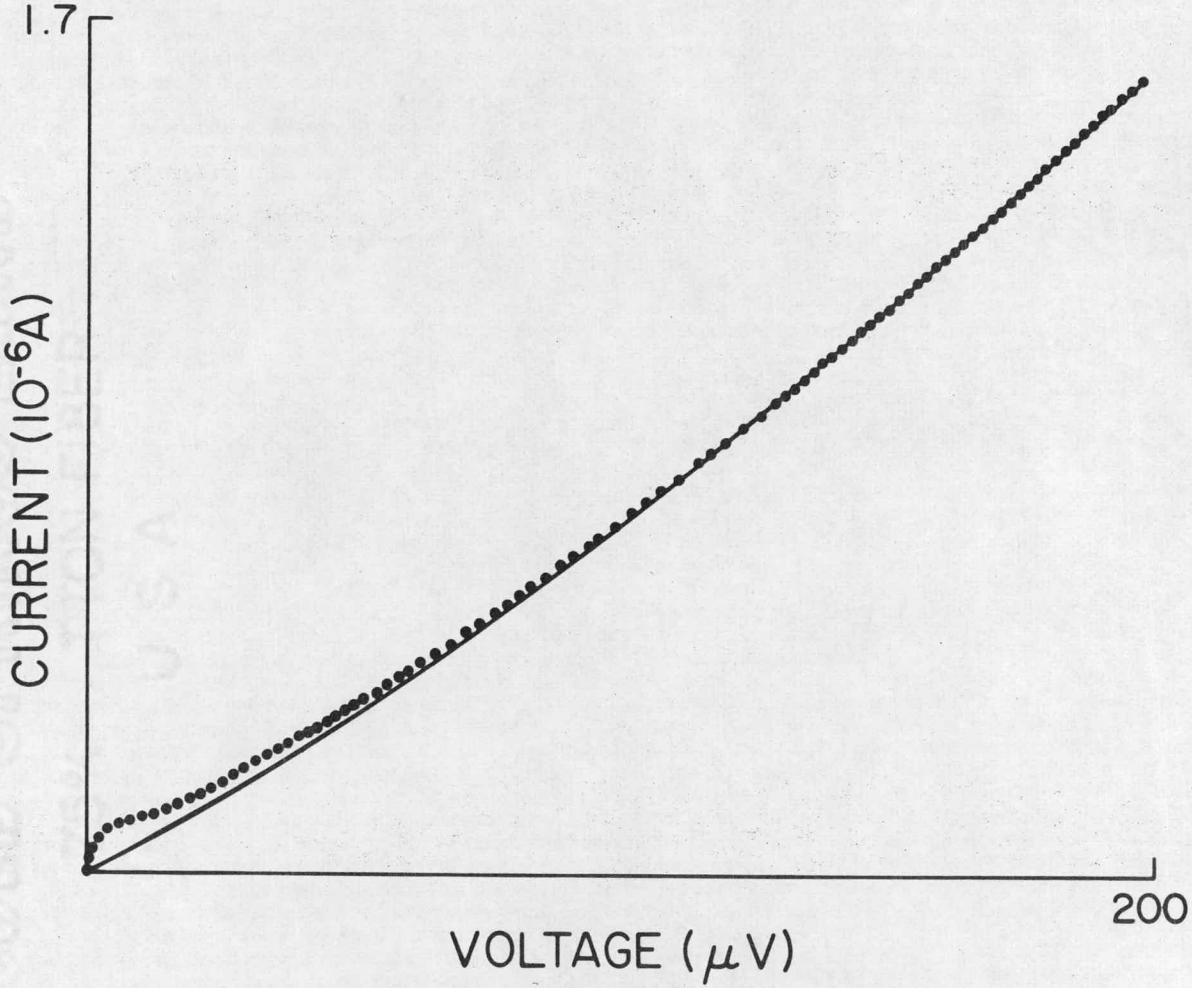

Fig. (7) Total I-V characteristic (points) for A12-36 at 1.96778 K. The solid line is the quasiparticle background determined from Eq. (54) and a least squares fit to the data from V = 150 μV to 200 μ V. The excess current is the portion of the curve above the solid line.

This expression is very nonlinear except close to the origin. To improve the characterization of the quasiparticle current, the first term of the above equation was used in the analysis of the data for sample Al2-5, 36, 61, 64, and 79. For every temperature and magnetic field, a fit of the experimental I-V characteristic to

$$I = A \sinh \frac{BV}{T} \tag{54}$$

was made with A and B treated as adjustable parameters. This fit was carried out for voltages between 150 μV and 200 μV, a region where the pair current due to fluctuations is small. The coefficients A and B were then used to compute the quasiparticle background at the very low voltages (0 - 50 μV) which were of interest.

This procedure was also used to approximate the background current when both halves of the junction were superconducting. Near T_c, where thermal smearing is large, the difference between the results of a fit based on this procedure and a more complicated calculation with two full energy gaps is negligible. Care must be exercised in the interpretation of the excess current obtained using the above analysis since the relatively elementary theory used to calculate the quasiparticle background does not include contributions from higher order single-particle processes or electron-pair interference effects. Thus some of the features of

the excess current-voltage characteristics may arise from processes not removed by the subtraction which are not related to the pair current associated with order parameter fluctuations.

IV. DATA AND ANALYSIS

The data[53] presented in this chapter was obtained from eight samples studied over an extended period of time. Sample preparation techniques and data acquisition methods were essentially the same for all samples, however, increasingly sophisticated techniques were used to handle and analyze data during the course of the investigations.

Measurements on samples A1-5, 6, 7, and 23 were made using apparatus built by J.T. Anderson. On-line data processing equipment was not available at the time. Consequently graphical techniques were used to determine the quasiparticle current, peak current, peak voltage, and zero voltage conductivity.

Measurements on sample A12-5 were made with the apparatus described in Section 3-C. A minicomputer and teletype were used to analyze the data. With the computer the quasiparticle current could be characterized accurately by a nonlinear least squares fit to the leading term of Eq. (53). The values of the peak current and peak voltage were determined by plotting the digitized values of the voltage and excess current from the computer and picking the maximum from the graph. A linear leasts squares fit was carried out to determine $\sigma(0)$ from the low voltage data.

Measurements on samples A12-36, 61, 64, and 79 were carried out with the electronics described in

Section 3-E. The usual procedure followed was to determine the I-V characteristic of the junction in the range from 150 to 200 μV at each temperature and magnetic field. An accurate fit of this data to Eq. (54) then determined the parameters of the quasiparticle current. The voltage gain on the lock-in amplifier and the series resistance in the measuring loop were then adjusted to permit a sweep of the I-V characteristic over the low voltage range required for the determination of the peak voltage and peak current. A simple program was written which subtracted the quasiparticle current from the total current and which could display any portion of the excess current-voltage characteristics on the screen of the computer display. The display was equipped with a cross-hair cursor with which the coordinates of any point on the screen could be input to the computer. This was used to record the peak voltage and peak current. A more accurate determination of the peak values was made by tracing a small region of the I-V characteristic around the peak with a high density of data points. Then with this portion of the excess current-voltage characteristic displayed on the terminal screen, the theoretical form of the excess current-voltage characteristic using Eq. (34) was superimposed on top of the data. The values of I_p and V_p were then adjusted to give the best agreement with theory. Below $T_c(H)$ Eq. (34) was not used for the determination of the peak voltage

and current. In most cases the peaks in the excess current-voltage characteristic were sufficiently well defined that the cursor alone could be used to select V_p (for example, see data in Fig. (21)). In some cases a detailed multiparameter fit to the data using a remote computer was carried out. This is discussed in Section IV-C.

All junctions exhibited negative dynamical resistances at low voltages over a range of temperatures in the vicinity of the superconducting transition. The width of the range was from 10 mK to 100 mK depending on the relative magnitude of the quasiparticle current as compared with the excess current. Peak voltages and peak currents could not be determined in the region of negative dynamical resistance because of a high susceptibility to noise which lead to switching instabilities in the current-voltage characteristics. $\sigma(0)$, the dynamical conductivity in the zero voltage limit is believed to be unaffected by these negative resistances and was therefore the only quantity determined in this region.

In this chapter we will present representative results of excess current-voltage measurements carried out on Al-Al_2O_3-Pb tunneling junctions. With the addition of digital data handling equipment to the laboratory, extensive data could be taken and immediately analyzed to document in detail the behavior of the excess current

as a function of both temperature and magnetic field. Only a small fraction of the data will be presented, since all junctions (except Al2-36) exhibited the same general behavior. Transition temperatures, zero temperature Josephson currents and aluminum film resistivities parameters over which there was little experimental control, varied from sample to sample. It is important to note that although these parameters varied, no sample-to-sample variation in the effects reported here were observed (except for Al2-36). Earlier data analyzed without the aid of the computer was not significantly different from later data except for larger scatter. No data was obtained below $T_c(H)$ for samples Al-5, 6, 7, and 23 and Al2-5.

The properties of the junctions used in the analysis are summarized in the next section. The presentation of the data is divided into two sections. First the data for $T > T_c$ is presented and compared in detail to the theories of Scalapino, and Shenoy and Lee. Since theoretical calculations for $T < T_c(H)$ are somewhat controversial and are currently in a state of flux, the next section contains only the experimental results for $T < T_c(H)$. A discussion of the comparison of the data with some of the theoretical explanations is postponed until after the data in that regime has been presented.

A. SAMPLE CHARACTERISTICS

The properties of the eight aluminum lead junctions analyzed in detail are summarized in Table I. R_N is the normal tunneling resistance, R_D is the quasiparticle resistance at zero voltage at a temperature of 2 K in zero magnetic field, I_0 is the dc Josephson current at approximately 1.1 K, C(F) is the capacitance of the junction determined from the spacing of the Fiske steps,[54] and T_c, d, and $\rho(N)$ are respectively the zero field transition temperature, the thickness and the normal state resistivity of the aluminum film. The thickness of the lead film is denoted by d'. The area of the plane of the junction is 7.34×10^{-4} cm^2.

The zero field transition temperature of the aluminum film was determined by extrapolating the graphs V_p, I_p^{-1} and $(\sigma(0))^{-\frac{1}{2}}$ versus temperature. By Eqs. (35), (36), and (37) these quantities are linearly decreasing functions of temperature with intercepts at $T = T_c$. The three values of T_c determined in this manner were usually within 1 mK of each other. The region near T_c where nonlinear behavior was observed (see Fig. (14)) was not used in this extrapolation. T_c could also be determined from the resistive transition of the film, however as a consequence of the edges of the film not being scribed, the transition temperature obtained in this manner was approximately .1 K higher than that obtained from the extrapolation of V_p, I_p^{-1} or $(\sigma(0))^{-\frac{1}{2}}$.

TABLE I

Junction[a]	R_N (Ω)	R_D (Ω)	I_o (mA)	T_c (K)	d' (Å)	d (Å)	N (Ω-cm) X 10^{-6}	C (F) X 10^{-9}
Al-5	.069	3.75	2.4	1.751	2250	1280	5.8	15.6
Al-6	.1	8.64	1.7	1.765	2400	1300	7.5	31.9
Al-23	.451	280	1.2	1.860	2670	1600	3.81	61
Al2-5	.513	301	.9	1.800	2400	1240	3	79
Al2-36	.952	129	1.6	1.935	2250	1280	6	16
Al2-61	.5	360	.6	1.679	2475	1240	2.75	4
Al2-64	.39	81	2.6	1.786	2250	1280	1	4
Al2-79	.6	140	1.2	1.945	3000	1240	9	not measured

a Al-7 not shown here but similar to Al-6.

Film edges which are excluded from the junction by the masking, are responsible for the higher transition temperature. No conductivity measurements were made on films with scribed edges. A third possible method to determine T_c, is to use the temperature dependence of the zero-voltage current. For an asymmetrical junction, the zero-voltage current should approach zero with infinite slope at $T = T_c$. No junctions were observed to exhibit such behavior. Zero-voltage currents were found to approach zero with a finite slope, actually extrapolating to zero at temperatures from 3 to 7 mK higher than those determined from the extrapolations of the $T > T_c$ behavior. Also, a tail in the zero-voltage current was present above the extrapolated transition temperatures (see Fig. (14)). Possible mechanisms responsible for this tail, discussed in the next section, may also explain the linear temperature dependence of the zero voltage current noted below T_c. A detailed fit to the theoretical temperature dependence of the zero voltage current well below T_c was not carried out. This fit would probably have indicated a T_c in agreement with the T_c determined from the $T > T_c$ behavior.

The aluminum electrodes of the junctions were all disordered with transition temperatures in excess of the 1.2 K bulk transition temperature of aluminum. The enhancement of T_c is believed to be a consequence of the granular nature of the films. Various explanations

of the correaltion of T_c with the grain size have been proposed.[55] The most widely accepted, implies that the presence of free surfaces in the granular film lowers the phonon frequency, thereby increasing T_c relative to that of bulk material.[56] The understanding of the actual mechanism responsible for the coupling between grains and the enhancement of T_c is not necessary for the interpretation of the results of this work. However, it is important that the granular films behave as homogeneous "dirty-limit" superconducting films. This is thought to be the case for films with short conduction electron mean free paths as long as grain diameters are smaller than the temperature dependent coherence length $\xi(T)$.[57] As discussed in the next paragraphs, the aluminum films used in this investigation fall into this category.

Transition temperatures and resistivities of the films used were in the range expected for aluminum films with grain sizes the order of 100 Å.[58] Electron microscope studies of grain sizes of films were not carried out. However, such studies were made on a film prepared under the same conditions as used in the present investigation. This film was a granular film which was found to have an average grain size of around 100 Å.[59]

The Ginzburg-Landau zero temperature coherence length for these films is of the order of 520 ± 50 Å. This was determined by relating the shift in the transi-

tion temperature of the aluminum film in the presence of a dc magnetic field, to $\xi(0)$ through the relation

$$\epsilon(H,T) = \frac{T_c(H) - T}{T_c(H)} = \epsilon(0,T) - \frac{1}{3}\left[e^2 d^2 \xi^2(0)/(\hbar^2 c^2)\right] H^2 \qquad (55)$$

The transition temperature in the presence of a magnetic field was easily determined from the dependence of the peak voltage on temperature in the vicinity of $T_c(H)$. When the temperature was reduced below $T_c(H)$, the temperature dependence of the slope of V_p versus T changed sign as a consequence of the change in sign of $\epsilon = \frac{T - T_c(H)}{T_c(H)}$. This point was defined as $T_c(H)$ (see Section IV-C). The values of $\xi(0)$ determined with Eq. (55) are also consistent with the coherence length calculated from the data for $T > T_c$ by using the relation for the peak frequency derived by Shenoy and Lee (Eq. (51)):

$$\omega_p = \Gamma_0\left(1 + q^2\xi^2(T) + \frac{1}{3}\left(\frac{2e}{\hbar c}\right)^2 \left(\frac{d}{2}\right)^2 \xi^2(T)\right) . \qquad (56)$$

The mean free path was estimated to be about 20 Å by using the "dirty-limit" value for the temperature dependent coherence length (Eq. (8)):

$$\xi(T) = .85\left(\xi_0 l\right)^{\frac{1}{2}} (\epsilon)^{-\frac{1}{2}},$$

with the BCS coherence length $\xi_0 = 16000$ Å and the Ginzburg-Landau coherence lenth $\xi(0) = 520$ Å. Thus the aluminum films used in this work should behave as homogeneous "dirty-limit" superconductors.

The critical field $H_{c2}(0)$ was not determined experimentally for any of the films studied, but would be expected to be the order of 1000 Oe based on results from films of similar thickness, coherence length and grain size.[57]

Transverse junction dimensions, .271 X .271 mm, were small compared to the Josephson penetration depth so that spatial inhomogeneities of the current flow pattern across the junction would not be expected.[60]

Thicknesses of the lead electrode were large in comparison with the penetration depth of lead so that the modification of the wave vector q, due to a variation of the field in the film is negligible (see Eq. (21)).

B. DATA FOR $T > T_c(H)$

B.1 Zero Field Results

In this section we present experimental excess current-voltage characteristics obtained in the temperature regime between the transition temperatures of the two electrodes of the junction. According to Eq. (24) this current is a direct measure of the pair-field susceptibility of the aluminum electrodes and enables us to critically probe the behavior of fluctuations above T_c. We have carefully examined the temperature and magnetic field dependence of the excess current. The result and comparison to theory are described in this section.

Figure (8) shows typical excess current-voltage characteristics obtained at several different temperatures in zero magnetic field. The points are experimental data and the solid line is the theoretical excess current determined by using the experimental values of I_p and V_p in Eq. (34). The difference between the experimental and theoretical curves at high voltages is a consequence of neglecting the small contributions of the pair-current to the total tunneling current in the range of voltages over which the parameters that characterize the quasiparticle current are determined. The resultant discrepancy between experiment and theory can be removed by carrying out an iteration of the analysis. The theory is used to calculate the pair current in the region of the I-V characteristic where the parameters of the quasiparticle current are determined. A corrected quasiparticle current can then be obtained and the whole fitting and subtraction procedure can be repeated. Since the values of the peak voltage and peak current were not significantly shifted by the small changes in the subtracted quasiparticle current resulting from the above analysis, this procedure was carried out only at a few selected temperatures. With the corrections, the various curves are in excellent agreement with the quasi-Lorentzian shape. It should be noted that the quasi-Lorentzian dependence of the excess current on voltage was observed qualitatively at temperatures as high as 1 K above T_c in some samples. However,

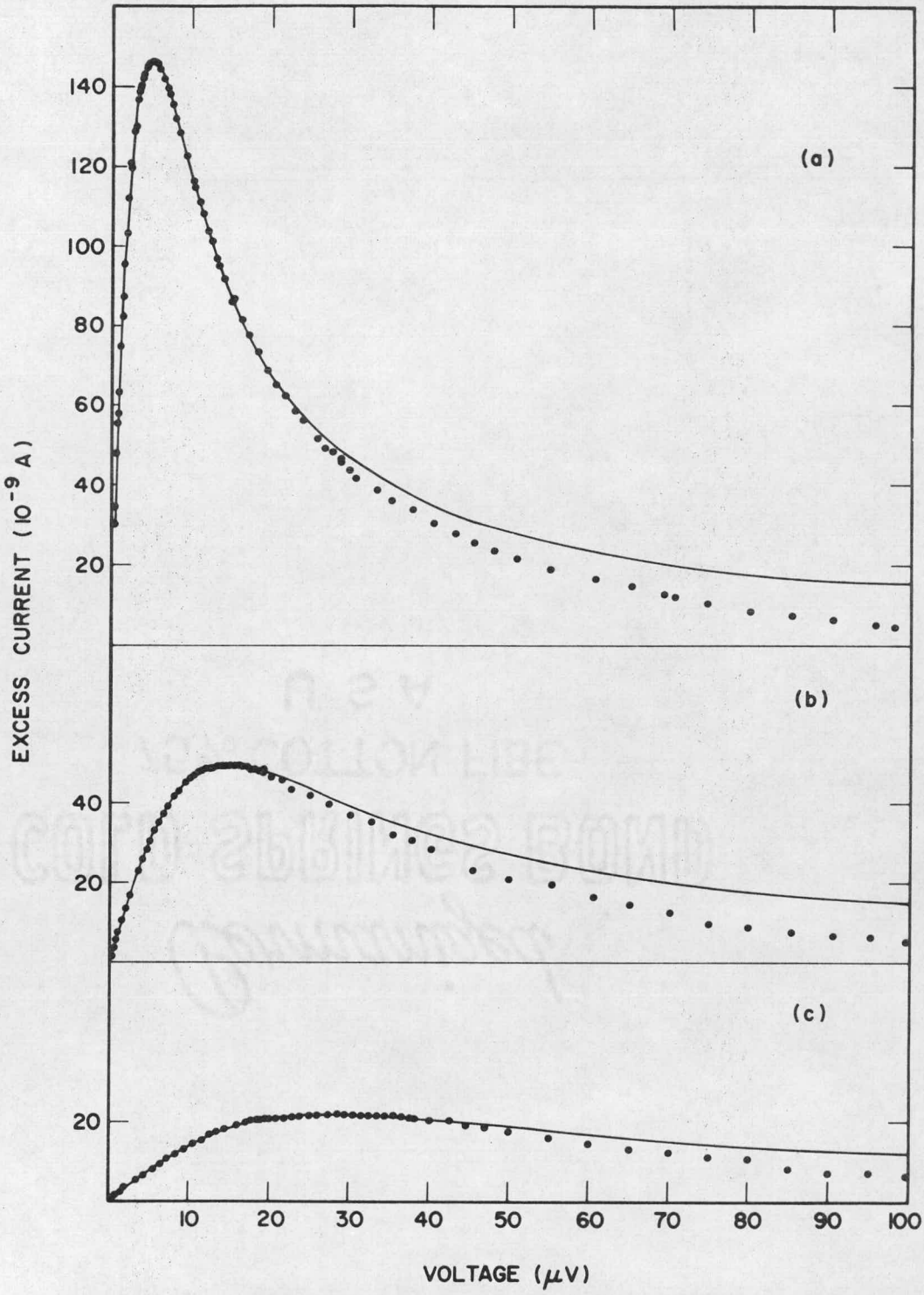

Fig. (8) Excess current-voltage characteristics of junction A12-5. Curves (a) - (c) correspond to T = 1.84726, 1.93276 and 2.09892 K. respectively. Solid line is computed from V_p and I_p using Eq. (34). The deviation at high voltages can be corrected by a model dependent analysis.

at the higher temperatures the excess current is such a small percentage of the total tunneling current that quantitative measurements are difficult. In this regime small errors in the determination of the quasiparticle current have large effects on the excess current obtained using the subtraction procedure.

Shown in Figs. (9) and (10) is the dependence of V_p on T, for samples Al-6 and Al2-64. The region near T_c is not accessible to experimental measurements because of the previously mentioned negative resistances which are found there. The dashed line in the figures is the theoretical value of the peak voltage, proportional to the relaxation frequency calculated from Eq. (35). Quantitative measurements of the peak voltage were carried out on junction Al2-5 to temperatures 250 mK above T_c with no departures from a linear dependence on temperature observed, except for the region near T_c. Equation (35) predicts a theoretical slope of $\frac{dV_p}{dT} = 1.098 \times 10^{-4}$ V/K dependent only on fundamental constants. The experimental slopes shown in Table II, are in good agreement with the theoretical predictions. Data from the first sample, Al2-5, was taken only in the nonlinear region close to T_c which explains the large value of the slope. The value of T_c for this junction given in Table I is also suspect since the extrapolation to find T_c from V_p versus T was also carried out using only data in the nonlinear region. As can be clearly seen from the data of the later samples, an extrapolation

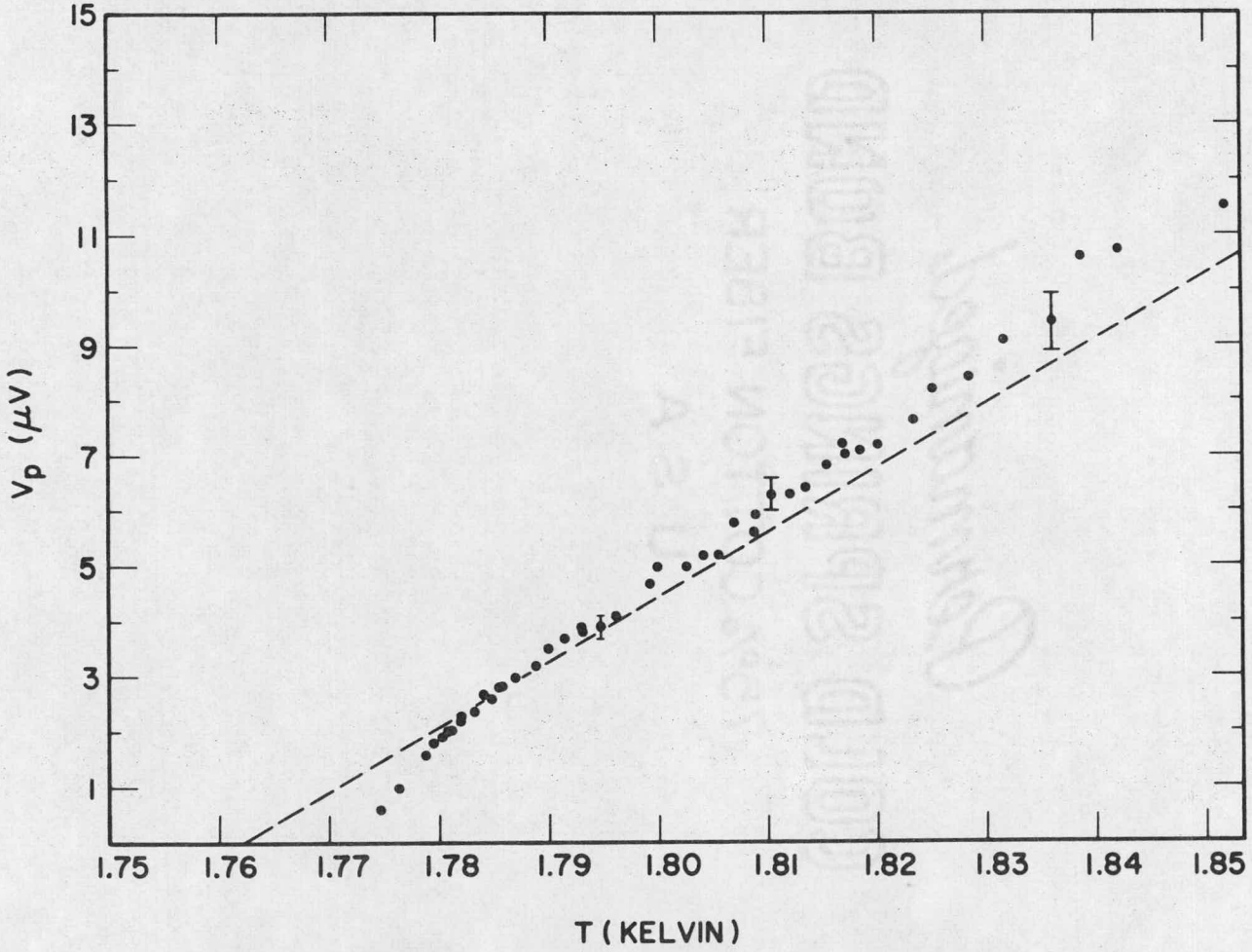

Fig. (9) Peak voltage V_p versus T for Al-6 in zero field. The dashed line is determined from theoretical value of the relaxation frequency.

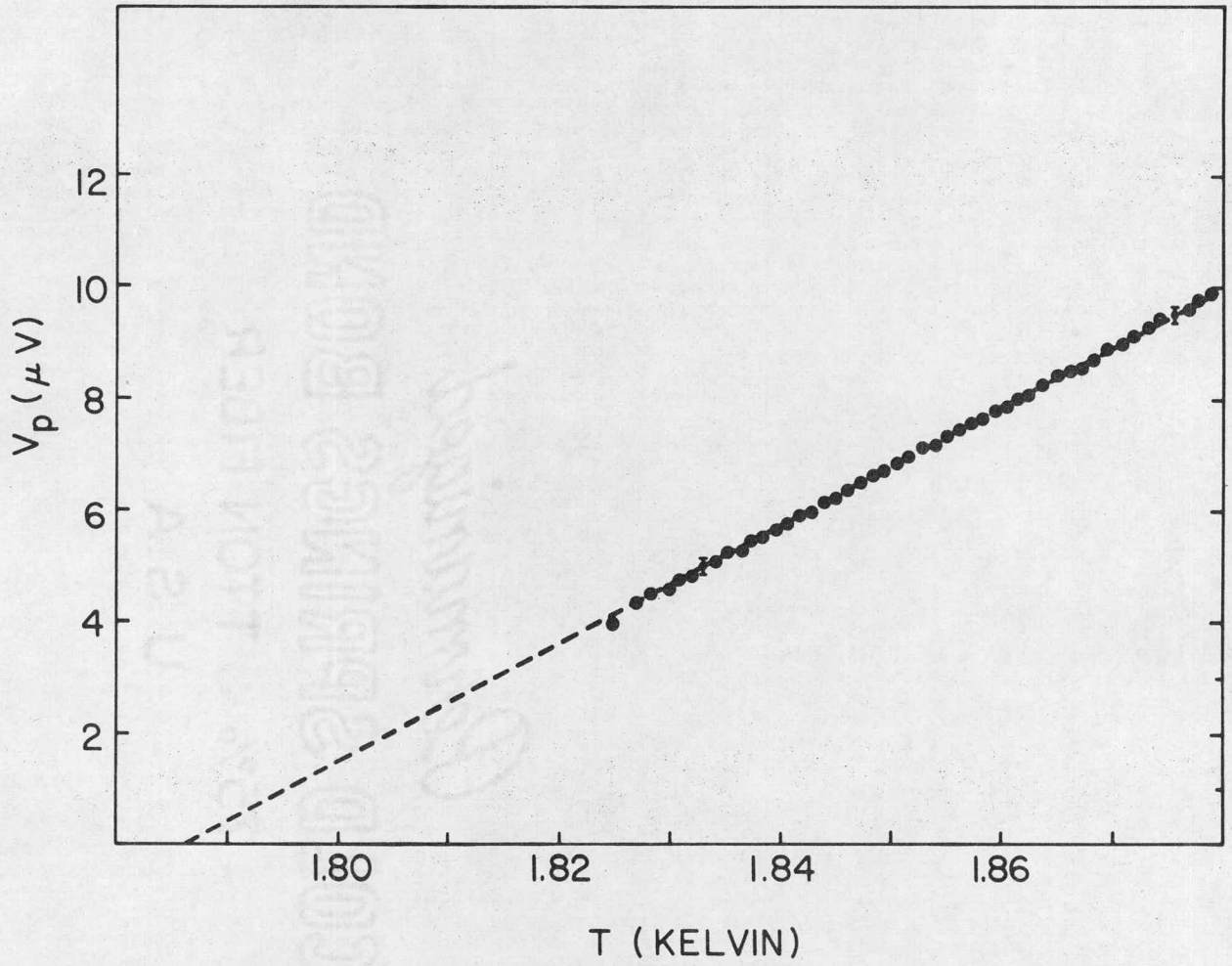

Fig. (10) V_p versus T for Al2-64 in zero field. Dashed line is theory.

TABLE II

Junction	dV_{p}/dT (V/K) $\times 10^{-4}$	dI^{-1}_{p}/dT (A^{-1}/K) $\times 10^{7}$		$d\sigma^{-\frac{1}{2}}/dT$ ($\Omega^{\frac{1}{2}}$)	
	Exp. [a]	Exp.	Theory	Exp.	Theory
Al-5	2.8 ± .4	5.07 ± .1	7.1	47 ± 2	63.3
Al-6	1.26 ± .2	.5 ± .08	2.45	52 ± 2	37.1
Al-23	.85 ± .2	15.0 ± 15	58	265 ± 10	185
Al2-5	1.026 ± .05	18 ± 1	26	91 ± 1	123
Al2-36	1.066 ± .03	45.5 ± 1.2	74.4	147 ± 1.3	199
Al2-61 [b]	.98 ± .06	72 ± .8	105	172 ± 2	238
Al2-64	1.069 ± .03	12 ± .05	29.6	63 ± .5	129
Al2-79	1.099 ± .01	42 ± .05	72	not measured	

a The experimental values were determined by a linear least squares fit to the linear portion of the data.

b Only limited data was taken on sample Al2-61.

from the nonlinear region will not give the correct T_c. The nonlinear behavior near T_c will be discussed at the end of this section.

The quantity dV_p/dT was determined more accurately for junctions Al2-64 and Al2-79 than for the earlier junctions. The reason for this was that after the experimental results for junction Al2-36 were published it was suggested that the aluminum films used in this work might be characterized by a rather large depairing parameter ρ.[37] The manifestation of depairing above T_c is a shift in the position of the peak in the excess current from that given by Eq. (35) to a form given by Eq. (88). The slope of V_p versus T would directly reflect this change. This motivated the extensive measurements of the temperature dependence of the peak voltage above T_c which were made on samples Al2-64 and Al2-79, to obtain an accurate result for dV_p/dT.

Equation (52) gives the expression for the temperature dependence of V_p, if the transmission of electrons across the barrier were diffuse in nature rather than specular. In the short mean free path limit Eq. (52) becomes

$$V_p = \frac{\Gamma_o}{2e} \left(1 + \frac{\xi(T)}{l}\right)^{\frac{1}{2}}, \qquad (57)$$

which is inconsistent with the experimental observations. Thus we conclude that the experimental results can be

taken as evidence that the dominant tunneling process involves specular transmission of electrons across the barrier rather than diffuse transmission.

In Figs. (11) and (12) the inverse of the peak current, I_p^{-1} is plotted as a function of temperature for samples A1-6 and A12-64. Except in the region close to T_c, I_p^{-1} is a linear function of temperature as predicted by Eq. (36). This linearity was observed in sample A12-5 out to $T - T_c = 250$ mK. The dashed line is drawn in the figures to indicate the linearity and to determine T_c. Table II contains the experimental values of dI_p^{-1}/dT for the junctions analyzed along with the theoretical value expected from Eq. (36). For most junctions the experimental value is only in qualitative agreement with theory. That this is true is not surprising, since the calculation of dI_p^{-1}/dT from theory depends on values of junction parameters which are imprecisely known. The errors in d, R_N and N(0) are probably large enough to account for the discrepancy between theory and experiment in most cases.

Except for junction A1-23, the experimental peak current is larger than the theory predicts. It is possible that this is due to locally thin regions of the insulating barrier resulting in an anomalously large excess current.

The experimental behavior of the inverse peak current in the region near T_c in which nonlinear effects are observed in the peak voltage is not repro-

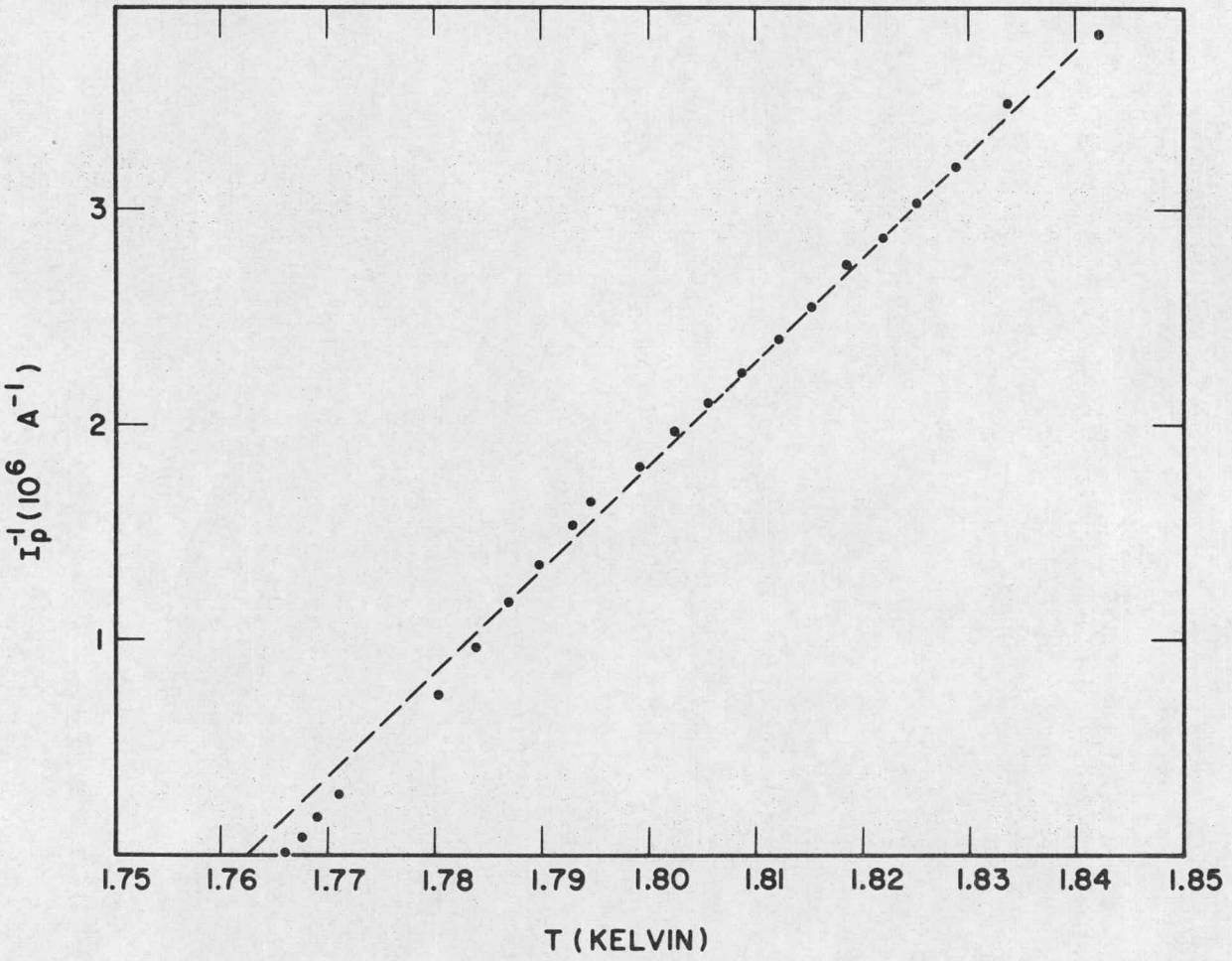

Fig. (11) Inverse peak current I_p^{-1} versus T for Al-6. Errors in the determination of I_p^{-1} are approximately .2 X 10^{+6} A^{-1}. The dashed line is to indicate linearity and determine T_c.

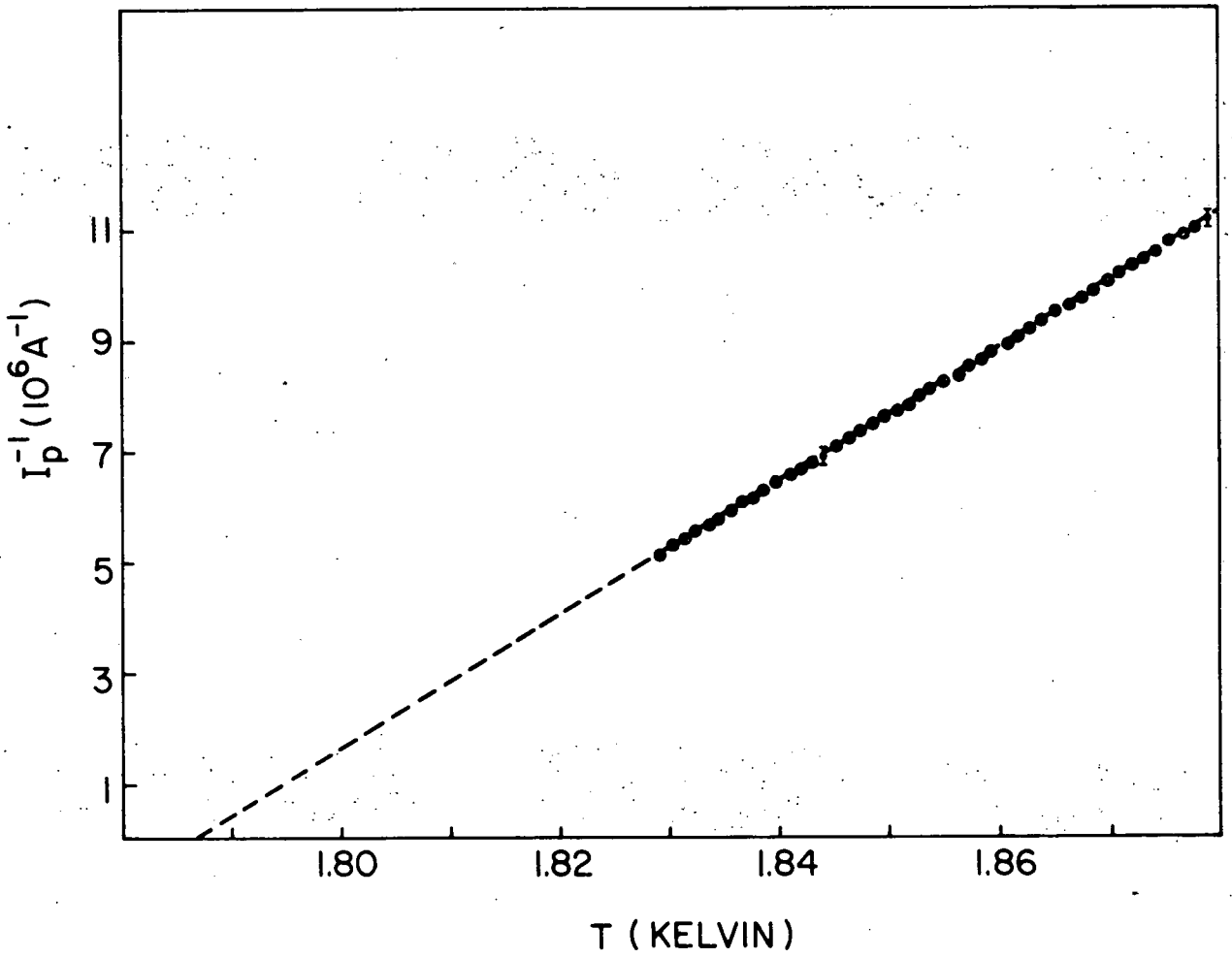

Fig. (12) I_p^{-1} versus T for A12-64. The dashed line indicates linearity and determines T_c.

ducible. In some junctions I_p^{-1} appeared to rise as T was decreased and in others it appeared to fall off with decreasing T, before the negative resistance region was reached.

Figures (13) and (14) show the variation of the reciprocal of the square root of the conductance in the limit of zero voltage, as a function of temperature, for junctions Al-6 and Al2-5. It should be noted that the data in Fig. (14) is a linear function of temperature over almost 500 mK. The dashed line in Fig. (13) is drawn to indicate linearities. In Table II the experimental values of the slope in the linear region of this plot, are listed and compared with theoretical values calculated from Eq. (37). Again the agreement is only qualitative, due to the imprecise knowledge of the parameters characterizing the aluminum film and the junction.

It is important to note that although the values of the slopes listed in Table II do not agree well with theory (except dV_p/dT) for a particular sample, they are completely consistent. Once the magnitude of the peak current is determined at a particular temperature, it is possible to show that the excess current-voltage characteristic and the values $\sigma(0)$ and I_p at all other temperatures, are consistent with theory.

The conductivity at zero voltage can be measured in the nonlinear region close to T_c where the peak current

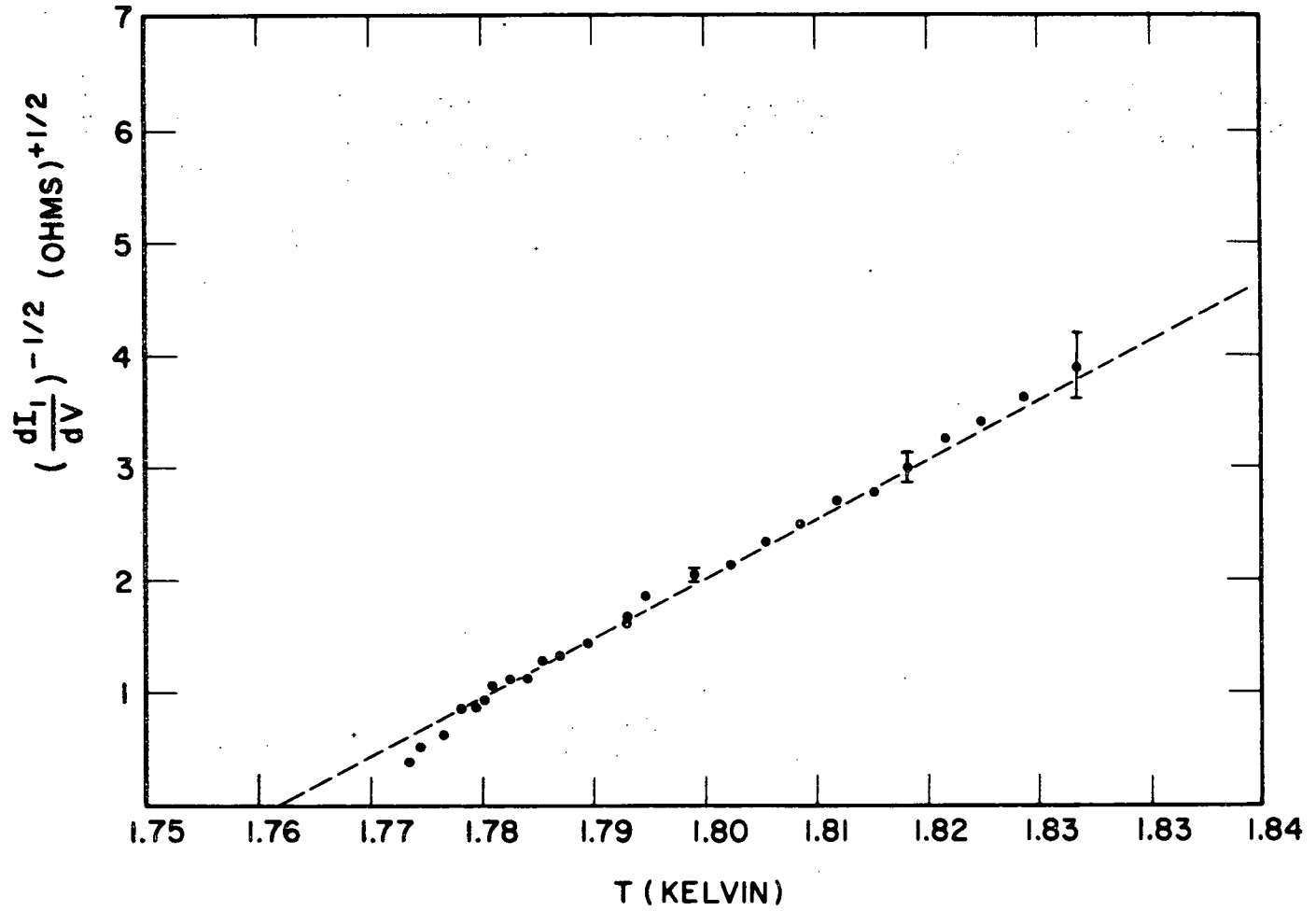

Fig. (13) $\sigma(0)^{-\frac{1}{2}}$ versus T for Al2-6. Dashed line indicates linearity and determined T_c.

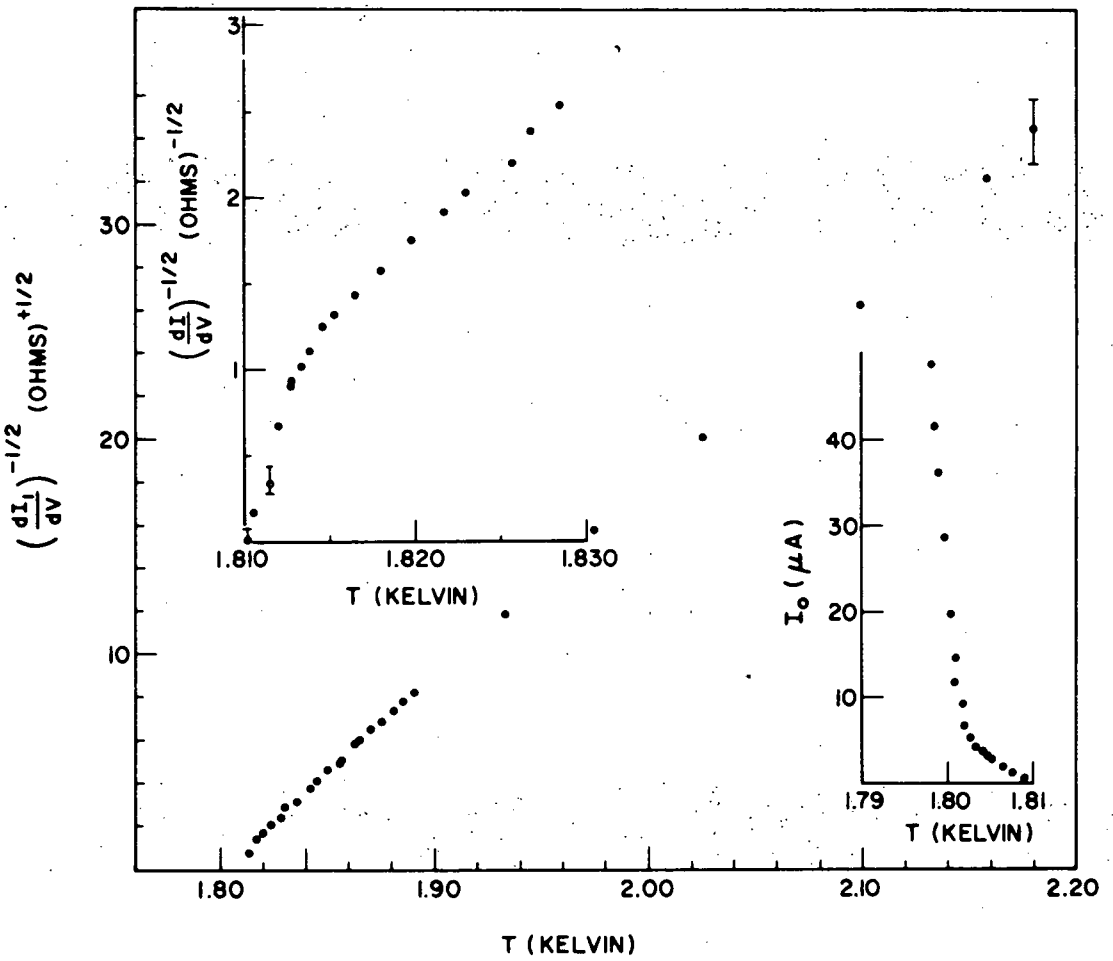

Fig. (14) The main figure shows $\sigma(0)^{-\frac{1}{2}}$ versus T for Al2-5 over the entire temperature range covered. The left insert shows the departure close to T_c from a linear temperature dependence. The right insert shows the behavior of the maximum zero voltage current near the transition temperature of 1.800 $\pm$ .001 K.

and peak voltage are inaccessible because of the negative resistances. The left insert in Fig. (14) shows the departure from linearity for sample A12-5 near T_c. Shown in Figs. (15) and (16) is the conductance for A12-36. The second figure is a log-log plot of the conductance as a function of $\epsilon = (T - T_c)/T_c$ where T_c has been chosen to be 1.9335° K. The linear region for large ϵ has a slope of -2, as expected from theory. If a line is drawn through the data for small ϵ, a slope of -6 is obtained. The value of this latter slope cannot be taken too seriously since it is highly dependent on the choice of the transition temperature.

As the temperature is reduced towards T_c the conductivity appears to become infinite above T_c and a zero voltage current appears. (The minimum detectable voltage drop across the junction is less than 1 nanovolt.) This effect is illustrated in the right insert in Fig.(14) where the temperature dependence of the apparent zero voltage current is plotted. Only for $T < T_c$ ($T_c = 1.800^{\circ}$K) does the zero voltage current increase rapidly. The infinite value of $\frac{dI_p}{dT}$ at $T = T_c$, expected for asymmetrical junctions was never observed in any of the junctions investigated. Though the current that is present in the temperature range from 1.80 to 1.81 K in sample A12-5 appears to be a zero voltage current, the maximum value of the current does not exhibit a well defined quasi-periodic diffraction pattern in a magnetic field that would be expected of a zero voltage Josephson current.

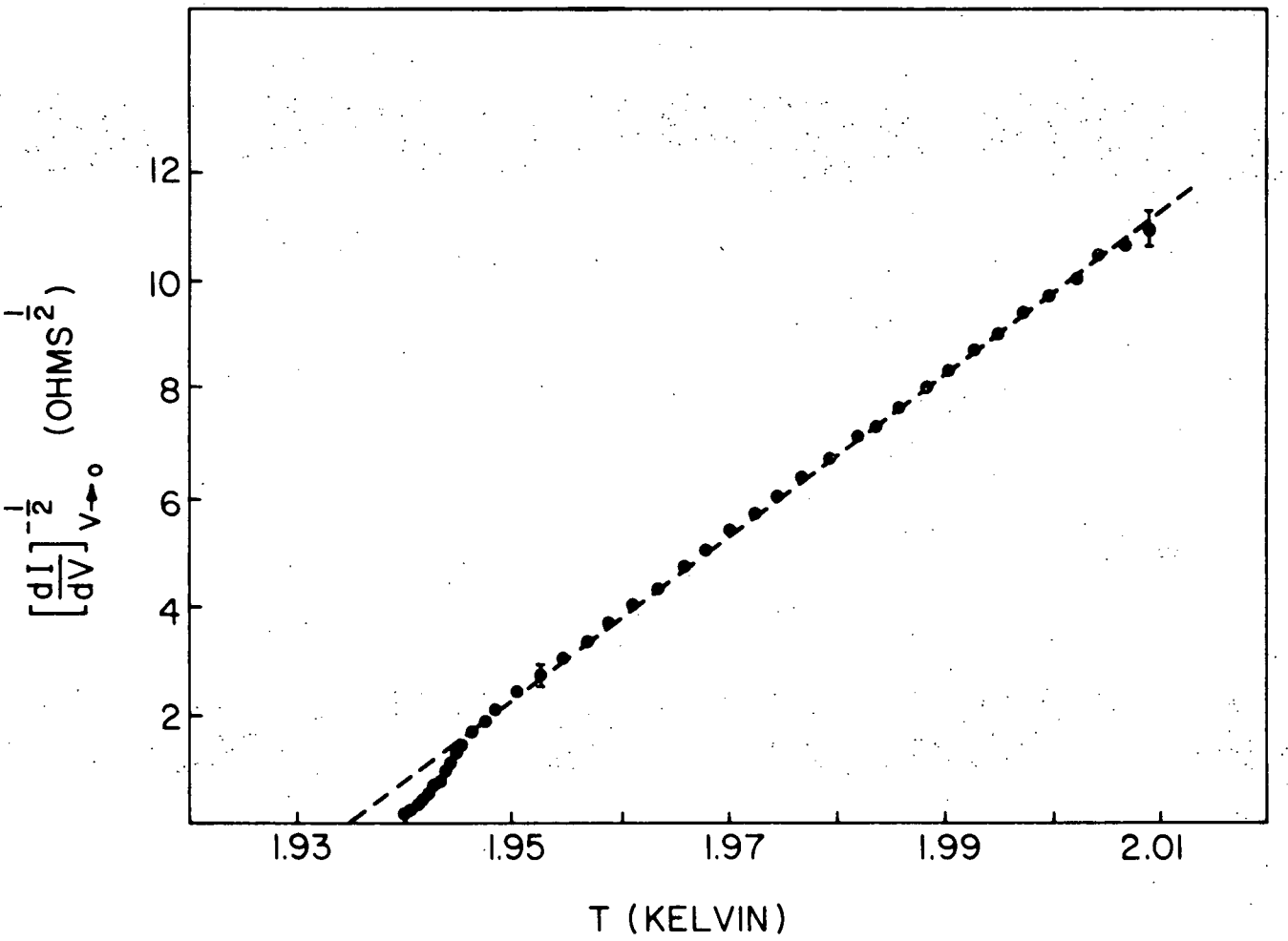

Fig. (15) $\sigma(0)^{-\frac{1}{2}}$ versus T for Al2-64.

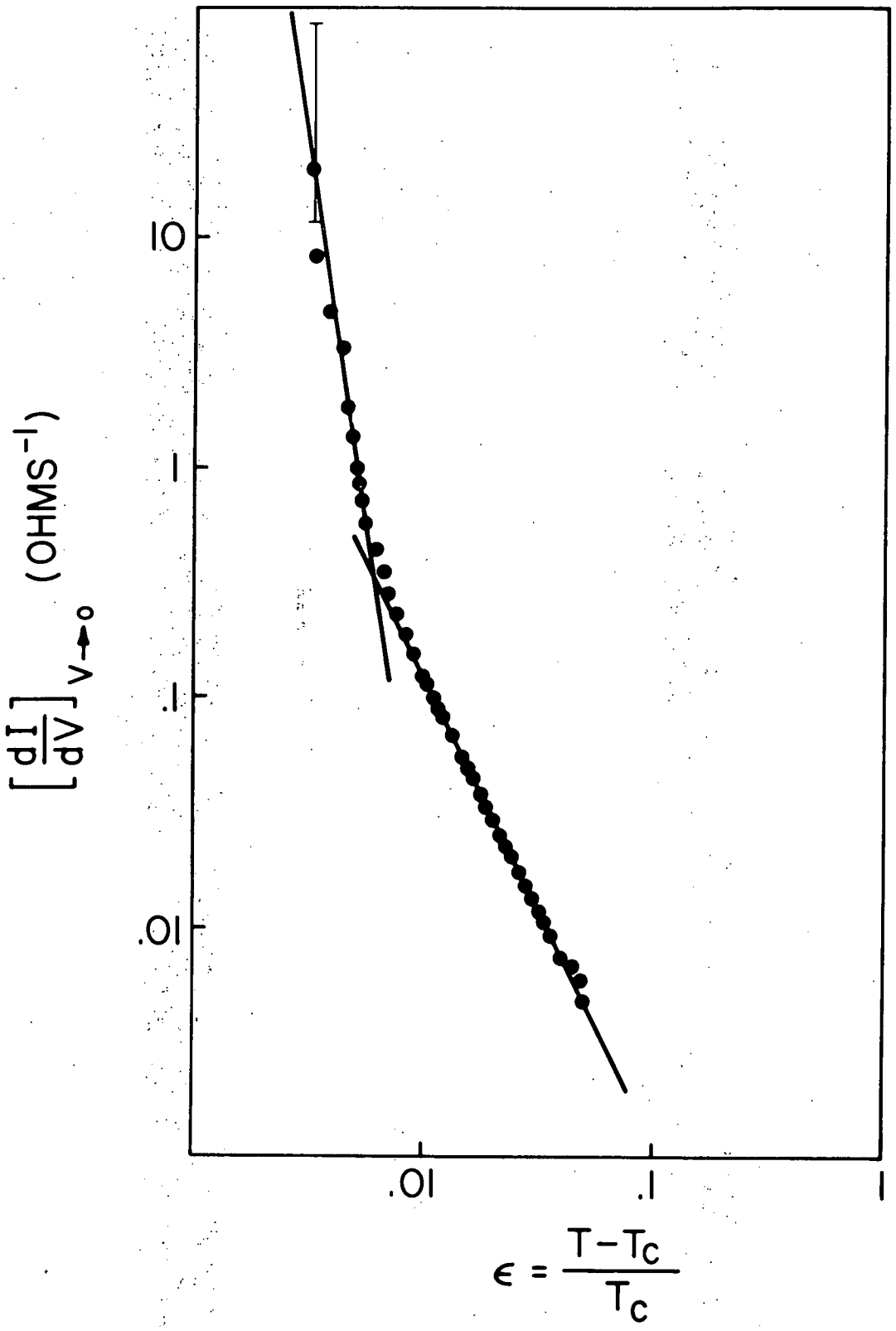

Fig. (16) $\sigma(0)$ versus ϵ for Al2-64. $T_c(0)$ has been chosen to be 1.9335 K. The slopes of the solid lines are -6 and -2 for small and large ϵ respectively.

To conclude this section on the zero magnetic field results, we consider some of the mechanisms which may be responsible for the drop in the relaxation frequency and increase in the static conductivity in the immediate vicinity of T_c and which also may account for the appearance of a zero voltage current above the extrapolated transition temperature of the aluminum film. One such mechanism which is suggested by the tail in the temperature dependence of the zero voltage current above T_c is the possibility of local regions of higher transition temperature occuring in the area of the aluminum film sampled by the junction. If the distribution of T_c's about an average transition temperature $\overline{T_c}$ is highly peaked, then variations in T_c would be of no consequence to the excess current-voltage characteristic far above $\overline{T_c}$. These contributions would be expected to be quasi-Lorentzians with slightly shifted resonances and significantly reduced magnitudes if the areas of such regions were a small fraction of the total junction area. However, when the temperature is reduced below one of the higher transition temperatures, a small zero voltage current could result. The quasiperiodic dependence of the maximum current might not be evident because of the small linear dimensions of the regions of higher transition temperature (see Eq. (28)). Only when T was reduced below $\overline{T_c}$ would the magnetic field dependence of zero voltage current behave as that of a Josephson junction because only then would there be phase coherence

across the entire junction. For most junctions, the onset of the tail in the zero voltage current was from 5 to 15 mK above the extrapolated T. Variations in T_c of this magnitude may not be unreasonable. In all of the junctions studied, there was no indication that the excess current-voltage characteristic far above T_c did not agree well with the predictions of Scalapino, so that if there were regions of varying T_c they were a small fraction of the total junction area. The above conjecture could also explain the fall off of both V_p and $(\sigma(0))^{-\frac{1}{2}}$ from a linear variation with temperature near T_c, since the extra conductivity near T_c could be due to weakly coupled Josephson junctions near their transition temperatures. Additional evidence that the behavior near T_c could be a result of Josephson tunneling current, is the data taken in a magnetic field. In magnetic fields of the order of 25 Oe, which are large enough to destroy the Josephson phase coupling, no drop in V_p or $(\sigma(0))^{-\frac{1}{2}}$ versus T was noted in the vicinity of $T_c(H)$. This suggests that the fall-off in zero magnetic field may be due to coherent pair transfer which is suppressed by a magnetic field. These arguments should be treated as conjectures as there may be other explanations for highly magnetic field dependent behavior. At present there does not seem to be any critical test of the hypothesis that these effects are a consequence of a spread in the transition temperatures of the aluminum films.

A suggestion by Šimánek and Walker[40] that the nonlinear behavior is a consequence of the nonuniform coupling across the junction is not satisfactory. Assuming a modulation of the junction coupling energy of the form $(1 + a \cos q_o x)$, they show the susceptibility to be of the form

$$\mathrm{Im}\,\chi(\omega,q) \propto \frac{\omega}{\Gamma_o^2 + \omega^2} + \tfrac{1}{2} a \frac{\omega}{\Gamma_o^2(1 + \xi^2(T) q_o^2)^2 + \omega^2} .$$

The resonance is at

$$V_p \underset{\epsilon \to 0}{=} \frac{\hbar \Gamma_o}{2e} \left(1 + \frac{a^2}{\xi(0)^4 q_o^4} \epsilon^2\right) \qquad (58)$$

For small ϵ this model predicts a peak voltage that is larger than the theoretical value opposite to the behavior which is observed experimentally.

In a more realistic calculation, the regular coupling energy variation described by a single q_o would be replaced by a distribution of q_o's. This would lead to a broadening of the excess current-voltage characteristics from the quasi-Lorentzian shape. Since the data fits a single quasi-Lorentzian for $T > T_c$, the proposed explanation is probably not correct.

Another possible source of nonlinear behavior near T_c which should be considered, is that the theory may break down when ϵ is small because of critical behavior. For two reasons it seems highly unlikely that this

mechanism is responsible for the observed nonlinearities. First, estimates of the width of the critical region for this system are usually an order of magnitude smaller than the temperature interval over which nonlinear effects are observed. Second, as Ferrell[4] has shown, inclusion of the fourth order term in the free energy functional tends to suppress fluctuations and postpone the onset of the phase transition in the tunneling junction. This is equivalent to the relaxation frequency, decreasing less reapidly with temperature in the critical region than in the high temperature limit. This is opposite to what is seen experimentally; the phase transition in some respects is occuring at a higher temperature than that which would be inferred from an extrapolation of data taken at high temperatures.

It has also been suggested that the change in the character of the data near T_c is due to a change in the nature of transmission of electrons across the barrier from specular to diffuse transmission.[42] If the transmission were diffuse, then the reciprocal of the dynamic conductance rather than the square root of the reciprocal would vary linearly with temperature. However, this does not appear to be borne out by the data in the vicinity of T_c (see Fig. (16)).

Finally we consider the suggestion that the proximity effect may be associated with the behavior near T_c. In fact, the excess current observed above T_c

can be thought of as resulting from a type of proximity effect in which the Josephson phase coupling energy between the pair-field of the lead film and the fluctuating pair-field in the aluminum film induces a finite value of the order parameter in the aluminum film above T_c. Ferrell and Scalapino[61] have derived the excess current by writing the free energy as

$$F = F + a \left|\psi\right|^2 - \lambda \left|\psi\right| \cos \phi , \qquad (59)$$

and using a form of the time-dependent Ginzburg-Landau equation

$$\frac{\partial \vec{\psi}}{\partial t} = - \gamma \vec{\nabla}_{\psi} F + \vec{V} \times \vec{\psi} , \qquad (60)$$

where ψ is treated as a vector in the two dimensional space spanned by its real and imaginary parts. The excess current which flows across the junction is then given by

$$J = \frac{\lambda^2}{a^2} \frac{V/V_o}{1 + (V/V_o)^2} . \qquad (61)$$

This result is equivalent to Eq. (33) derived by Scalapino. In the above equations γ is a parameter describing the relaxation of the order paramter, $-\lambda \left|\psi\right| \cos \phi$ is the Josephson coupling energy, $\bar{V} \times \vec{\psi}$ describes the effects of a voltage V on ψ, and $V_o = a \gamma$.

In "conventional" proximity effect experiments,[62] a normal metal N is deposited on top of a superconducting metal S. If the electrical contact is good, Cooper pairs can leak from S to N and N may take on superconducting properties. If N is a superconductor, its transition temperature is raised as a consequence of S, while the transition temperature of S is lowered because of N. With good electrical contact, the proximity effect is comparatively long range. The penetration depth of the pair-field of S into N is of the order of 10^3 Å. However, if there is a thin insulating layer between N and S, the Cooper pair density or pair-field decays very rapidly in the layer and a proximity effect usually is not observed. In the insulating layer a reasonable form for the wave function is exp - (k_f x), a barrier of only 10 Å thickness will reduce the Cooper pair density by e^{-20}, whereas with no oxide, the pair-field in the normal metal will have only dropped by a few percent at 10 Å into the normal metal.

Although a "conventional" proximity effect occuring across an oxide layer would thus be very weak, it would tend to raise the transition temperature of the aluminum film.

In order to explain some of the effects seen in this investigation near T_c, it may be argued that when the temperature is far away from T_c the effect proposed by Scalapino dominates the behavior and the film appears

to have a transition temperature T_c. When T approaches T_c, the conventional proximity effect might become large enough to produce an observable shift to a higher transition temperature. This conjecture is not yet supported by detailed calculations of a proximity effect of this type in junctions.

Evidence that may possibly rule out the proximity effect is that there is apparently no correlation between the width of the temperature range over which V_p and $(\sigma(0))^{-\frac{1}{2}}$ fall below theoretical predictions and the magnitude of the low temperature Josephson current. If the proximity effect acting across the oxide layer were responsible for the apparent shift in T_c, one would expect the magnitude of the shift to depend on the strength of the tunneling interaction. The latter would be proportional to the magnitude of the low temperature Josephson current.

We thus conclude by stating that at the present time it is not clear as to the origin of the behavior in the immediate vicinity of T_c. It may be a consequence of one or a combination of the above mentioned mechanisms or some other mechanism not considered.

B.2 Finite Field Results for $T > T_c(H)$

The magnetic field dependence of excess current-voltage characteristics for junction A12-5 is shown in Fig. (17) along with the field dependence of the inverse

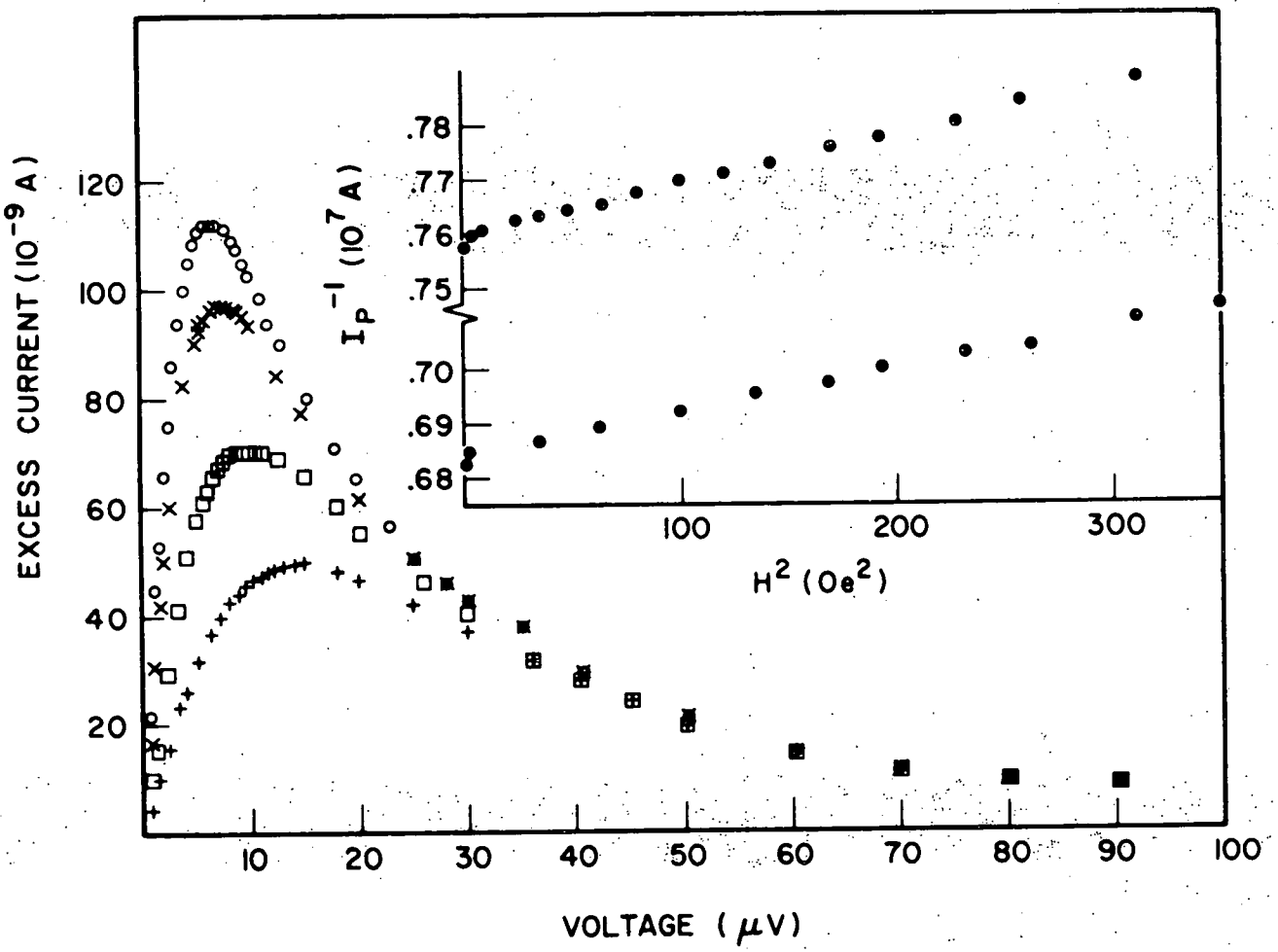

Fig. (17) The main figure shows the excess current-voltage characteristics in several magnetic fields at a constant temperature. T = 1.86015 K for Al2-5. The curves labeled 0, X, □, and + correspond to H = 0, 40.8, 81.3 and 122 Oe respectively. The insert of I_p^{-1} versus H^2 at T = 1.85202 K (upper) and T = 1.84726K(lower).

peak current. The excess current-voltage characteristics are quantitatively identical to the quasi-Lorentzian shape in zero magnetic field. The fit to Eq. (34), using the values of I_p and V_p is in excellent agreement with the experimental data. For small magnetic fields, Eq. (50) predicts the same quasi-Lorentzian shape for the excess current-voltage characteristic.

Both Eqs. (37) and (51) predict a linear temperature dependence of the relaxation rate for finite q values. This is shown in Fig. (18) for sample Al2-36. The theoretical slope, $^{dV}p/dT$ is independent if H and is identical to the zero field result. For larger fields, the slope of V_p versus T is modified by a term dependent on the pair breaking parameter ρ. These effects are small for the magnetic fields used in this work.

Shown in Fig. (19) is the dependence of the peak voltage on H^2 at several temperatures for junction Al2-36. Equation (37) predicts linear dependence of V_p on H^2 for all fields while Eq. (51) is linear, only for small fields. The slope of the linear region differs in the two cases since in Eq. (37) the shift in T_c due to the magnetic field has been neglected while it is included in Eq. (51). For this reason, the latter equation is used for the comparison of data to theory. Using $\xi(0) = 540$ Å, d = 1280 Å and $\lambda' = 390$ Å, we have determined $^{dV}p/dH^2$ according to Eq. (51) to be

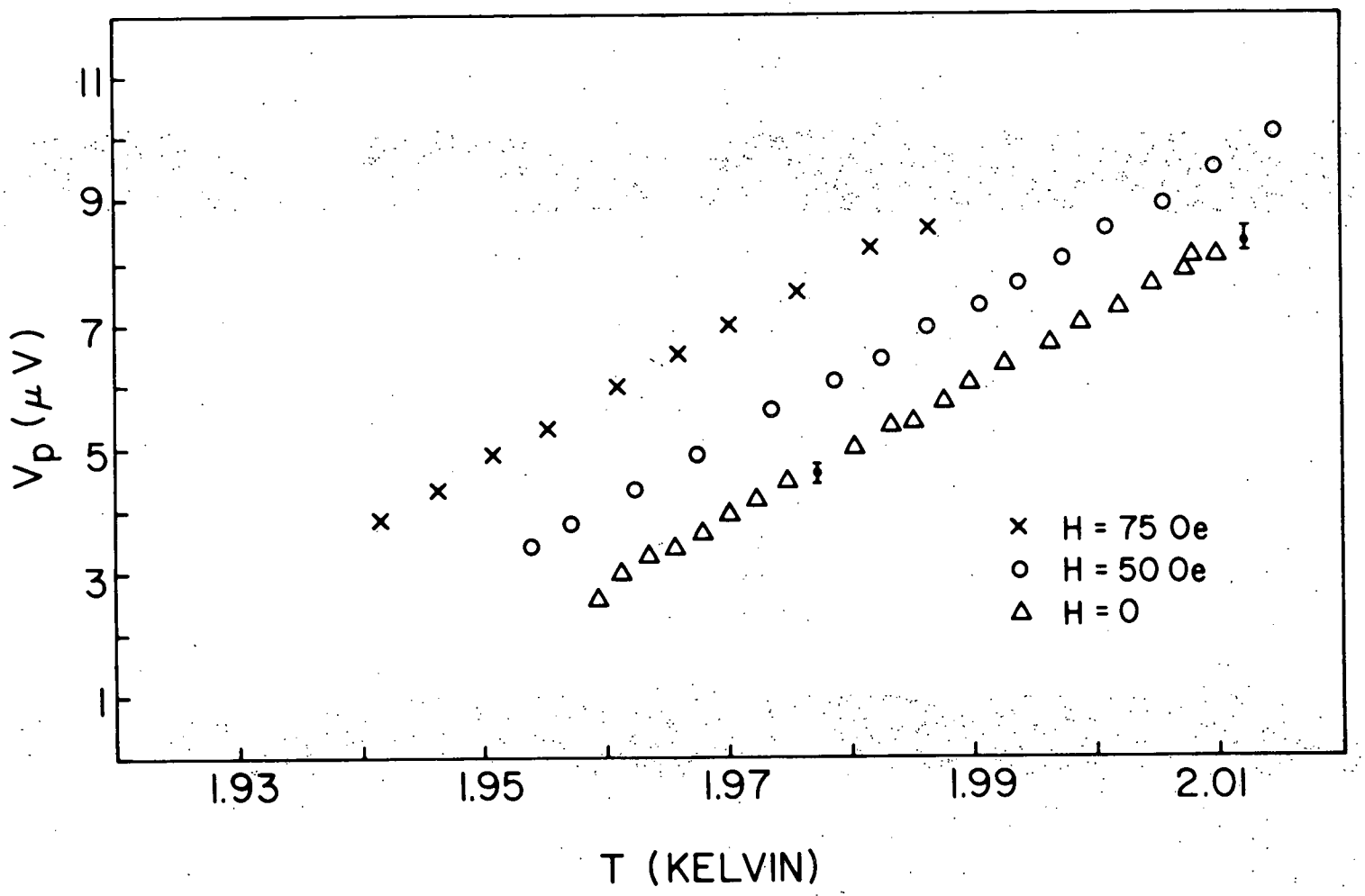

Fig. (18) V_p versus T for A12-36 in several fields. The slopes are $1.066 \pm .03 \times 10^{-4}$, $1.08 \pm .04 \times 10^{-4}$ and $1.05 \pm .04 \times 10^{-4}$ V/K for H = 0, 50 and 75 Oe, respectively.

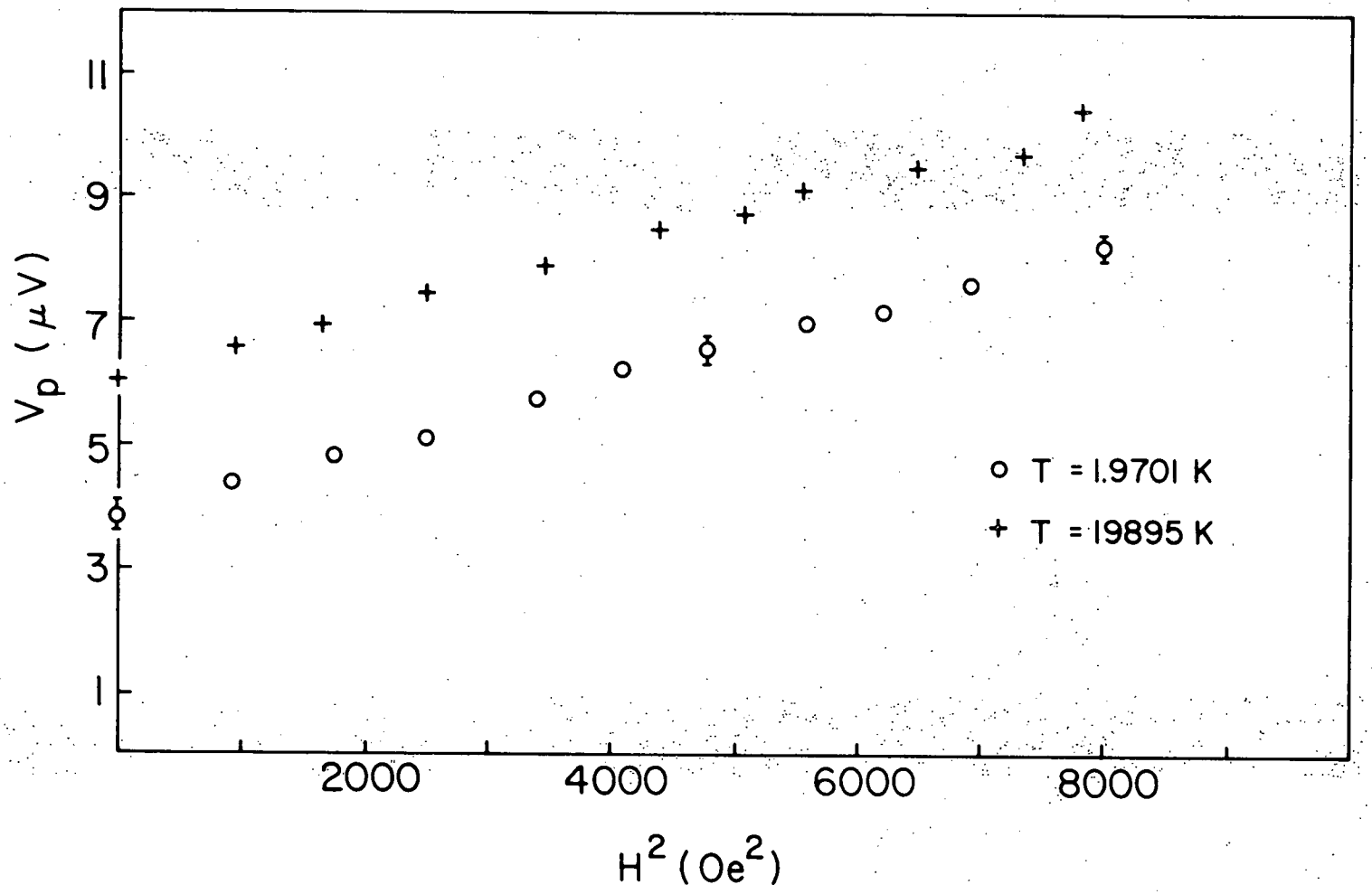

Fig. (19) Dependence of V_p on H^2 for A12-36.

$5.98 \pm .6 \times 10^{-10}$ V/Oe^2. Slopes calculated from the data in Fig. (19) are $5.63 \pm .3 \times 10^{-10}$ and $5.375 \pm .3 \times 10^{-10}$ V/Oe^2 for T = 1.9701 and 1.9895 K respectively. It is important to note the slope calculated from Eq. (75) is highly dependent on the choice of $\xi(0)$. The insert in Fig. (17) shows the expected linear variation of I_p^{-1} with H^2 for small magnetic field. Slopes determined from the data are 845 (upper) and 797 $A^{-1}Oe^{-2}$ (lower) compared to 880 $A^{-1}Oe^{-2}$ from theory.

The abrupt increase in I_p^{-1} as the magnetic field is initially applied, shown in Fig. (17) is not understood and is an effect which was only seen in this sample.

To critically test the theory of Shenoy and Lee, the nonlinear high field region of V_p versus H^2 must be investigated. The solid line in Fig. (20) is the predicted behavior of Eq. (51) for large H. The coherence length has been adjusted to $\xi(0) = 546$ Å to give the correct experimental slope for small H. The agreement between theory and experiment is only qualitative because of the uncertainty in determining the value of the peak voltage when the magnetic field is high.

Although the agreement with theory is only qualitative, the deviation of the data at high field from the linear dependence on H^2 is a real effect. This result is important because it is a qualitative feature of the data whose explanation depends on the idea that

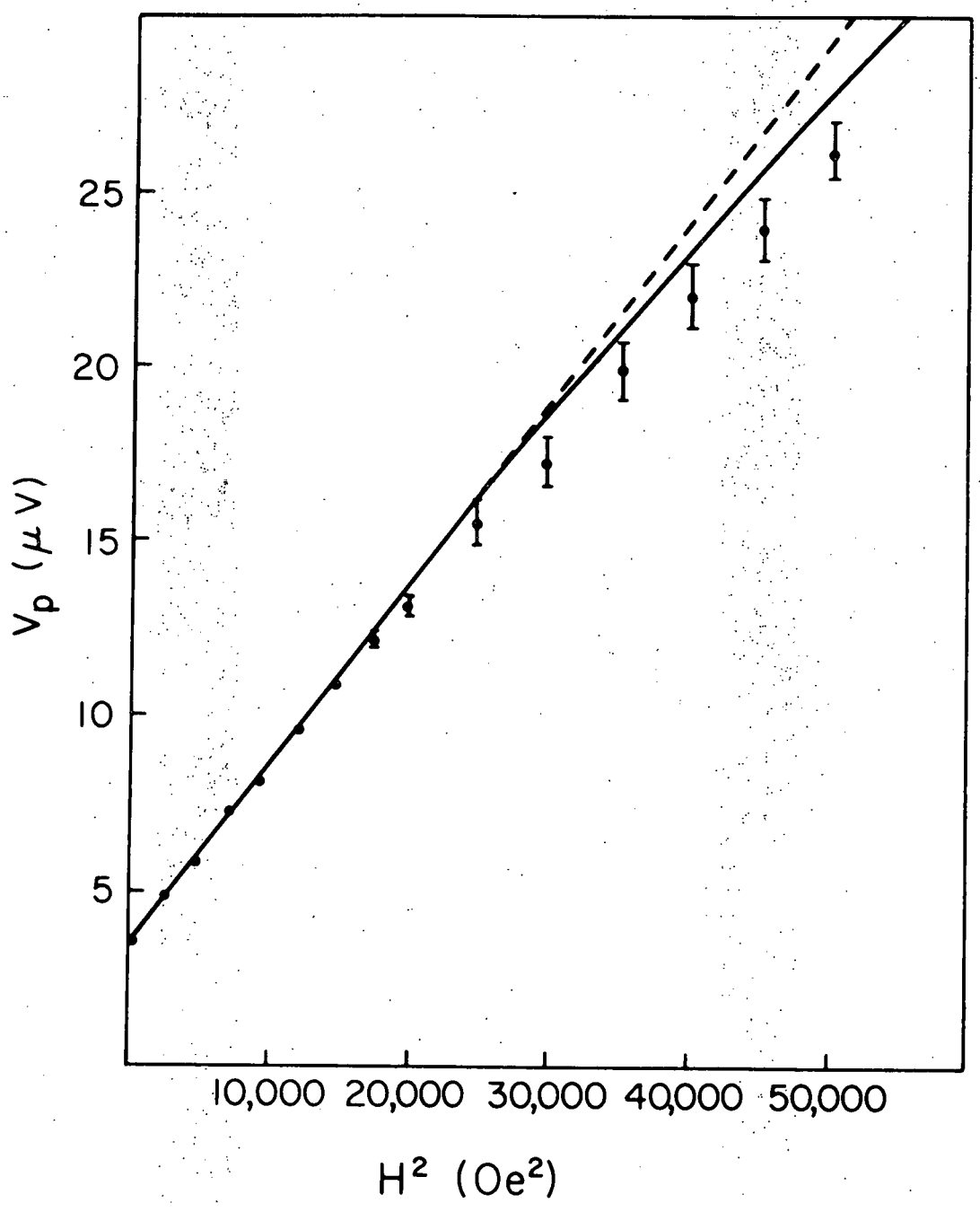

Fig. (20) V_p versus H^2 for Al2-36. The solid line is determined from Eq. (51) using $\xi(0)$ = 546 Å, d = 1280 Å, λ' = 390 Å, and δ = 10 Å. The dashed line indicates the departure from linearity for high fields.

fluctuations of a given wave vector $q = {}^{2e}/_{\hbar c}\,(\lambda' + {}^{d}/_{2})$ are picked out by the magnetic field. If the shift in the pattern in a magnetic field were only the result of the dependence of T_c on H, there would be no departure from linearity at high fields. At low fields, the dependence on magnetic field through the shift in T_c and by the selection of a particular wave vector have identical functional forms. Their simultaneous presence can be determined only by accurate parameterization of the slope.

No quantitative conclusions can be drawn from this work about the contribution to the excess current from the excited states of Eq. (50). The conditions necessary to observe these effects (dirty, thick $d > \xi(T)$ films) were not satisfied in any of the junction used.

C. DATA FOR $T < T_c(H)$

In this section we present experimental excess current-voltage characteristics obtained when both metals were superconducting. As has been discussed in Chapter II, the excess current-voltage characteristic observed below T_c is expected to be a measure of the pair-field susceptibility of the aluminum film. Measurements are made only at finite q because of the necessity of applying a magnetic field to suppress the dc Josephson effect so that the higher order effects may be observed. It should be noted that the magnetic field applied in the plane of the junction was not greater

than the critical field of the lead electrode. Care was taken to distinguish the structures in the excess current-voltage characteristic which could be attributed to fluctuation induced pair tunneling from remnant features of the standard Josephson effect. In the regime of weak coupling of the metals of the junction near T_c, thermal fluctuations can cause a rounding of the zero voltage Josephson current, which could be confused with fluctuation induced pair tunneling.[63] A definite transition between "Josephson-like" behavior (I_o increasing as T is decreased and interference effects due to an applied field), and "non Josephson-like" behavior (decrease in the magnitude of the excess current as T is decreased and no interference effects) was observed for magnetic fields of the order of 10 to 15 Oe, depending on the junction.

Also care must be taken in the interpretation of some of the structures in the excess current as they may arise from quasiparticle tunneling processes or quasiparticle-pair interference processes not removed by the background subtraction. These features would not be related to the fluctuating pair current and would thus not be a part of the pair-field susceptibility of the aluminum film.

We first present the data analyzed in terms of the excess current or equivalently the pair-field susceptibility. From this data it will be evident that the

dynamical nature of the fluctuations below T_c is quantitatively different from that above $T_c(H)$. By studying the structure factor rather than Im $\chi(\omega,q)$, the nature of the fluctuations is more clearly demonstrated. Therefore, in the second part of this section we analyze the data in terms of $S(\omega,q)$ or equivalently I_{ex}/V.

Figure (21) shows the main features of the excess current for junction Al2-36 as the temperature is reduced below the transition temperature of the aluminum film. The applied field is 100 Oe. In Fig. (21.a) the temperature is above $T_c(H)$ and the behavior is the same as discussed in the previous section. Figures (21.b - d) show the behavior for $T<T_c(H)$.

The offset in Fig. (21.d) is a consequence of an asymmetry in the I-V characteristic of sample Al2-36 resulting from a ground loop in the electronics which was later corrected. Figure (21.d) is then only a qualitative representation of the behavior of the excess current in this voltage range.

The solid lines in Fig. (21.a - c) are fits to the theory using Eq. (34). Data in Figs. (21.b - d) were obtained below $T_c(H)$ and are not in agreement with the form of the theory which holds above $T_c(H)$.

Figures (22) and (23) show the detailed behavior of the excess current in the vicinity of $T_c(H)$ for sample Al2-64. The magnetic field is 125 Oe and the transition temperature in this field is $1.780 \pm .001$ K, where

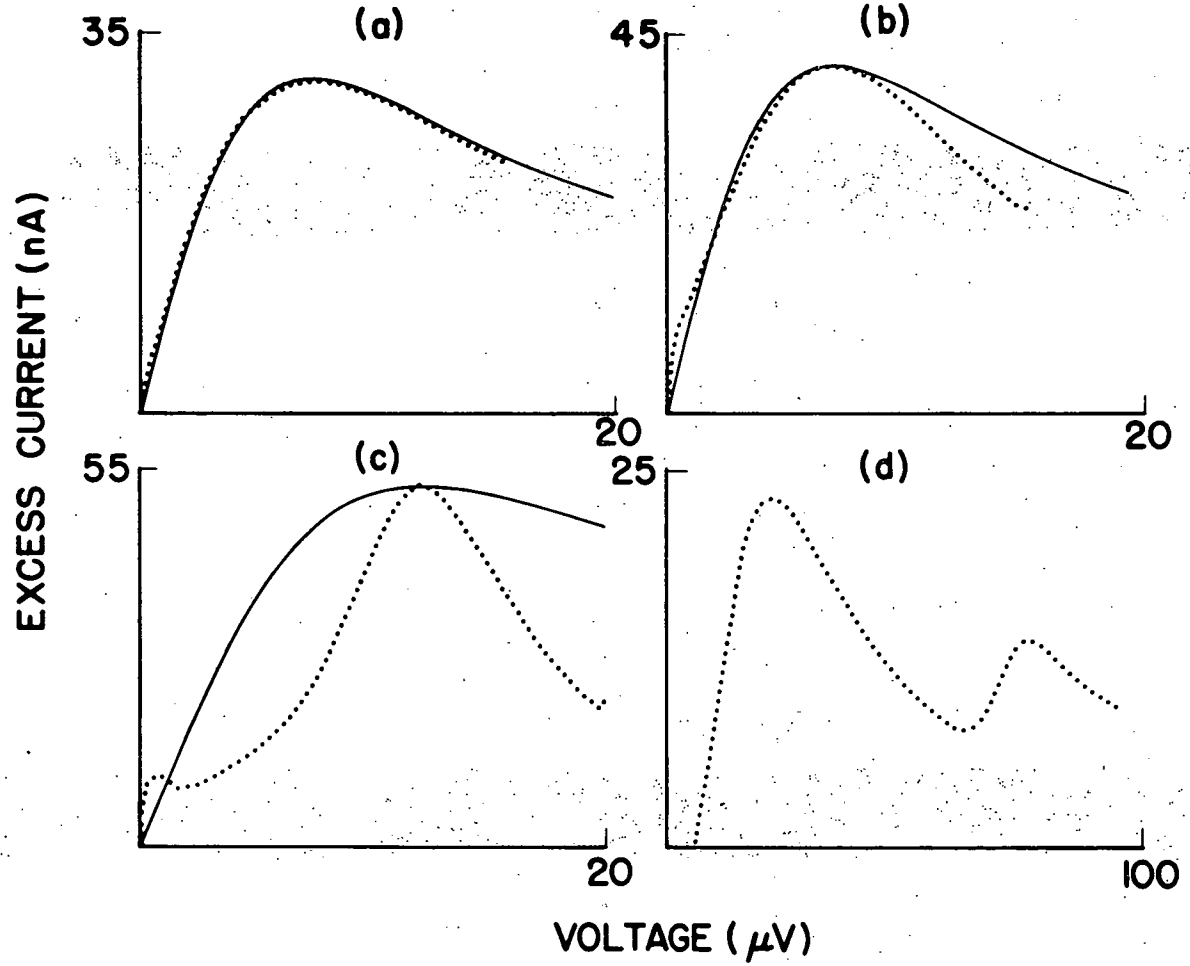

Fig. (21) Excess current-voltage characteristics of junctions Al2-36 at H = 100 Oe. Points are experimental data and solid lines are calculated from Eq. (34). Curves (a), (b), (c), and (d) correspond to T = 1.95465 K, 1.93341 K, 1.92719 K, and 1.89329 K respectively.

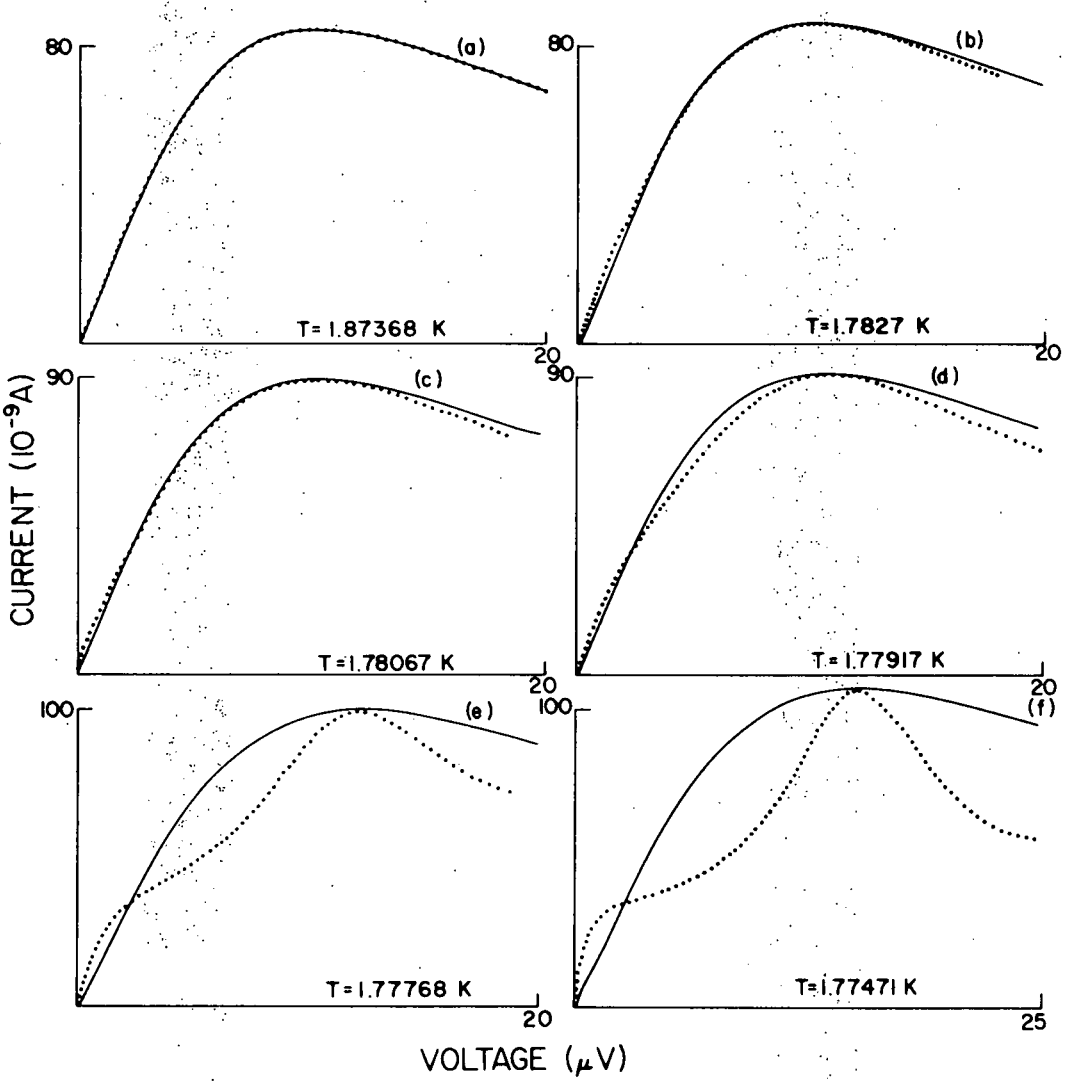

Fig. (22) Detailed temperature dependence of excess current-voltage characteristic for Al2-64 at H = 125 Oe and $T_c(H)$ = 1.7995 K.

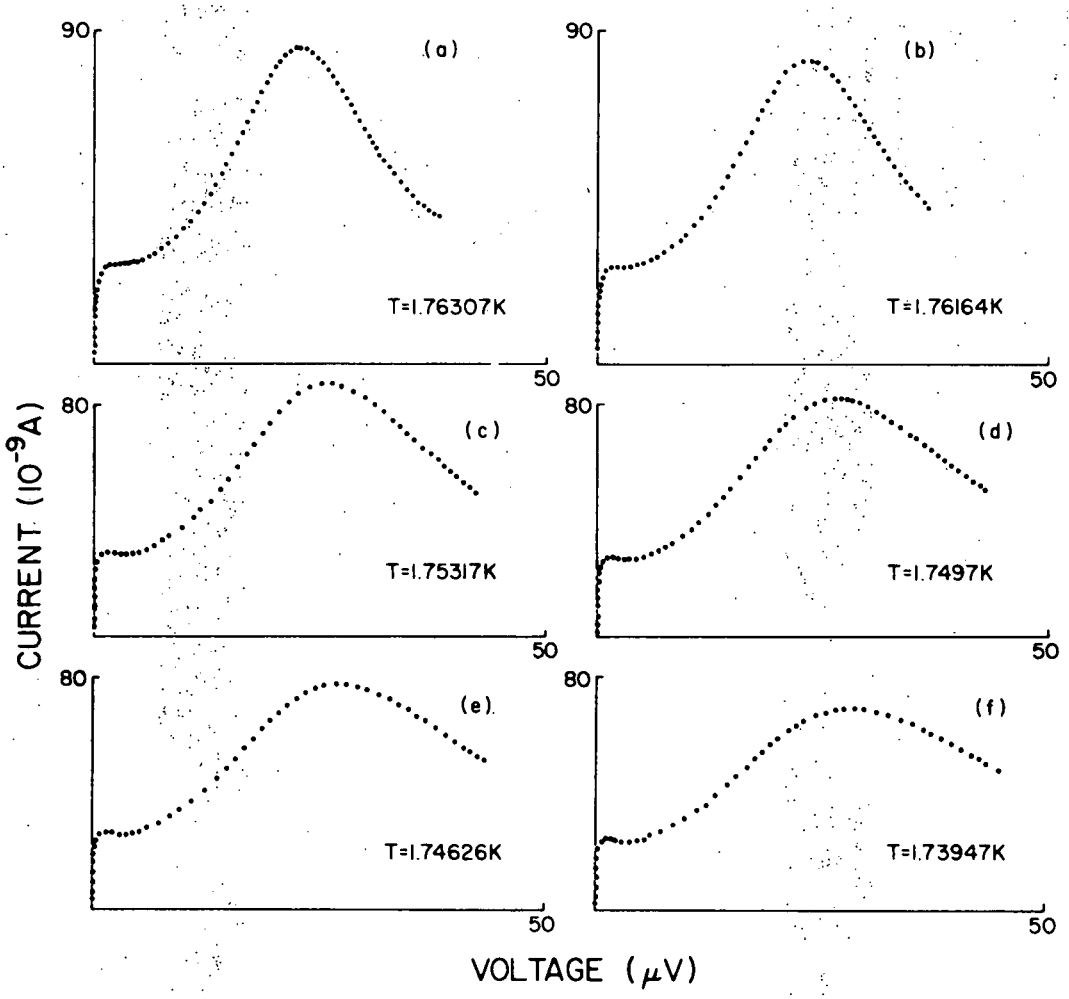

Fig. (23) Excess current characteristics for Al2-64 for H = 125 Oe and $T_c(H)$ = 1.7995 K.

the method used to set $T_c(H)$ will be described shortly. The high voltage peak shown in Fig.(21.d) is not in the range of these traces. These figures clearly indicate how the contribution to the excess current below $T_c(H)$ develops in a continuous manner from the features above observed $T_c(H)$ that are known to be a measure of the pair-field susceptibility of the aluminum film. Thus we are naturally led to the conclusion that the excess current-voltage characteristic, except for the secondary peak which we will show shortly is most likely due to quasiparticle processes, is a measure of the pair-field susceptibility of the aluminum film below $T_c(H)$.

The distortion of the excess current-voltage characteristic from the behavior of $T > T_c(H)$ begins several mK above $T_c(H)$. In this region, close to $T_c(H)$, the inverse coherence length $\xi(T)^{-1}$ is comparable to the wave vector q and the system is in the nonhydrodynamic limit. The transition is also smeared out over a temperature interval of several mK. This is also evident in the plots of V_p versus T (Figs. (28) and (29)) where the change in slope at $T_c(H)$ is gradual rather than abrupt.

Three features of the excess current should be noted. First, at the transition temperature, a shoulder develops on the low voltage side of the main peak. As T is reduced below $T_c(H)$ this shoulder moves to a lower voltage and for some junctions becomes a peak in the excess current-voltage characteristics at low

temperatures. For very low temperature, it usually appears as a rounded step at the origin whose magnitude slowly decreases or appears to remain constant as T is decreased. At fixed T if the magnetic field is reduced, the shoulder grows slowly until for small fields (10 - 15 Oe) the dc Josephson effect becomes dominant and obscures the fluctuation induced pair current.

The second feature of the excess current is a change in the behavior of the main peak as the transition temperature is crossed. The shape of the peak distorts from the quasi-Lorentzian shape of $T > T_c(H)$, to a much more peaked function for $T < T_c(H)$. In addition, the sign of the temperature dependence of the position of the maximum of the main peak changes, at the transition temperature. As T is decreased, the amplitude of the peak gets smaller and the shape becomes less peaked, although it does not become quasi-Lorentzian again in the temperature range in which the effect is observed.

The third feature of interest is the high voltage secondary peak shown in Fig. (21.d). The development of this peak from the main peak is shown in Fig. (24) Measurements of the position of the maximum as a function of temperature were only made when the secondary peak was sufficiently far removed from the main peak for it to be well defined. The insert in Fig. (28)

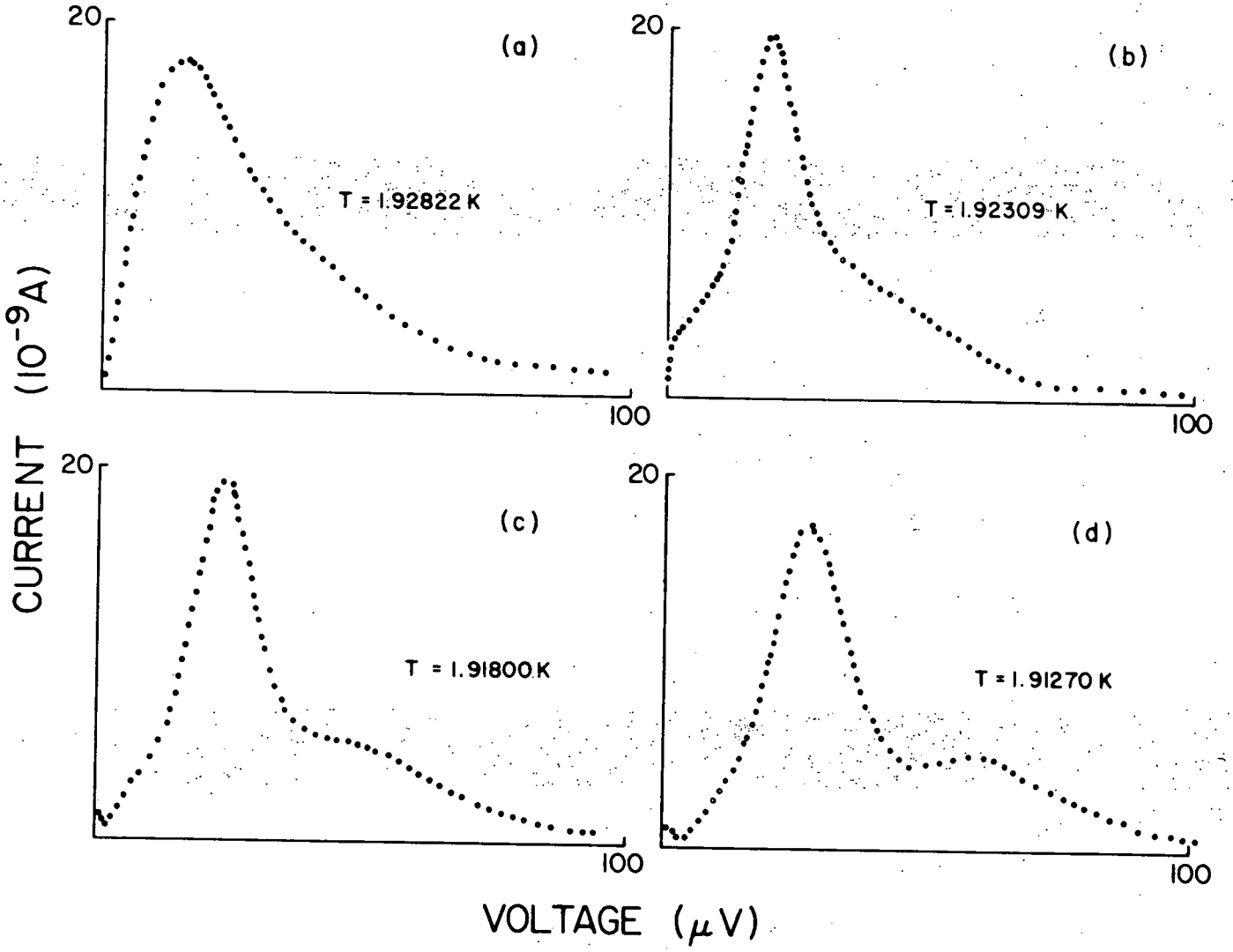

Fig. (24) Development of the secondary high voltage peak for sample Al2-36 at H = 150 Oe.

shows the temperature dependence of the secondary peak voltage which is found to be equal to the voltage corresponding to the energy gap of the aluminum film. This is shown in Fig. (25) where we have plotted data from sample Al2-64 obtained in a magnetic field of 75 gauss. The solid line is the temperature dependent energy gap of the aluminum film near $T_c(H)$ calculated from

$$V_g = \frac{\Delta_{Al}(T)}{e} = \frac{3.1\ k_B T_c}{e} (1 - T/T_c(H))^{\frac{1}{2}}, \qquad (62)$$

where only $T_c(H)$ has been adjusted to give the best fit to the theory.

Figure (26) shows the temperature dependence of the magnitude of the current at the peak. Since the peak is found at high voltages, small errors in the subtraction of the background quasiparticle current can cause significant errors in the amplitude of the peak. Another source of error in the magnitude of the secondary peak is the main low voltage structure in the excess current. Since the height and position of the secondary peak were determined without subtracting the contribution from the main peak, the apparent magnitude may be larger, however the position is not affected because the magnitude of the tail of the main structure does not change over the voltage region where the secondary peak is observed. For these reasons the data shown in Fig. (26) should be taken only as approximate. The fall

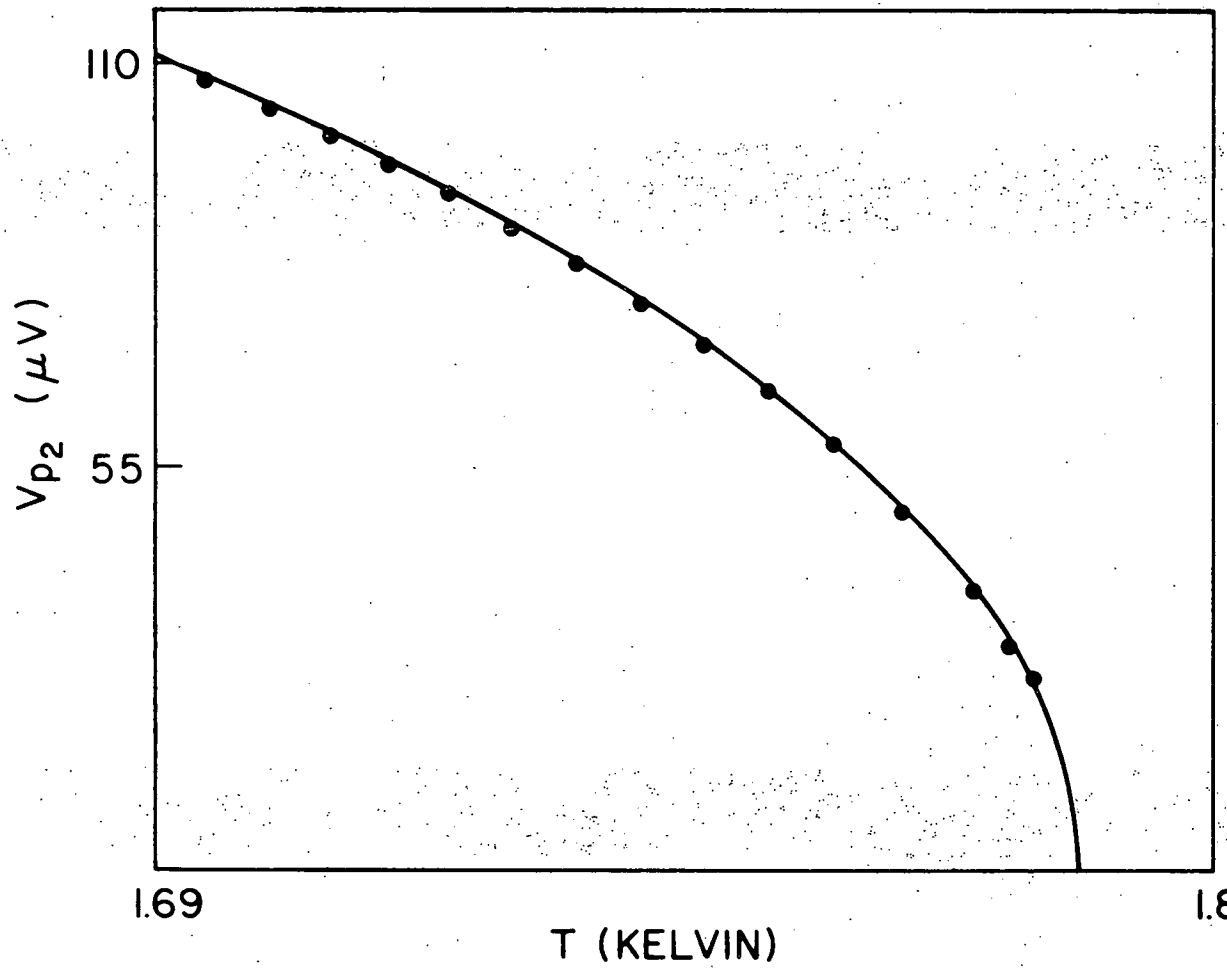

Fig. (25) Temperature dependence of the secondary voltage peak for sample A12-64 in a field of 75 Oe. The points are data while the solid line is the fit to Eq. (62) for the temperature dependence of the voltage corresponding to the energy gap. Only $T_c(H)$ has been adjusted.

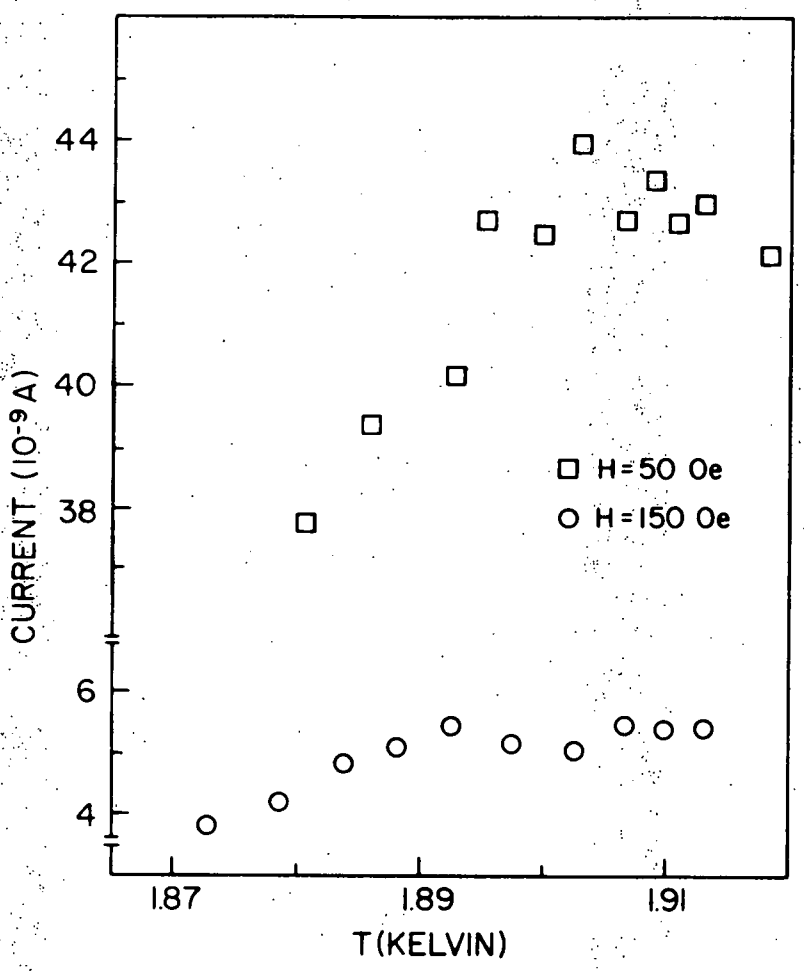

Fig. (26) Peak current of secondary voltage peak for Al2-36 as a function of temperature for several magnetic fields. The fall off at low temperatures may be due to errors in background subtraction.

off at low temperatures is probably the result of errors in the base line subtraction since the peak is moving into the region where the quasiparticle subtraction parameters are determined.

In Fig. (27) we show the low temperature total current-voltage characteristic of the Al2-64. The structures at the voltage of the energy gap has moved to approximately .23 mV which is very close to the low temperature energy gap of aluminum determined by other measurements. The low voltage shoulder is a small step at the origin and the main peak has become a very broad peak. As the field is increased, these structures are reduced in magnitude appreciably, however they do not disappear. It is surprising that other experiments have not observed these low voltage structures in the I-V characteristic.

Several mechanisms have been suggested which may be responsible for the secondary peak. The fact that the position of the peak is found at the same voltage as the energy gap of the aluminum film and is only weakly dependent on magnetic field suggests that it is a consequence of quasiparticle processes rather than coherent pair tunneling processes. One such mechanism suggested by Šimánek and Hayward[64] is dynamical pair breaking produced by oscillating electromagnetic fields in the junction. They have shown that the interaction of the order parameter in the aluminum film with the ac voltage induced by the ac currents in the junction

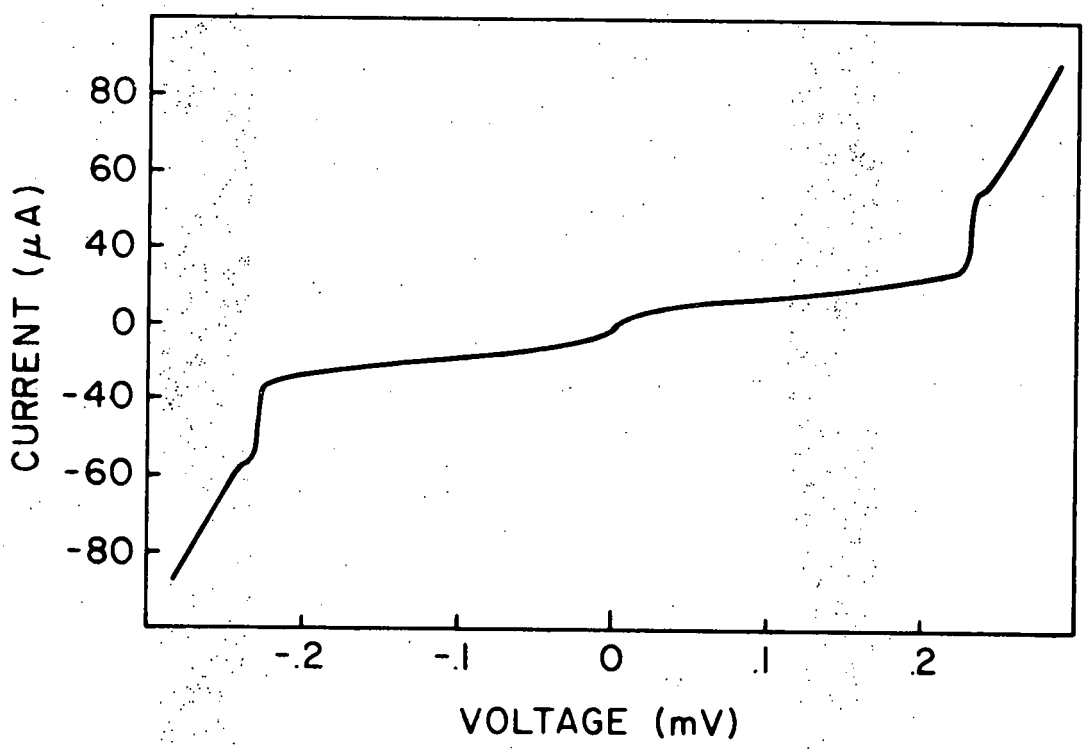

Fig. (27) Total I-V characteristic of Al2-64 at T = 1.12 K and H = 75 Oe. The step at the voltage of the gap is evident at V = .23 mV and the excess current at lower voltages is still evident.

can produce a structure at the gap voltage. When the dc bias across the junction is such that the Josephson frequency $\omega = 2eV/\hbar$ becomes equal to the gap frequency $2\Delta_{Al}(T)/\hbar$ real excitations of quasiparticle pairs begin to contribute to the dc current. The position of the secondary peak as a function of temperature is associated with the threshold of this excitation process and is a measure of the temperature dependence of the energy gap. Šimánek and Hayward found that at the gap voltage the I-V characteristic exhibits a discontinuous jump. The inclusion of pair breaking effects[37] due to the magnetic field rounds off this step at the gap voltage in a manner qualitatively similar to the experimental rounding. The magnitude of the dc current peak is given by

$$\Delta I = \frac{\pi e^2 V_o \Delta (T) g N(0) |\bar{C}| H}{h^2 q^2 v_f} \qquad (63)$$

Here g is the strength of the BCS interaction and V_o is the amplitude of the ac voltage. A numerical estimate of the current jump for H = 100 Oe and $\Delta_{Al}(T) = 70 \times 10^{-6}$V is approximately 10×10^{-9} Å which is in qualitative agreement with the experiment.

Another mechanism which may be related to the structure we observed at the gap is the multiparticle tunneling processes originally proposed by Wilkins and Schrieffer[65] to explain the gap structure observed in superconducting tunneling junctions.[66] Šimánek[67] has estimated

the magnitude of this effect in the temperature range of interest and finds a current jump at $\Delta_{Al}(T)$ to be three orders of magnitude smaller than the effects experimentally observed.

A third explanation of the secondary peak which should be considered is that pair-field susceptibility itself contains a peak at $\hbar\omega = 2eV = 2\Delta(T)$. Understanding this mechanism would require a detailed theory for $\chi(\omega,q)$.

Figures (28) and (29) show the temperature dependence of the maximum of the main peak in the excess current-voltage characteristic for several values of magnetic field for samples Al2-36 and Al2-64. The position of the peak was determined by selecting the maximum in the excess current from a plot on the computer display rather than from a detailed fitting scheme which folded out the various structures in $\chi(\omega,q)$. The onset of superconductivity in the aluminum film is marked by the "turn-around" of the data. This is a consequence of the fact that ϵ, the quantity characterizing fluctuations near $T_c(H)$, is an increasing function of temperature when $T > T_c(H)$ and a decreasing function of temperature when $T < T_c(H)$. The gap in the data for fields of 50 and 75 gauss is due to the existence of negative resistance regions in I-V characteristic for this temperature range. Measurements in this range are unreliable because of switching. At larger fields and lower temperatures

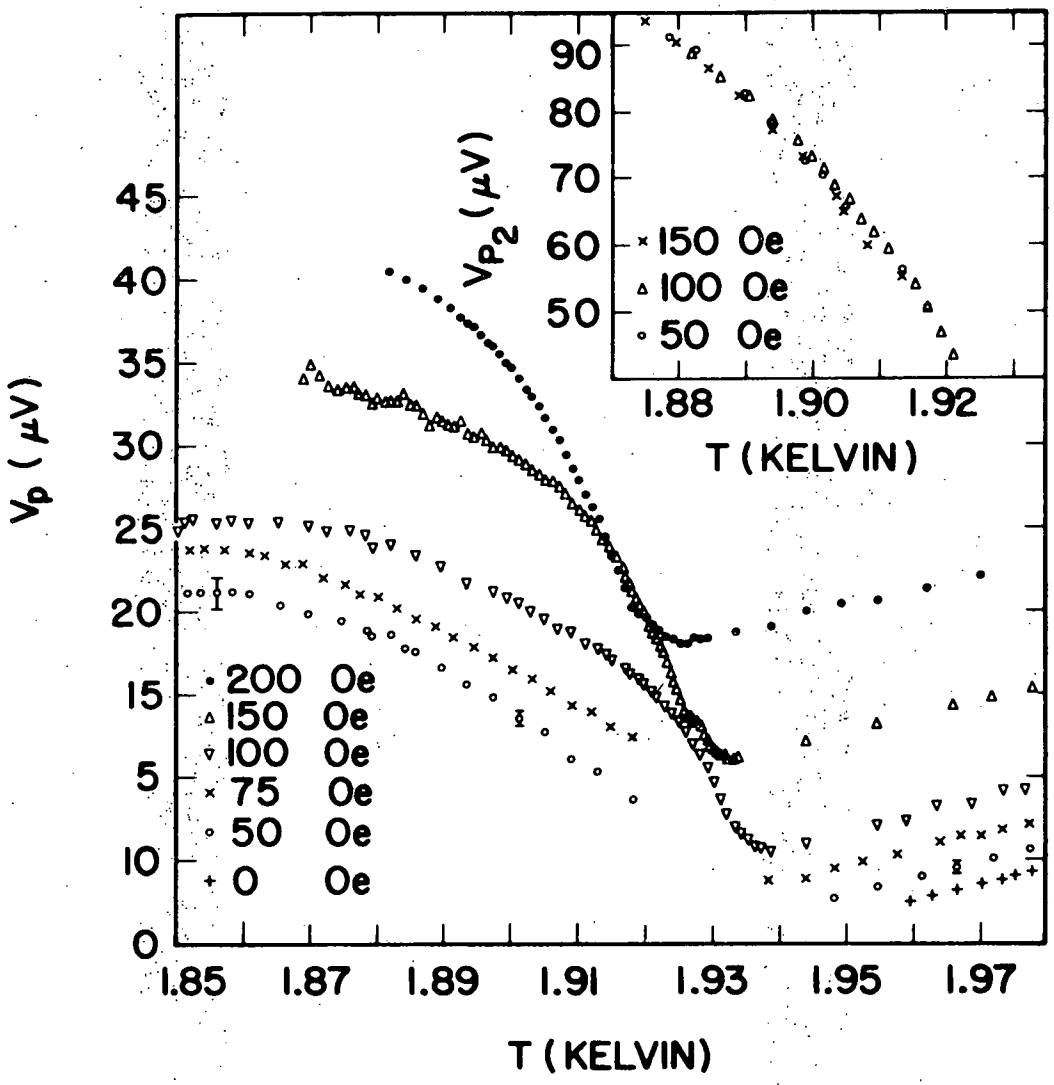

Fig. (28) Temperature dependence of the voltage of the main peak of the excess current for Al2-36 for several magnetic fields. Data is not shown for low fields in the vicinity of T_c due to the negative dynamical resistances. In the insert the temperature dependence of the secondary peak is shown for various magnetic fields.

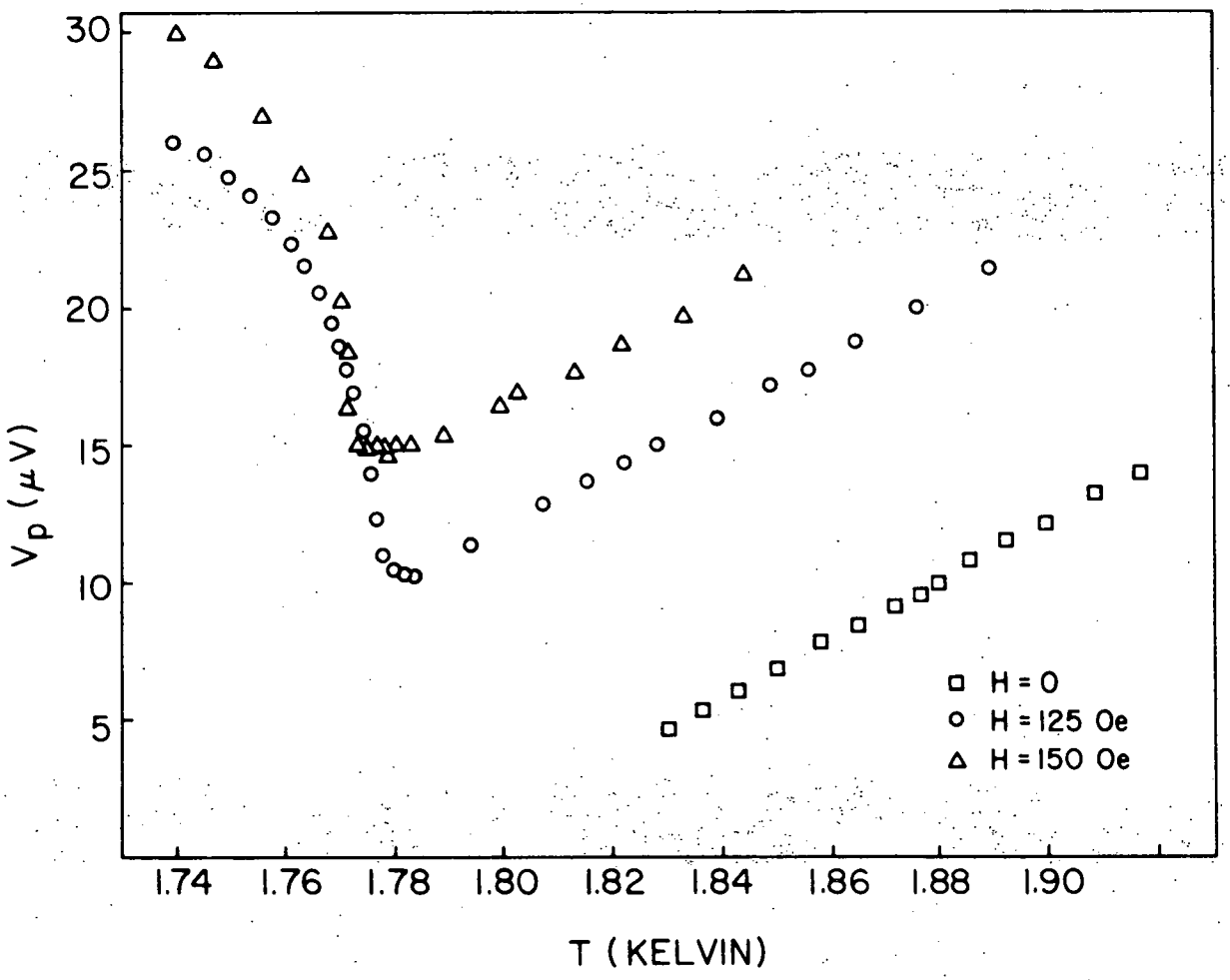

Fig. (29) Temperature dependence of the peak voltage in the excess current for sample Al2-64 for several magnetic fields.

the fluctuation effects are smaller, resulting in positive dynamical resistances over the entire range of the I-V characteristic.

The transition temperature of the film is defined as the temperature at which the plot of V_p versus T in finite field changes sign. This temperature was not well defined from the data as a result of rounding of the V_p versus T curve in the vicinity of $T_c(H)$. If the temperature at which $dV_p/dT = 0$ was used as $T_c(H)$, then the value of the coherence length calculated from Eq. (55) did not agree with values of $\xi(0)$ determined from different values of $T_c(H)$ in different magnetic fields. The transition temperature was actually determined from the interaction of the extrapolated behavior for $T > T_c(H)$ with that for $T < T_c(H)$. Then the values of $\xi(0)$ determined from Eq. (55) with different values of $T_c(H)$ for different fields, were within 5 to 10% of each other.

In Figs. (30) and (31) we plot the inverse peak current I_p^{-1} as a function of temperature in several magnetic fields for junctions A12-36 and A12-64. The anamalous nonmonotonic variation of I_p^{-1} versus T in the form of a peak in I_p^{-1} near $T_c(H)$ was observed only in sample A12-36. This behavior is observed at the same temperatures as the step in V_p versus T and is most evident in data of Fig. (28) taken in 150 gauss and at 1.925 K. At the present time, it is not known if this effect is an unusual consequence of sample inhomo-

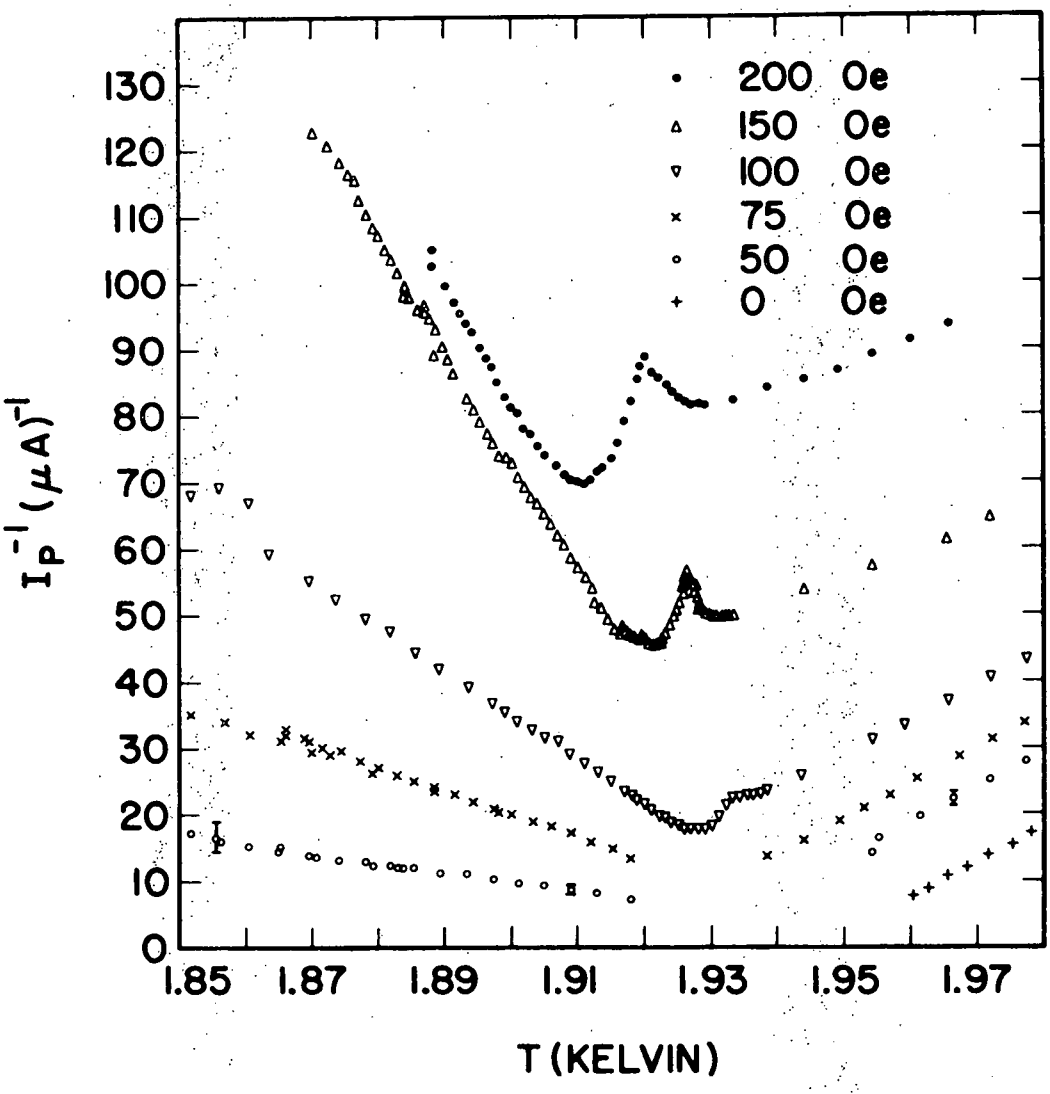

Fig. (30) Inverse peak current as a function of temperature for Al2-36. The nonmonotonic behavior just below $T_c(H)$ was only observed in this sample.

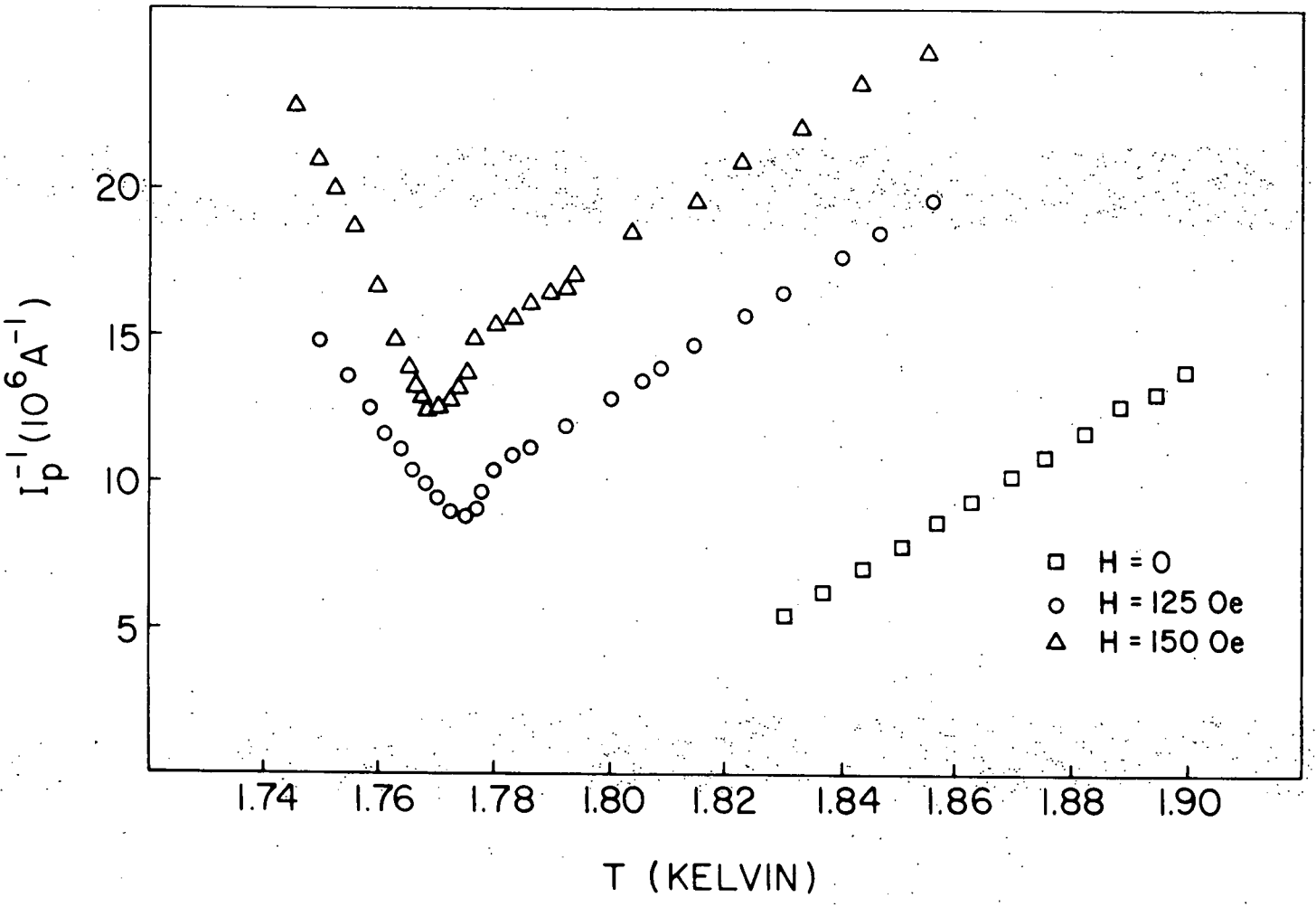

Fig. (31) Temperature dependence of inverse peak current A12-64 for several magnetic fields.

geneity such as a multiple transition or is a fundamental property of the junction.

A theoretical calculation of $\chi(\omega,q)$ below T_c for a gapless neutral superconductor, which is discussed in Section IV-D, predicts this type of behavior for the temperature dependence of the inverse peak current below T_c. However as discussed in that section, the evidence for such a description is not strong, especially since the effect was only observed in one sample, A12-36, whose physical properties (ρ_N, R_N, $T_c(0)$ etc.) did not differ significantly from those of other samples. There may still be a undefined parameter in the system which characterizes this type of behavior which is not understood.

More characteristic behavior of the temperature dependence of the inverse peak current is shown in Fig. (31). The fall off of I_p^{-1} from the linear behavior of $T>T_c(H)$ occurs at $T_c(H)$. The rapid increase in the peak current as $T_c(H)$ is crossed is not well understood at this time. It is unlikely that the decrease in I_p^{-1} is a consequence of the presence of the secondary high voltage peak under the main peak. If the explanation given by Šimánek and Hayward[64] is correct, the magnitude of the peak is proportional to the temperature dependent gap. Near $T_c(H)$, the magnitude of the peak is too small to account for the decrease in I_p^{-1}. As the peak current is a measure of the strength of the fluctuations, the drop in I_p^{-1} in the vicinity of $T_c(H)$ implies an

enhancement of fluctuation effects. Again this behavior occurs over a temperature range within which the inverse correlation length $\xi(T)^{-1}$ is of the order of the wave vector so that effects occuring in this region may be manifestations of critical behavior. As in the discussion of the drop in the relaxation frequency above T_c, any enhancement of fluctuation effects is opposite to what would be expected in the critical region. However for sample A12-36 the inverse peak current falls, near T_c, indicating a supression of fluctuations in a manner which is expected in the critical region.

The data presented in Fig. (21) suggests that fluctuations of the order parameter cannot be described by a diffusive time-dependent Ginzburg-Landau equation, but rather should be described by an equation with propagating solutions. In this case the structure factor, $S(\omega,q)$, should be studied rather than $\chi(\omega,q)$ since from the former it is easier both to demonstrate the nature of such modes and, in principle, to ascertain their dispersion relations. A peak in the structure factor at non-zero frequency implies the existence of a propagating mode, with the damping of the mode proportional to the half width of the peak. The structure factor is easily obtained from the data by dividing the excess current by the voltage (Eq. (15)). So that these results will be displayed in a manner more consistent with data presented for the study of other phase transitions, the

voltage is writtern in terms of frequency $\omega = \frac{2eV}{\hbar}$ and the magnetic field is written in terms of wave vector $q = \frac{2e}{\hbar c} H (\lambda' + d/2)$.

The structure factor for sample Al2-64 is shown in Fig. (32). The magnitude of the structure factor is in arbitrary units. A magnetic field of 125 Oe is applied to the junction, reducing the transition temperature from 1.786 K to approximately 1.7795 K. Although only the $\omega > 0$ portion of the data is shown, all curves are actually symmetrical about $\omega = 0$. The high frequency peak in the excess current at the gap is out of the range of the graphs. Above $T_c(H)$ the structure factor is Lorentzian centered at $\omega = 0$, with a half width equal to the pair relaxation frequency Γ_o. Below and in the immediate vicinity of T_c, $S(\omega, q)$ has a peak at finite frequency ω_p in addition to the usual peak at the origin. As the temperature is reduced below T_c, this peak moves out in the frequency, its half width broadens and finally for $T_c(H) - T \approx 40$ mK the peak becomes very broad and is obscured by the tail of the central peak. The amplitude of the peak at the origin grows as $T_c(H)$ is crossed and decreases slowly below $T_c(H)$. Its half width after decreasing at $T_c(H)$ appears to increase as the temperature is reduced further.

Shown in Fig. (33) is the magnetic field dependence of $S(0,q)$ at $\epsilon(H,T) = 6.3 \times 10^{-3}$ for sample Al2-64. The nonmonotonic behavior as a function of magnetic field

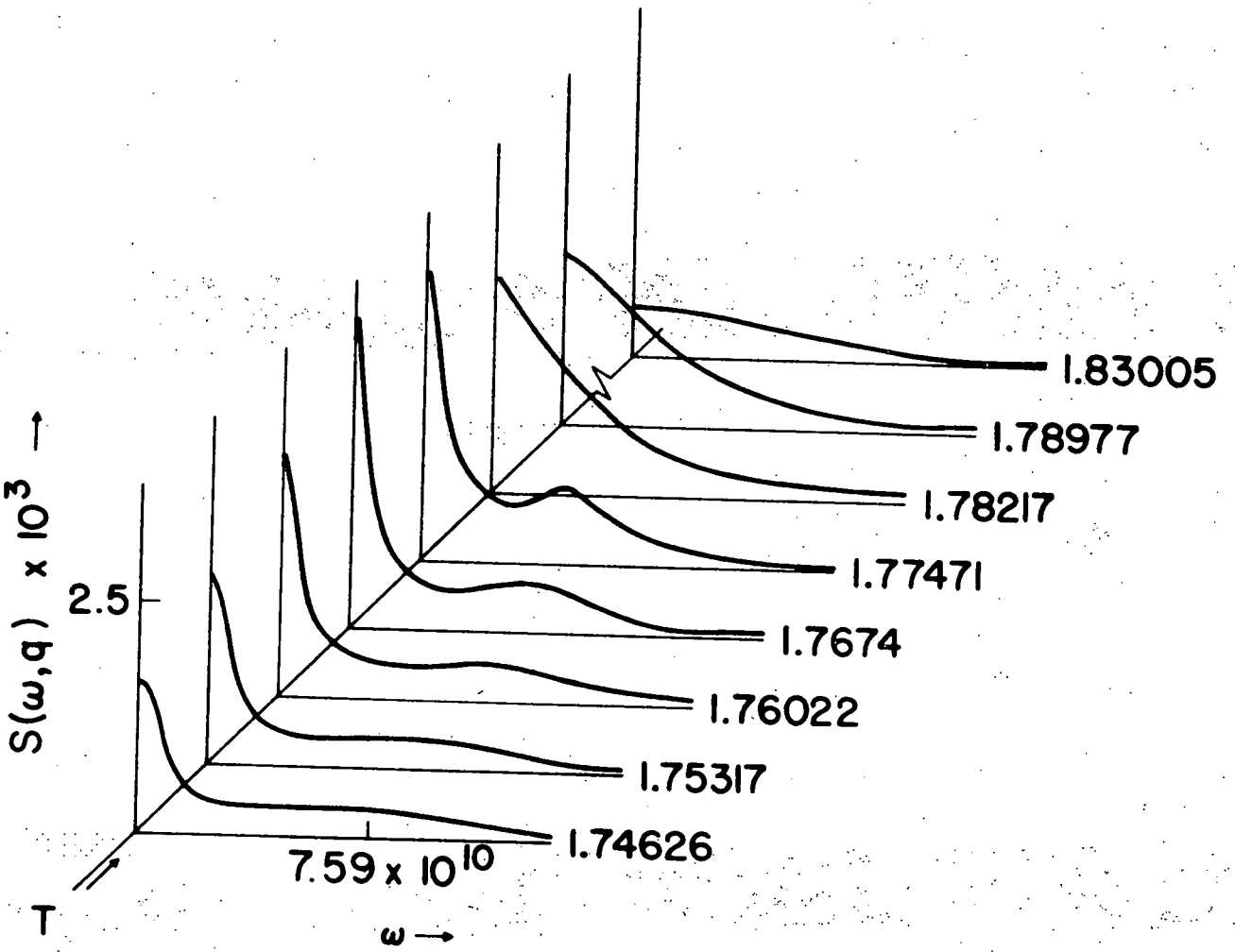

Fig. (32) Structure factor (I_{ex}/V) in arbitrary units for A12-64 plotted as a function of temperature. The magnetic field is 125 Oe. Curves are only shown for the $\omega > 0$ portion; they are actually symmetrical about $\omega = 0$. $T_c(H) = 1.780$.

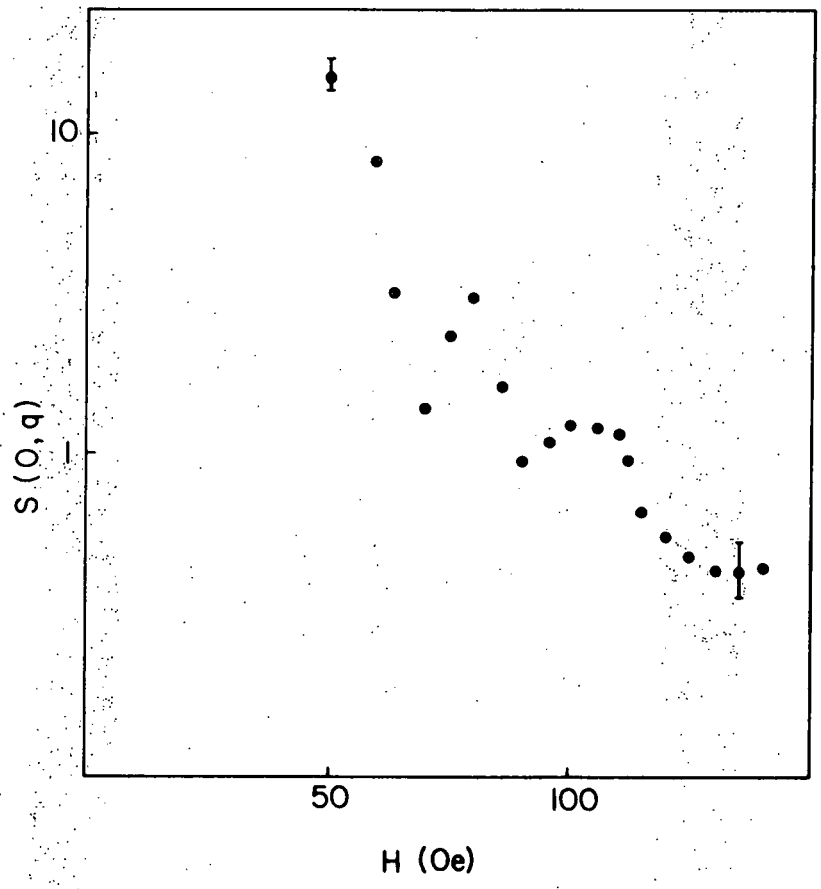

Fig. (33) Value of the structure factor at zero frequency for ϵ (H,T) = 6.32 X 10^{-3} for junction Al2-64. The nonmonotonic behavior was present in Al2-61 and 79 also.

was observed in junctions A12-61, 64 and 79, which were the only junctions for which this quantity was measured. It may be possible that the observed behavior is a consequence of locally thin regions or even small filamentary shorts through the insulating layer which result in coherent pair transfer with interference effects. The period of the nonmonotonic behavior implies a wave length of 2000 Å (Eq. (28)) which may be a reasonable size for such regions. The nonmonotonic behavior may also be a real feature of the central mode in $S(\omega,q)$ not contained in any known model.

The dispersion relation for the propagating mode can be determined by measuring the wave vector dependence of the finite frequency peak in the structure factor, where the wave-vector is set by the magnetic field in the plane of the junction. Figures (34) and (35) show the results for junctions A12-64 and A12-79. In Figs. (34.a) and (35) the dispersion relation is plotted at fixed temperature and in Fig. (34.b) at fixed $\epsilon(H,T)$, Eq. (55). The bending over of the curves in Figs. (34.a) and (35) is a consequence of the approach to the superconducting-normal phase boundary with increasing magnetic field. Because the applied field shifts T_c as well as determines the wave vector, the physically significant curves are believed to be plots at fixed reduced temperatures. These are shown in Fig. (34.b). The curves A and B correspond to $\epsilon(H,T) = 6.32 \times 10^{-3}$ and 1×10^{-3},

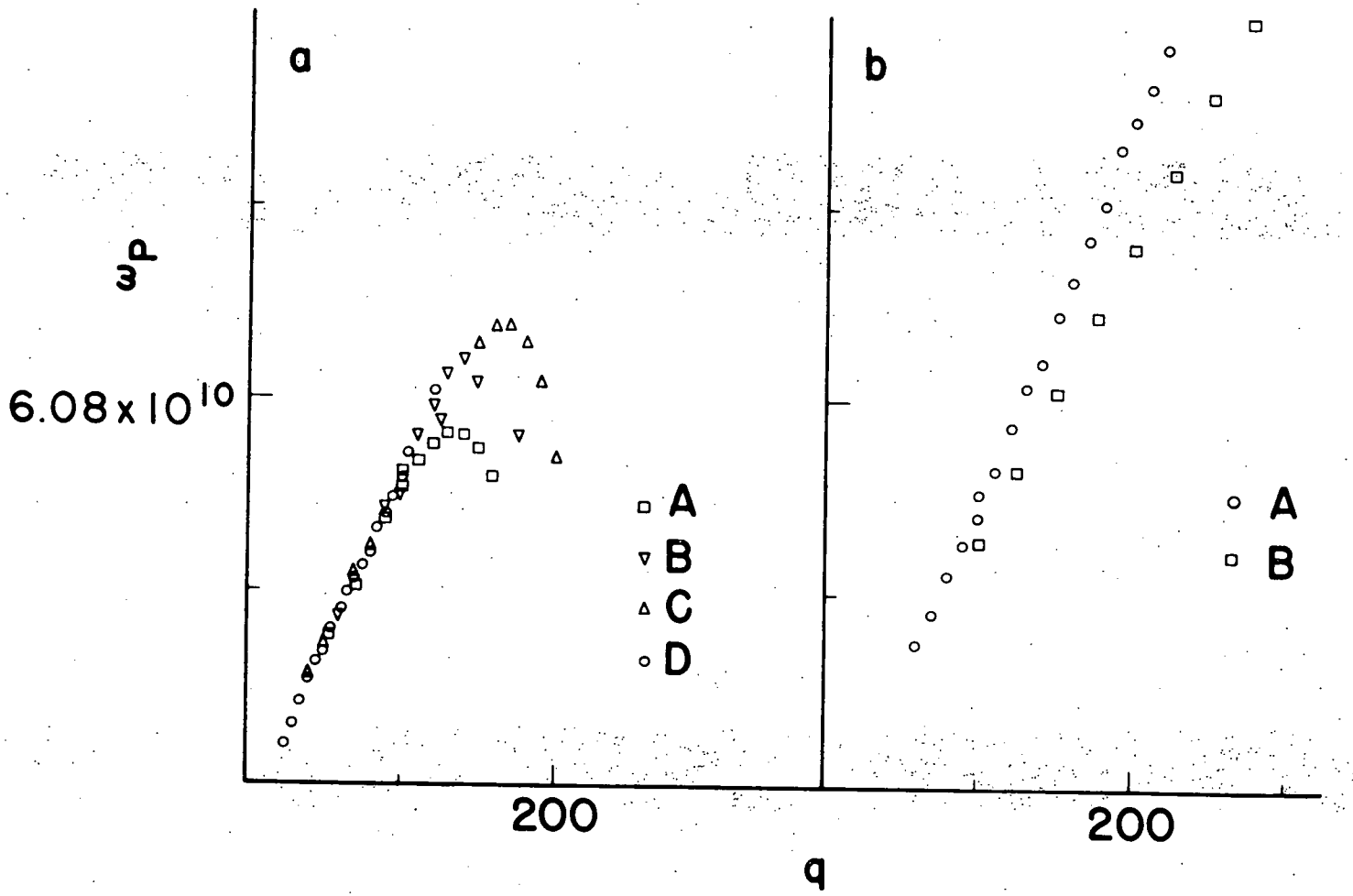

Fig. (34) a) Position of finite frequency peak in $S(\omega,q)$ plotted as a function of q in units of magnetic field $(2e/\hbar c\ (d/c + \lambda'))$ of sample A12-64 at several fixed temperatures. The points (a), (b), (c) and (d) correspond to T = 1.77104, 1.76740, 1.76379 and 1.75317 respectively.
b) Frequencies of peaks in $S(\omega,q)$ at fixed $\epsilon(H,T)$. Points labeled A,B correspond to $\epsilon = 6.32 \times 10^{-3}$ and 1.0×10^{-3} respectively.

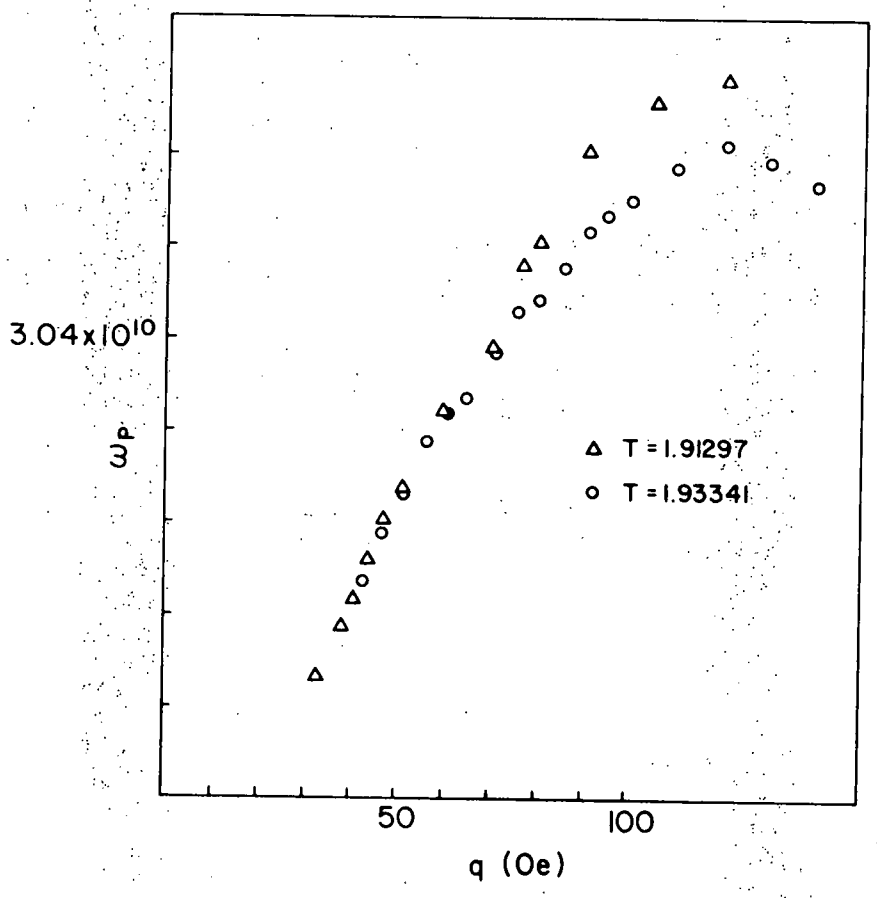

Fig. (35) Position of finite frequency peak in $S(\omega, q)$ of Al2-79 at several temperatures plotted as a function of magnetic field. The apparent negative frequency is evident.

respectively where at each field, ϵ (H,T) was calculated from Eq. (55) with $\xi(0) = 5.46 \times 10^{-6}$ cm and $T_c(0)=1.786$ K. Over the apparent linear range where the dispersion relation is measured, the propagation velocities can be obtained from the slopes of the curves and they are $1.74 \times 10^{+6}$ cm/sec for $\epsilon = 6.32 \times 10^{-3}$, and 1.35×10^{6} cm/sec for $\epsilon = 1 \times 10^{-3}$. The propagation velocity appears to be independent of ϵ for $\epsilon > 4 \times 10^{-3}$ to the extent that it is possible to observe a peak in $S(\omega,q)$. For $\epsilon > 4 \times 10^{-3}$ the velocities are greater than the sound velocity in aluminum (5×10^{5} cm/sec) but are lower than the Fermi velocity (2.02×10^{8} cm/sec) in aluminum.

From the data in Figs. (34) and (35) it is evident that the extrapolation of the linear portion of the dispersion relation to small q gives an apparent negative frequency intercept. It should be emphasized that this experiment does not measure the dispersion relation for low q. For small wave vectors, quantitative measurements on the finite frequency peak cannot be carried out for several reasons: first, in low magnetic fields the Josephson effect dominates, second, the I-V characteristic has regions of negative dynamical resistance and finally, the width of the central peak at small q and large ϵ is usually large enough to obscure the behavior of finite frequency peak at small ω. Measurements on voltage biased junctions that are carefully shielded from external noise, along with a detailed fitting scheme

could possibly probe more of the small wave vector region.

However, the negative-frequency intercept of the curve suggested by the high data is not inconsistent with a model in which a phononlike mode is coupled to a plasmonlike mode.[68]

Shown in Fig. (36) is the temperature dependence of the finite frequency peak for Al2-64 in two magnetic fields. The saturation of ω_p for $\epsilon > 4 \times 10^{-3}$ is consistent with the saturation of the propagation velocity for low q, evident from the dispersion curve. In Figs. (34), (35), and (36) the limits on the ranges of q and ω for which data are plotted are determined by limitations on the quantitative definition in the peak of $S(\omega,q)$ which is a consequence of the graphical technique used to analyze the data. Instead of determining the peak frequency with a detailed fitting scheme in which the various components in the structure factor are folded out from the raw data, ω_p was found by selecting the maximum from the graph of $S(\omega,q)$. The lower limit for the range of q was thus set by a requirement that the peak be far enough separated from the tail of the zero frequency peak, that it could be well defined. For values of q and ω as large as 300 Oe and 6×10^{-2}, respectively, an effect was still evident but could be characterized only in a marginal manner. Over the range plotted, the error in the determination of peak frequencies

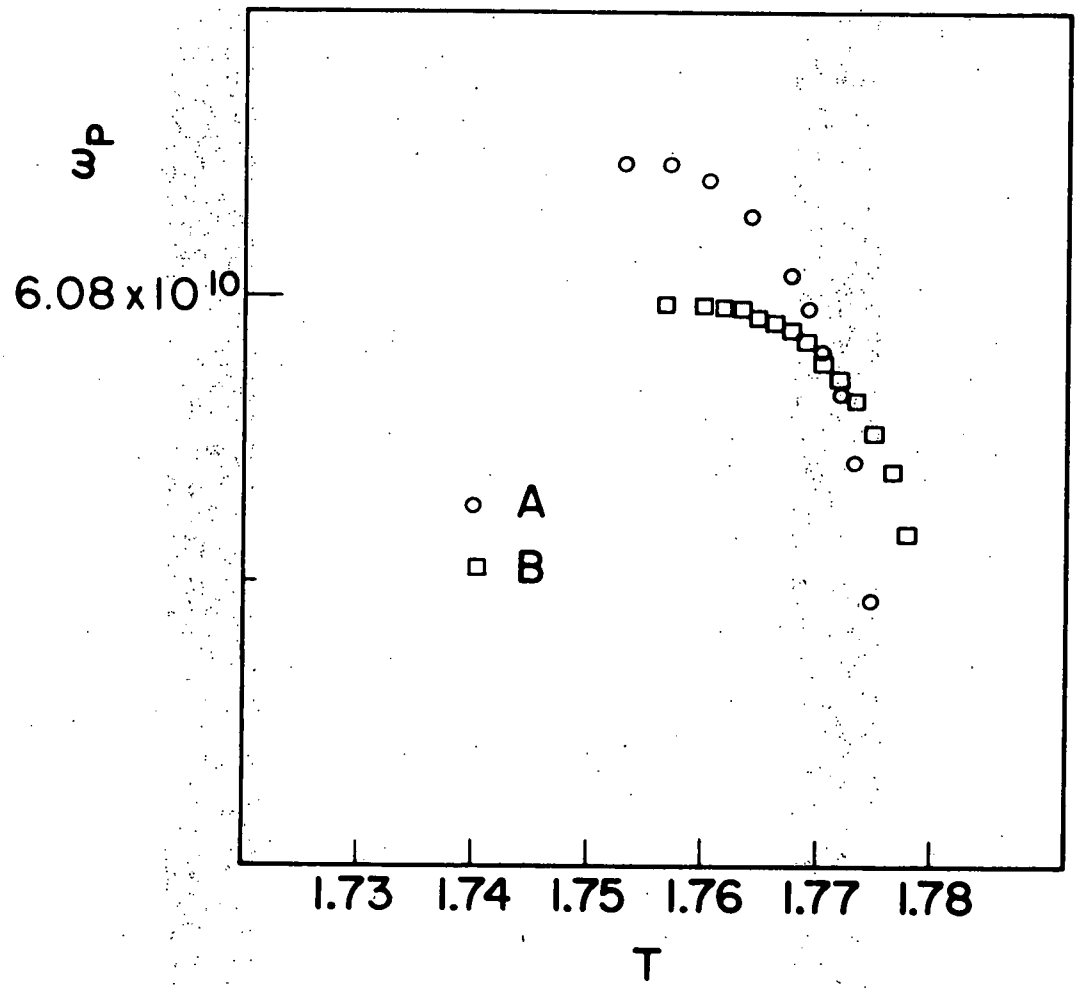

Fig. (36) Temperature dependence of peak of $S(\omega,q)$ in fields of 150 Oe (A) and 125 Oe (B).

using a graphical technique rather than a fitting scheme was estimated to be at most $\pm$ 3 X 10^{-9} rad/sec if all the peaks were Lorentzian or shifted Lorentzians.

The errors in determination of the peak frequencies are not large enough to account for the fact that all the graphs of ω_p versus q extrapolated to a small negative frequency as q goes to zero. A systematic error in the analysis may possibly be responsible for the negative intercept. A contribution from a remnant of the fluctuation broadened dc Josephson current would make an increasing contribution to the excess current at low voltages as the magnetic field is reduced. This would appear as a contribution to the central peak in $S(\omega,q)$ and would shift ω_p to a lower frequency. However, since the height of the central peak decreases as T is lowered below T_c in fields in excess of 15 Oe, this effect is probably unimportant. A contribution to the central peak from the Josephson effect would increase with decreasing temperature.

We have also obtained preliminary results using a nonlinear fitting scheme applied to the data shown in Fig. (32). The structure factor has been assumed to be the sum of a central Lorentzian and two shifted Lorentzians at $\omega = \pm\omega_p$. The parameters characterizing the peaks determined from the fitting program are given in Table III, along with the value for the peak frequency which had been determined graphically. We can conclude

TABLE III

Temperature (K)	A[b] X 10^{-3}	B[c] X 10^{10}	C[b] X 10^{-3}	D[c] X 10^{10}	F[c] X 10^{10}	F[c] Graphical
1.78977	16.8 ± .1	3.12 ± .2	-	-	-	-
1.78217	18.5 ± .1	2.86 ± .2	-	-	-	-
1.77417	28 ± .5	.62 ± .1	6.3 ± .2	1.97 ± .1	4.5 ± .06	4.5 ± .2
1.7674	25 ± .5	.61 ± .2	4.1 ± .4	3.03 ± .2	5.77 ± .1	5.68 ± .1
1.76022	20 ± .1	.69 ± .3	3.3 ± .7	3.65 ± .2	6.14 ± .2	6.04 ± .1
1.75317	16 ± .1	.66 ± .1	2.6 ± .1	4.56 ± .1	6.08 ± .1	6.07 ± .1
1.74626	14.5 ± .1	.65 ± .1	2.2 ± .02	5.32 ± .1	6.23 ± .1	6.07 ± .1
1.73947	14.1 ± .1	.65 ± .1	2.0 ± .03	5.71 ± .1	6.13 ± .1	6.07 ± .1

a The parameters are defined from the equation $S(\omega,q) = A/(1 + \omega^2/B^2) + C/(1 + (\omega \pm F)^2/D^2)$

b Arbitrary units

c ω in rad/sec

from the values listed in Table III that the fitting technique does not significantly shift the position of the finite frequency peak from the values which had been previously determined graphically. The fitting technique does give information about lifetimes and relaxation times associated with the finite frequency peak and the central mode respectively. Because errors in this technique appeared to be large, the use of more sophisticated fitting techniques is being explored. No quantitative statements can be made at this time as to the validity of the relaxation times and lifetimes listed in Table III.

It is of some interest to indicate explicitly the regions of the superconducting-normal phase diagram in which measurements have been made. This is shown in Fig. (37). The boundary of hydrodynamic region was determined with condition $\xi(T)/\lambda$, which is actually only a qualitative measurement of the width of the non-hydrodynamic region.

To summarize this section, we list the important features of the data to be explained by theory. First the peak of the excess current which is a measure of the pair-field susceptibility, distorts as the transition temperature is crossed. Analysis of the structure factor suggests this peaking to be a consequence of the existence of a propagating mode in the system which appears at $T = T_c(H)$. This mode has a linear dispersion relation over the range it is observed however it appears to

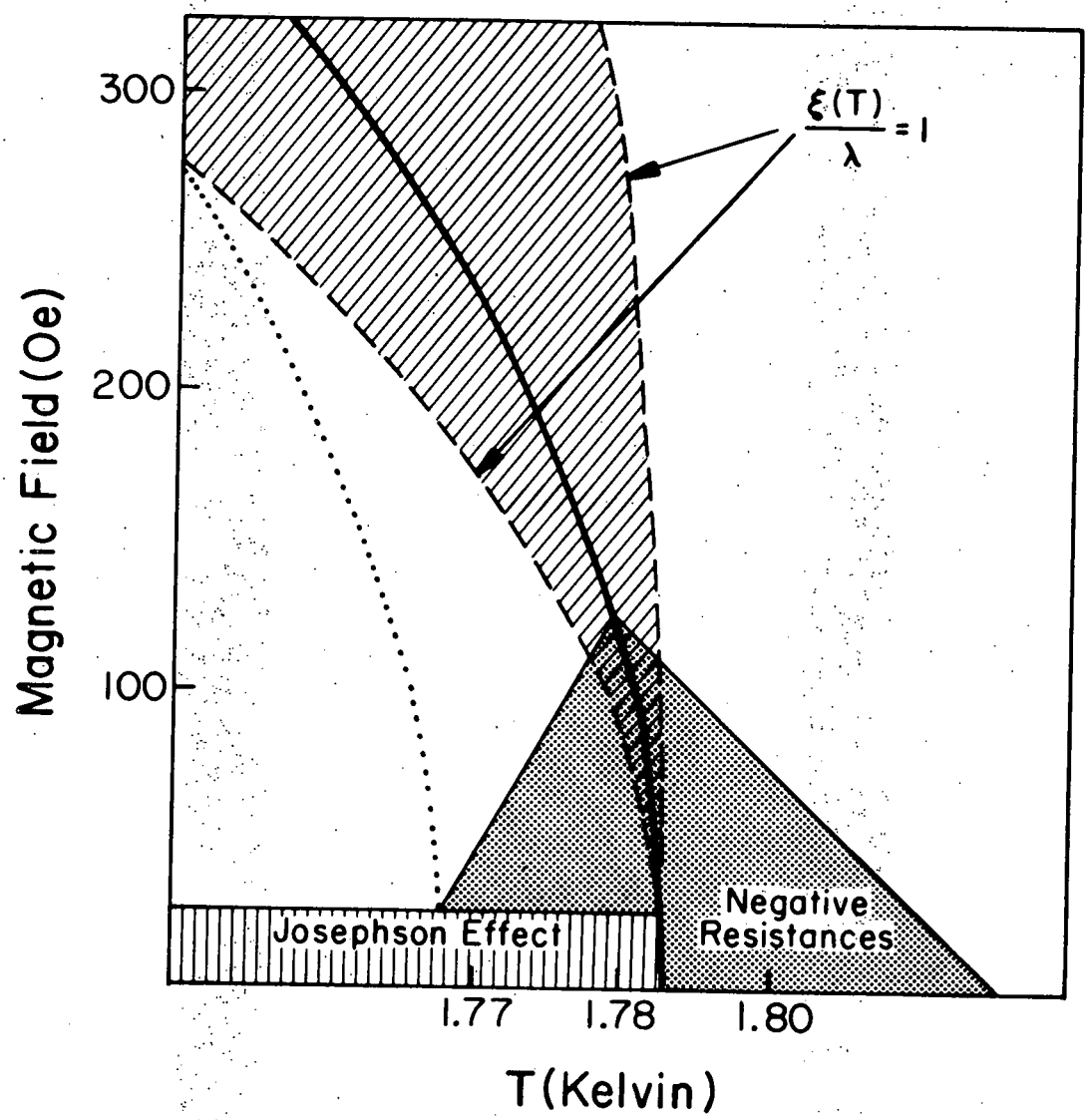

Fig. (37) Regions in the H-T plane where measurements on sample A12-64 were carried out. Similar drawings could be made for other samples. The heavy solid line corresponds to the superconducting normal phase boundary. The shaded region in the center is approximately the non-hydrodynamic region. The dotted line below $T_c(H)$ corresponds to the lower temperature limit where the propagating mode is observed.

extrapolate to a negative frequency as q goes to zero. Second, on the low frequency side of the main peak in the susceptibility, a shoulder develops. This shoulder is associated with the diffusive peak at zero frequency in the structure factor.

D. DISCUSSION OF DATA FOR $T < T_c(H)$

Although there has been substantial experimental and theoretical investigations of dynamical fluctuation effects above the superconducting transition temperature, little quantitative information about the dynamics below T_c is available. The measurements of Lehoczky and Briscoe,[69] of the effects of order parameter fluctuations on the ac conductivity of thin lead films below T_c, have been claimed to be in agreement with a description of fluctuations by a diffusive time-dependent Ginzburg-Landau equation. However, this equation does not adequately describe the effects reported in this investigation for $T < T_c(H)$.

That the diffusive time-dependent Ginzburg-Landau equation is inadequate below T_c is well known. As derived from microscopic theory by Abrahams and Tsuneto,[26] it is strictly valid only for $T > T_c$, or $\Delta(r,t) = 0$. In their derivation they found the following three equations for the relaxation of the order parameter, for supercurrent density, and for the charge density:

$$\hbar\gamma\left(\frac{\partial}{\partial t} + \frac{2\mu_i}{\hbar}\right)\psi = \frac{\delta_F}{\delta\psi^*}, \qquad (64)$$

$$\vec{j}_s = \frac{ie\hbar}{m}(\psi^*\vec{\nabla}\psi - \frac{ie2}{\hbar c}\bar{A})\psi - c.c. \qquad (65)$$

$$\delta\rho = \frac{3ie\hbar}{mv_f}(\psi^*(\frac{\partial}{\partial t} + \frac{2i\mu}{\hbar})\psi - c.c. - \frac{3ne^2}{mv_f^2}V. \qquad (66)$$

In the above μ is the electrochemical potential, γ is a parameter characterizing the relaxation rate:

$$\gamma = \frac{\pi}{8k_BT_c}\frac{h^2}{2m\,\xi^2(0)}$$

and eV is the electrical potential energy. Unfortunately, when a gap exists, Eqs. (65) and (66) do not satisfy a continuity equation

$$\vec{\nabla}\cdot\vec{j} + \frac{\partial\rho}{\partial t} = 0\,, \qquad (67)$$

where

$$\vec{j} = \vec{j}_s + \vec{j}_n$$

and

$$\rho = \rho_s + \rho_n\,.$$

This violation of charge conservation is the central difficulty with the time-dependent generalizations of the Ginzburg-Landau theory and appears to arise from the nonlocality of the theory of superconductivity when there is an energy gap. Physically the problem of the conversion of normal fluid (thermal excitations) to superfluid has not been treated properly.

To avoid the difficulties associated with the energy gap, Gor'kov and Eliashberg[19] considered the case of a superconductor with a sufficient concentration of paramagnetic impurities to exhibit a gapless regime below T_c. They derived a set of local-charge conserving, time-dependent equations valid in the gapless regime. In their theory, a new function, the anomalous term U was introduced to describe the coupling of order parameter fluctuations to density fluctuations:

$$U = V + \frac{vf^2}{3ne^2} \delta\rho \tag{68}$$

Here eU may be identified with the electrochemical potential. Associating the electrochemical potential with the anomalous term U, the time-dependent Ginzburg-Landau equation (Eq. (64)) derived by Abrahams and Tsuneto is seen to be equivalent to the equations of Gor'kov and Eliashberg in the gapless regime. However the chemical potential is given by

$$\mu = \mu_0 + \frac{\partial\mu}{\partial\rho} \delta\rho \tag{69}$$

and the charge density is not given by Eq. (66) but is calculated from Eq. (60), the equation of continuity, and Eq. (65), the equation for the supercurrent.

Detailed calculations of the pair-field susceptibility have been carried out by Brieskorn et al.[17] and Maki and Sato[18] using the Gor'kov-Eliashberg equations.

The principle feature in these calculations is the appearance of a collective mode involving fluctuations in the phase of the order parameter, which resembles the "fourth sound" mode of liquid He^4.

Another time-dependent generalization of the Ginzburg-Landau equation which is of interest is that of Schmid and Schön.[70] They have used the microscopic theory of Eliashberg and Eilenberger to derive a set of linearized equations for the deviations from equilibrium of both the quasiparticle distribution function and the order parameter. Recently they have used these equations to derive a dispersion relation for a collective mode in the phase of the order parameter which is similar to the mode seen in this investigation.[23]

Since it is apparent from the data that a propagating mode exists in the junction-superconductor system, the next section contains a brief review of the subject of propagating modes in Josephson junctions and superconductors. Following this a discussion of theoretical calculations of the pair-field susceptibility and collective modes which have been carried out as a result of these investigations is given. To conclude this section, a brief discussion of the relationship of this investigation to other experimental work on non-equilibrium processes below T_c is given.

D.1 Collective Modes

The finite frequency peak in the structure factor clearly demonstrates the existence of a propagating low frequency order parameter collective mode in the superconductor-junction system. In this section we discuss the known collective excitations of Josephson junctions and superconductors that could be related to the phenomena observed in this investigation.

The collective excitations in the phase differences across a Josephson junction are described by the equation of motion[60]

$$\left(\frac{\partial^2}{\partial y^2} + \frac{\partial^2}{\partial z^2} - \frac{1}{\bar{c}^2} \frac{\partial^2}{\partial t^2} \right) \phi = \lambda_J^{-1} \sin \phi , \qquad (70)$$

where the geometry of the junction is that shown in Fig. (1). Here ϕ is the phase difference across the junction, λ_J is the Josephson penetration depth given by

$$\lambda_J = \left(\frac{\hbar c}{8\pi e (\lambda + \lambda' + \delta) j_1} \right)^{\frac{1}{2}} , \qquad (71)$$

where δ is the thickness of the insulating barrier and the penetration depth of the electrodes are λ and λ'. The wave velocity is

$$\bar{c} = c \left[\frac{\delta}{(\lambda + \lambda' + \delta)} \frac{1}{\epsilon} \right]^{\frac{1}{2}} , \qquad (72)$$

where ϵ is the dielectric constant and c is the velocity of light.

Magnetic fields completely penetrate the low transition temperature electrode in this investigation because measurements were carried out at temperatures close to T_c. Consequently, the penetration depth may be replaced by the thickness d. The electric field in the junction is related to the phase difference by the Gor'kov-Josephson equation

$$\frac{\partial \Phi}{\partial t} = \frac{2eE_x \delta}{\hbar} \quad . \tag{73}$$

Using Eq. (73) in Eq. (70), the free fluctuations of the electric field are found to be the so-called Swihart modes of a superconducting junction.[71] These are slow transverse magnetic waves in the junction which have a phononlike dispersion relation and a phase velocity (and group velocity) $\bar{c}$. For the junction used in this investigation, $\bar{c}$ is approximately 1/20 the speed of light ($\lambda' = 370$ Å, $\lambda = d = 1200$ Å, $\epsilon = 5$). Swihart modes have been observed in experiments with superconducting strip transmission lines[72] and in an experiment by Eck et al.[73] in which they were both driven and detected by the Josephson current.

In the experiments of Eck et al., the ac Josephson current density across the junction is given by

$$j = j_1 \sin (\omega_o t - qy + \phi_o) \ , \tag{74}$$

where Eq. (19) gives the relationship between ω_o and q, and the dc voltage and magnetic field, respectively. When the phase velocity ω_o/q matches the phase velocity of the Swihart modes $\bar{c}$, the Josephson current transfers energy into the TM electromagnetic modes of the junction. The energy is dissipated by losses in the barrier region and by external radiation. The dc current-voltage charactertistic of a voltage-biased junction is affected by the build-up of the fields in the barrier in a fashion qualitatively similar to what was seen here, but quantitatively very different. The wave velocity $\bar{c}$ is always much higher than the velocity of the mode of the present investigation.[73]

If Eq. (70) is solved for small fluctuations of the phase about zero, the so-called Josephson plasma oscillations are obtained.[32] Their dispersion relation is

$$\omega = \left[\omega_p^2 + \bar{c}\, q^2\right]^{\frac{1}{2}} . \tag{75}$$

Here ω_p is the Josephson plasma frequency which is given by

$$\omega_p = \left(\frac{(2e)^2 E_1}{\hbar^2 C}\right)^{\frac{1}{2}} \tag{76}$$

where E_1 is the Josephson coupling energy and C is the capacitance of the junction. ω_p is approximately 1 to 5 X 10^{10} sec $^{-1}$ for the junctions investigated in this work in the temperature range of interest.

The plasma mode is quantitatively different from what is observed experimentally. The positive intercept of the frequency which would be large enough to be evident is not observed, and the velocity of these plasma modes is also much larger than the velocity of the experimentally observed mode.

There is also the possibility of collective modes associated with the motion of vortices found in the barriers of wide Josephson junctions in a magnetic field. Since the linear dimensions of junctions investigated were small compared to λ_J, it is unlikely that modes of this type play any role in explaining the observations.

The most convincing evidence that an order parameter collective mode rather than a junction mode is being observed is that the features of the excess-current voltage characteristic below T_c which we have associated with the mode, develop <u>continuously</u> from the behavior above T_c which may be related to the pair-field susceptibility. There is no reason to believe that any mode of the junction itself would behave in this manner.

In the past, the existence of a low-frequency collective excitation of the order parameter with a phonon-like dispersion relation in an isolated charged superconductor, has been thought to be highly unlikely.[74] It is well known that when the long-range Coulomb interaction is taken into account, any phonon-like

mode involving charge density fluctuations will be shifted to a high frequency plasma mode. If the collective mode involves only oscillations in the phase of the order parameter, the Gor'kov-Josephson relation implies the existence of a time-dependent fluctuation in the electric field which will produce charge density fluctuations. The Coulomb interaction again drives the frequency up to the electrom plasma frequency.

The above discussion neglects the possibility of a screening of the Coulomb interaction. Three possible screening mechanisms have been suggested. First, since the frequency of the collective mode found in this work is low, the ions of the lattice could screen the electrons by following their oscillations.[67] A second idea is that normal fluid itself could move relative to the superfluid to maintain charge neutrality. A third possibility is the conjecture that the mode is not a free mode of the superconductor but propagates only because of the presence of the junction. That is, one might conjecture that the ac currents in the junction somehow provide a screening mechanism. The first two ideas are discussed in the next section.

In neutral superfluids (He II and He^3) or superconductors in which the Coulomb interaction is completely screened, conditions are favorable for the existence of propagating order parameter modes. In particular, there is a question of the existence of

hydrodynamic modes in superconductors, analogous to the second and fourth sound modes in liquid helium that exist below the lambda point. In helium, second sound is a temperature-entropy wave with a phonon-like dispersion relation. In a two-fluid model it corresponds to a relative oscillation of the normal and superfluid such that the total density of the fluid is constant. There has been some discussion in the literature as to the possibility of the propagation of second sound in superconductors, with most authors coming to a negative conclusion.[75-77] Since second sound is a wave in the amplitude of the order parameter with constant total density, the Coulomb interaction would not prevent its existence, however the hydrodynamic requirement that $\lambda > l_T$ where l_T is a characteristic thermalizing length, is not satisfied in the normal electron fluid. In most practical superconductors and in particular, in the disordered films used in this investigation, the electron-electron scattering length is much longer than the electron-lattice interaction length. Thus the normal fluid is not in local thermal equilibrium and a hydrodynamic mode involving the motion of the normal fluid is not possible.

There has also been some discussion of the existence in a charged superconductor near T_c of a nonhydrodynamic second sound like mode, in which the normal fluid and superfluid are in relative motion but neither

are in local thermal equilibrium. A wave-like motion somewhat similar to this mode is discussed in the next section.

The situation in which the normal electrons are strongly scattered by lattice impurities and phonons resembles the fourth sound mode in helium. There, the motion of the normal fluid is inhibited by its viscosity, as the geometry of the containing vessel is one in which the liquid helium fills a porous stationary matrix of solid material. Fourth sound is a temperature-density wave in which only the superfluid is in motion. In a superconductor, a fourth sound like mode would be one in which the normal fluid is clamped to the lattice, with the motion of the superfluid satisfying a phonon-like dispersion relation. Such a mode has been predicted to propagate in neutral superconductors in the gapless region by Brieskorn et al.[17] and independently by Maki and Sato.[18] Its velocity in the $q \to 0$, $\omega \to 0$ limit is given by

$$c_4 = \left[\frac{\Delta(T)}{\pi} \frac{T_c}{T} \frac{8}{\hbar} \xi^2(0) \psi' (\rho + \tfrac{1}{2}) \right]^{\frac{1}{2}} \tag{77}$$

The quantities ρ and $\psi'(t)$ are the depairing parameter characterizing the gapless state and the trigamma function respectively.[37] The fourth sound mode corresponds to a wave in the imaginary part of the order parameter, which to first order is equivalent to a wave in the phase of the order parameter. This mode

is discussed in the next section.

It must be emphasized that there is a danger that analogies between propagating modes in helium and superconductors may be superficial. Fourth sound in helium involves fluctuations in the amplitude of the order parameter, while the mode suggested to be the analogy in a superconductor involves fluctuations in the phase of the order paramater. In helium, local thermal equilibrium is required for the existence of fourth sound while the fourth sound mode in a gapless superconductor is a microscopic mode which exists outside the hydrodynamic regime.

Finally, no discussion of collective modes would be complete without mentioning both the well-known Anderson-Bogoliuvbov [74, 78, 79] mode and excitons.[79] The Anderson-Bogoliuvbov mode is longitudinal long wavelength nonhydrodynamic density fluctuation of the electronic system as a whole. In a neutral superconductor at T = 0 it has a dispersion relation of the form

$$\omega = \sqrt{\frac{1}{3}} \; v_f \, q \; . \tag{79}$$

This mode was originally included in the BCS theory to restore gauge invariance. It is a plasmon in a charge system.

The existence of a microscopic, gapless, low-frequency collective mode appearing at the phase transition follows from the Goldstone Theorem [79, 80] and the

idea that symmetry breaking occurs at the transition. Qualitatively,[79] the Goldstone Theorem states that if an infinitesimal uniform change of the ground state produces a new ground state degenerate with it, an infinitesimal slowly varying change in the state (which interpolates between the ground states) will result in a state of low energy provided only (as is almost always the case) that the restoring force is proportional to the gradient of the variation. In an isotropic ferromagnet, the fact that there are ground states for each direction of magnetization implies that states in which the magnetization direction varies slowly in space, have a low energy. These states are spin waves. In a superconductor, the degeneracy is connected with the phase of the condensed pairs of fermions which make up the superconducting ground state. Thus a low energy wave in the phase of the order parameter is expected at the superconducting phase transition. This mode, a Goldstone-Boson is identified with the mode which has been called fourth sound which is discussed in Refs. 17 and 18 and the Anderson-Bogoliuvbov mode. That oscillations in the phase of the order parameter couple to longitudinal density fluctuation is easily seen from Eq. (69) and the Gor'kov-Josephson relation.

We conclude this section by mentioning excitons.[79] Roughly speaking, exciton states having energies lying within the energy gap may be pictured as excited bound

pairs. However, it is not known whether these modes contribute to the susceptibility, or indeed if they are relevant to this work.

D.2 Pertinent Theoretical Calculations

In this section we will describe theoretical calculations of the pair-field susceptibility of a superconductor and of collective modes in a superconductor which have been carried out to explain the results of these experimental investigations. The calculation of $\chi(\omega,q)$ for the idealized case of a gapless neutral superconductor described first. Although it is probably not actually applicable to the present investigation, it does provide valuable insight into the interpretations of the results. After the results of these calculations were published, Šimánek suggested a phenomenological method whereby a phonon-like mode similar to the fourth sound mode could be obtained for the case of a charged superconductor by considering the coupling of electron density to the lattice phonons. This calculation is described next. Finally we describe the recent calculation carried out by Schmid and Schön in which a propagating order parameter mode is found near T_c in a charged superconductor with a gap. The dispersion relation of the mode is qualitatively similar to that observed in the experiments.

D.2.a Calculation of the Susceptibility for a Gapless Neutral Superconductor. The calculations of Brieskorn, Dinter and Schmidt,[17] and Maki and Sato,[18] of the pair-field susceptibility of a neutral, gapless superconductor yield results qualitatively very similar to the data. These calculations are carried out for the gapless regime because in this regime a set of time-dependent macroscopic equations for the order parameter have been derived from microscopic theory. The case of a neutral superconductor is considered to avoid the problems associated with the long-range Coulomb interaction.

A gapless superconductor[37] is characterized by depairing parameter ρ which is a measure of the strength with which a particular perturbation acts to destroy pairs. A thin film in a parallel magnetic field will have a depairing parameter given by

$$\rho = \frac{1}{12\pi k_B T_c} \frac{e^2 H^2 d^2}{\hbar^2 c^2} . \qquad (80)$$

Paramagnetic impurities in a film provide a depairing mechanism with a value of ρ given by

$$\rho = \frac{1}{2\pi k_B T_c} \frac{nm\, p_o}{2\pi^2} S(S+1) \left| \bar{J} \right|^2 . \qquad (81)$$

Here n is the density of magnetic impurities, m is the mass of the electron, S is the impurity spin, p_o is the Fermi momentum, and J is the exchange integral.

A nonzero value of ρ has several quantitative effects on the superconducting state of a film. The transition temperature is shifted to a lower value given by solutions of

$$\ln T_c(0)/T_c(\rho) + \psi\left(\tfrac{1}{2}+\rho\right) - \psi\left(\tfrac{1}{2}\right) = 0 , \tag{82}$$

where $\psi(\rho)$ is the digamma function. Over a range of temperatures below $T_c(\rho)$ the superconductor may be gapless. The boundary between the gapless region and the region where a gap in the excitation spectrum exists, is given by the temperature at which the order parameter is equal to the pair breaking strength:

$$\hbar\Gamma = \Delta(T) = 2\pi\rho\, k_B T_c(\rho) . \tag{83}$$

For $T > T_c(\rho)$ the pair-field susceptibility is also modified. A time-dependent generalization of the Ginzburg-Landau theory including the depairing mechanism, and the magnetic field can be used in the region above T_c to calculate $\chi(\omega,q)$. The result given in Ref. 17 is

$$\chi(\omega,q) = \frac{4\pi k_B T}{N(0)\psi(\rho+\frac{1}{2})} \left[-i\hbar\omega + \hbar D(q^2 + 2m\alpha)\right]. \tag{84}$$

Here D is the diffusion constant, related to the coherence length through

$$D = \tfrac{1}{3} v_f l = \frac{8 k_B T_c}{\pi\hbar} \xi^2(0) , \tag{85}$$

and α is the coefficient of $\Delta^2(T)$ in the free energy,

$$\alpha = \frac{4 k_B(T - T_c(\rho))}{\pi m\hbar D} f(\rho) , \tag{86}$$

where

$$f(\rho) = \frac{\pi^2}{2} \frac{1 - \rho \psi'(\rho + \frac{1}{2})}{\psi'(\rho + \frac{1}{2})} . \tag{87}$$

The quasi-Lorentzian shape of the excess current ($I \propto \text{Im } \chi(\omega,q)$) is the same as in the absence of a pair breaking mechanism. However, the peak in Im $\chi(\omega,q)$ is not at the pair relaxation frequency Γ_o but is shifted to a lower frequency. This is easily seen by maximizing Im $\chi(\omega,q)$ at fixed T, ρ, and H. The maximum is at

$$\omega_m = Dq^2 + f(\rho)\Gamma_o \tag{88}$$

Thus the function $f(\rho)$ determines the shift of the peak of the excess I-V characteristic, and measurement of the peak voltage of the excess current-voltage characteristic, in principle, can serve to determine the pair breaking strength through Eqs. (87) and (88).

In References 17 and 18 essentially equivalent expressions for the pair-field susceptibility are obtained. The fluctuations of the order parameter are found to consist of two distinct modes: one associated with amplitude fluctuations and the other, phase fluctuations. Fluctuations of the amplitude are described by a diffusion equation and are thus nonpropagating, whereas the fluctuations

of the phase of the order parameter propagate with a phonon-like dispersion relation in the hydrodynamic limit.

The calculation of the pair-field susceptibility below T_c is carried out either by using the Gor'kov-Eliashberg equations for a gapless neutral superconductor with paramagnetic impurities or equivalent microscopic methods. The order parameter in the gapless state is linearized with respect to its deviation about its average value

$$\Delta = \Delta_o + \Delta_{||} + i \Delta_{\perp} ,$$

where $\Delta_{||}$ is associated with amplitude fluctuations and $\Delta_{\perp}$ to first order, is associated with phase fluctuations. The deviations $\Delta_{||}$, $\Delta_{\perp}$ then satisfy the equations of Gor'kov and Eliashberg. The amplitude fluctuations couple to the real part of the anomalous term U, while phase fluctuations couple to the imaginary part of U. The anomalous term $U_{||} + iU_{\perp}$ describes the coupling between the order parameter and density fluctuations. $\Delta_{||}$ satisfies a diffusion equation and $\Delta_{\perp}$ satisfies a wave equation. The pair-field susceptibility obtained by Breiskorn et al. is

$$\chi(\omega,q) = \frac{2\pi k_B T\,\hbar}{N(0)\,\psi\left(\rho+\frac{1}{2}\right)}$$

$$\left\{\left[i\omega + D(q^2 - 4m\alpha) - \frac{i\omega\,\Delta_o^2\,g(\rho)}{(i\hbar\omega + \hbar Dq^2)\,\pi k_B T\,\psi\left(\rho+\frac{1}{2}\right)}\right]^{-1} + \left[Dq^2 - \frac{i\omega/\psi'\left(\rho+\frac{1}{2}\right)}{A/\left(\psi'\left(\rho+\frac{1}{2}+B\right)\right)}\right]^{-1}\right\} . \qquad (89)$$

Here $\Delta_o^2 = -\alpha/\beta$ where α is given by Eq. (86), and β is the coefficient of the fourth order term in the expansion of the free energy which in the gapless regime is given by

$$\beta = \frac{\psi''\left(\rho+\frac{1}{2}\right) + \frac{\rho}{3}\,\psi'''\left(\rho+\frac{1}{2}\right)}{\pi m k_B T \hbar D\,\psi'\left(\rho+\frac{1}{2}\right)} . \qquad (90)$$

The quantities A and $g(\rho)$ are functions of the depairing parameter ρ given by

$$A = \left(1 + \Delta_o^2/\left(\pi\rho\,k_B T\hbar(-i\omega - Dq^2)\right)\right)^{\frac{1}{2}} \qquad (91)$$

and

$$g(\rho) = \frac{\psi'\left(\rho+\frac{1}{2}\right) + \rho\psi''\left(\rho+\frac{1}{2}\right)}{2\rho} . \qquad (92)$$

If the Gor'kov-Eliashberg equations are used to determine $\chi(\omega,q)$, B = 0, however in the alternate microscopic calculation

$$B = -i\hbar\omega\,\frac{|\lambda|\,N(0)\,\Delta_o^2}{\pi k_B T\hbar^2(-i\omega - Dq^2)} . \qquad (93)$$

where λ is the strength of the effective electron-electron interaction. $\chi(\omega,q)$ determined by Maki and Sato[18] is qualitatively similar to the above expressions, however it differs quantitatively because of technical theoretical errors in its derivation.

The first term in the brackets of Eq. (89) represents the contribution to the susceptibility from the nonpropagating amplitude fluctuations. The second term is a consequence of the propagating phase fluctuations. In the limit $q \to 0$, $\omega \to 0$, the dispersion relation for the latter is given by

$$\omega = \left(\Delta_o^2 \frac{\hbar D \psi'(\rho + \frac{1}{2})}{\pi k_B T} \right)^{\frac{1}{2}} q = \left(\frac{1}{3} v_f^2 \frac{\rho_s}{\rho} \right)^2 q \,, \tag{94}$$

where ρ_s/ρ is the superfluid fraction defined by

$$\frac{\rho_s}{\rho} = \frac{\lambda \Delta^2}{\pi k_B T} \psi'(\rho + \tfrac{1}{2}) \,. \tag{95}$$

For finite q the dispersion relation is not actually a linear function of wave vector and must be explicitly calculated from the q dependence of the peak in the structure factor.

The relevance of the above results to the present experiments depends on the existence of a gapless region in the phase diagram of the aluminum film below $T_c(\rho)$ in which the theory can be applied. If the pair breaking is assumed to be entirely due to the applied magnetic field, the width of the gapless region is the order of

1×10^{-5} K. However, if there are paramagnetic impurities in the aluminum film, the pair breaking increases significantly, with a corresponding increase in the size of the gapless region. With a concentration of magnetic impurities of 100 ppm, ρ is approximately .075 and the aluminum film is gapless in the temperature range $(T - T_c)/T_c = -2 \times 10^{-2}$. There is no reason to believe a priori that concentrations of this magnitude could exist in the films. Analysis of the actual films used in the measurements was not possible. Auger analysis of an aluminum film prepared in the same manner as the film used in the experiments indicated a contamination of iron at a concentration of .1%, uniformly distributed through the film. This was extremely surprising since the assay of the aluminum wire which was supplied by United Mineral and Chemical Company reported an iron impurity concentration of less than 5 ppm. A subsequent analysis of the aluminum wire showed a large concentration of iron (5%) and trace amounts of chromium and nickel in a surface layer (1000 Å deep). The wire apparently had been drawn through a stainless steel die leaving impurities in the surface layer. This contamination is most likely the source of the iron in the test films. Junctions A12-61, 64 and 79 were made with this wire while A12-36 was made from a differernt batch of wire obtained from Johnson, Matthey and Company. We are presently attempting to determine the iron impurity

level of the latter by analyzing an old film used in a different experiment which was made from wire specimen. As of the time of this writing, results were not available. If films made from the earlier batch do not have iron contamination, then it is possible that the absence of such contamination may have produced the "anomalous" behavior noted in sample Al2-36.

Admitting the possibility of contamination does not imply the existence of significant depairing however. It is well known that dilute concentrations of iron in aluminum do not exhibit localized moments.[81] The effect of the iron on the superconducting state has been termed a pair weakening rather than a pair breaking effect.[82] The former produces a downward shift in the transition temperature not accompanied by a region of gaplessness.

Further experimental and theoretical work is necessary. Experimentally, films must be made that are known to be free from magnetic or paramagnetic impurities, while the effect of pair weakening mechanisms on the pair-field susceptibility should be investigated theoretically.

If the contamination of the aluminum film does result in a depairing, then Eqs. (87) and (88) in principle, give a method to determine ρ directly from the experimental data of V_p versus T in zero field for $T > T_c$. Brieskorn et al. have determined a value of ρ of .074. In their analysis ρ was found by using the data shown in Fig. (28) for sample Al2-36, which had been published previously

in Ref. 10. Because of the limited data shown in Fig. (28) this determination of ρ is subject to large errors.

We have determined limits on the values of ρ for samples Al2-5, 36, 64, 79 by using detailed measurements of V_p versus T for $T > T_c$ obtained in zero field. The values of the depairing parameters determined in this manner are listed in Table IV along with the corresponding width of the gapless region calculated from Eq. (83). ρ was determined by assuming the shift in the slope of V_p versus T was entirely a consequence of the existence of a pair breaking mechanism. Sample Al2-61 is not included because only limited data was taken on this sample, making an accurate determination of $^{dV}p/dT$ impossible. Extensive measurements of the temperature dependence of V_p were make on samples Al2-64 and 79 to obtain an accurate value of $^{dV}p/dT$, for the determination of ρ. Although these values are very close to the theoretical prediction, the scatter in the data still allows a sizable value of ρ to be chosen if one used the largest error in $^{dV}p/dT$ to determine ρ.

The values of ρ listed in Table IV do not provide evidence for the existence of a relatively large depairing parameter, but set an upper limit on ρ. The depairing parameters determined in this manner are a reflection of the experimental errors in the

TABLE IV

Junction	Depairing Parameter	Width of Gapless Region (K)
A12-5	.046	15.8×10^{-3}
A12-36	.020	3.2×10^{-3}
A12-61	.078	42.2×10^{-3}
A12-64	.024	4.6×10^{-3}
A12-79	0	0

calculation of the slope of V_p versus T rather than an indication of pair breaking in the aluminum films. Thus, because of the errors involved in the calculation of dV_p/dT (usually around 3% to 5%) Eqs. (87) and (88) do not provide an accurate method to determine the value of ρ, when ρ is small ($\rho < .06$).

Further evidence against the existence of a large depairing mechanism in the aluminum film can be obtained by considering the secondary high voltage peak in the excess current-voltage characteristic which occurs at the aluminum gap voltage. If the explanation of this peak given by Šimánek and Hayward[64] is correct, then the existence of this peak is dependent on the existence of the gap in the excitation spectrum at that particular temperature. An upper limit on the width of the gapless region can be set by noting the temperature at which the peak first appears. In all the junctions studied, this is about 8mK below T_c, which corresponds to an upper limit on ρ of .032. Also, the shape of the peak is strongly dependent on the strength of the depairing. A ρ of about 1×10^{-4}, due entirely to the applied magnetic field, is enough to account for the experimental shape. If ρ is increased to .024, the peak is substantially washed out and becomes only a broad maximum at the gap voltage.[83]

Considering the preceding discussion, we believe there is no strong evidence to indicate that the films are gapless over a wide enough range of tempera-

ture for the calculations of Brieskorn et al. and Maki and Sato to be applicable to these experiments. However, we will assume for the sake of comparison to theory that the values of ρ listed in Table IV which are upper limits on ρ actually describe the films. When we compare the data to theory over the temperature range below $T_c(H)$ in which the superconductors are gapless then substantial differences between theory and experiment are still observed.

Brieskorn et al., using a value of ρ =.074 found that the theoretical results reproduced quite well the observed excess current voltage characteristic (see Fig. (1-d) of Ref. 17). Using a more realistic value for ρ from Table IV for sample A12-64, we find the agreement between theory and experiment not nearly so good. Figure (38) shows the susceptibility calculated from Eq. (89) with B=0, H=125 Oe, compared to the data for sample A12-64 at T = 177768K and H=125 Oe. The constants in Eq. (89) have been adjusted so that the magnitude of the theoretical excess current agrees with the experimental maximum. If a larger value of ρ is chosen, the theoretical distribution, peaks up more, becoming closer to that seen experimentally.

Shown in Fig. (39) is the temperature dependence of the peak voltage and inverse peak current determined with ρ = .024 from Eqs. (84) and (89) for $T > T_c$ and $T < T_c$ respectively and compared to data from sample

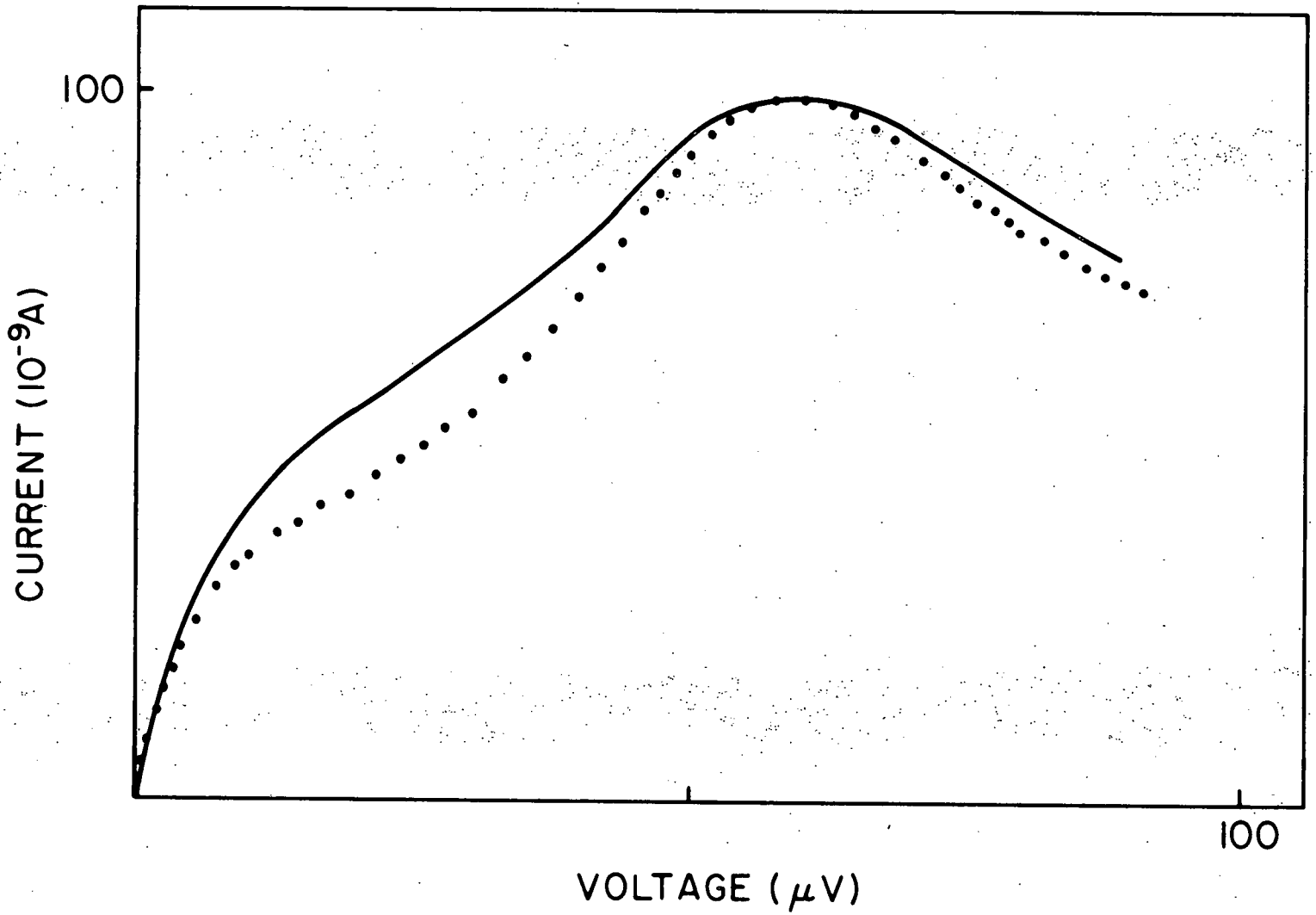

Fig. (38) Theoretical excess current (solid line determined from Eq. (89) at H = 125 Oe using ρ =.024, $\xi(0)$ = 520 Å and T = 1.77768 compared to the data (points) for Al2-64. The constants have been adjusted to make theory agree with experiment at the peak.

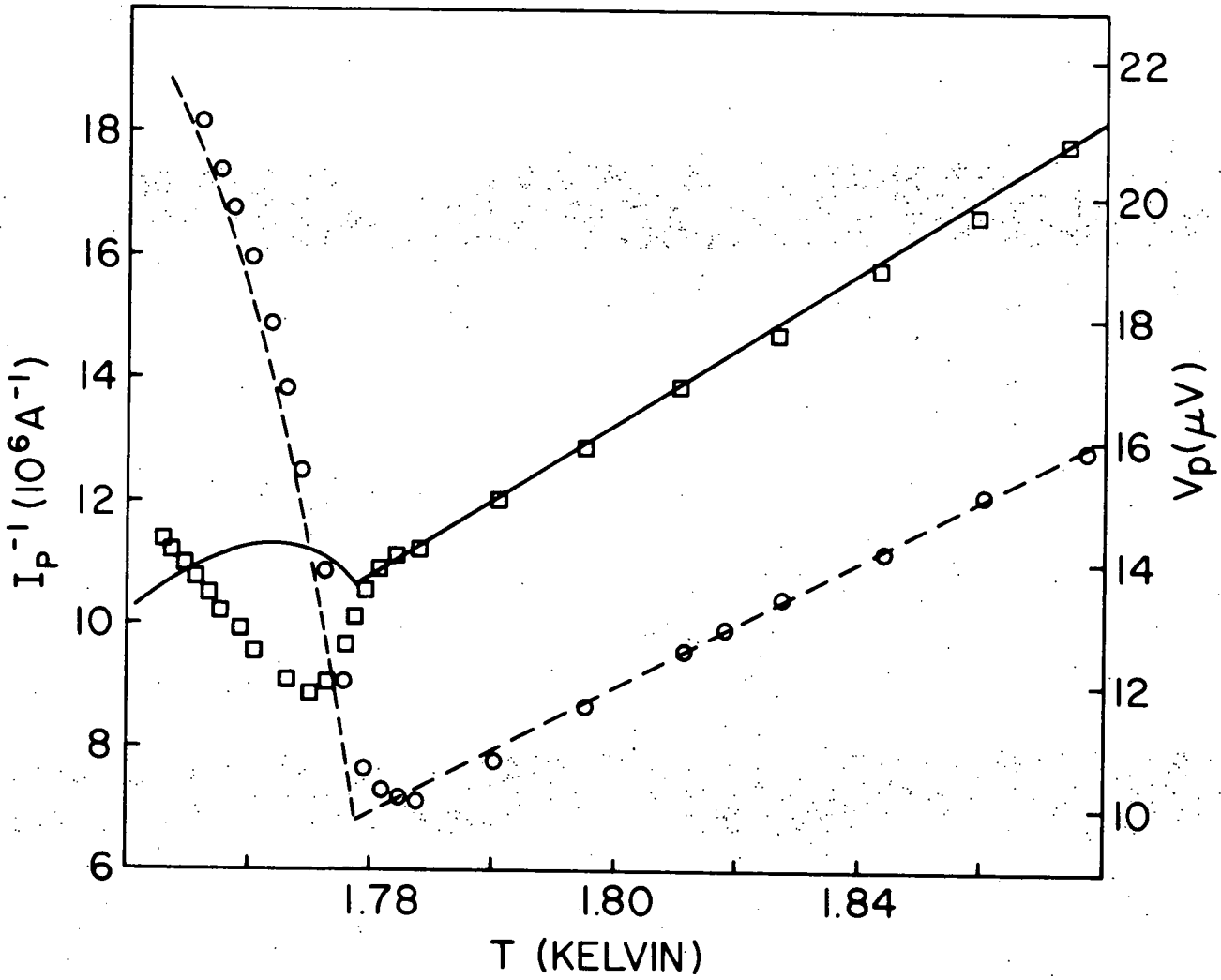

Fig. (39) Temperature dependence of experimental peak voltages (0) and peak current (□) of the excess current for Al2-64 compared to theoretical predictions of Eq. (89) with B = 0 and $\rho = .024$. Solid line is theoretical peak current and dashed line is the theoretical peak voltage. The magnetic field is 125 Oe.

Al2-64 at H=125 Oe. The constants in the theoretical expression for the excess current again have been adjusted to give the experimental slope and intercept for I_p^{-1} versus T. The theoretical prediction of the temperature dependence of the position of the peak is is excellent agreement with experiment for $T < T_c$, over a wider range of temperature than the width of the gapless region. However, the theoretical behavior of the inverse peak current is substantially different from experiment. Whereas the theoretical inverse peak current begins to rise at the transition and fall off a few mK below $T_c(H)$, the experimental curve falls off at $T_c(H)$ and turns around at 3-6 mK below $T_c(H)$. Increasing ρ tends to level off the peak in I_p^{-1} versus T.

If the theoretical predictions for the behavior of I_p^{-1} versus T are compared to data from sample Al2-36, the agreement between theory and experiment is qualitatively better; however there are still differences. As the field is increased, the relative nonmontonic behavior at T_c increases for sample Al2-36 (see Fig. 30). However, Eq. (89) predicts that as H is increased, the amplitude of the peak in I_p^{-1} versus T should get smaller rather than larger. The nonmontonic behavior in I_p^{-1} versus T below T_c has still not been adequately explained; however it does not seem to be a property of the gapless state.

Brieskorn et al. have also determined the structure factor and found qualitatively the same behavior as is observed experimentally. As T is reduced below T_c, a peak appears in $S(\omega,q)$ at finite frequency. This peak is a sensitive function of ρ. If instead of the value of ρ they use, we take $\rho = .024$ as is indicated for sample A12-64 in Table IV, we find the finite frequency peak in $S(\omega,q)$ to be substantially washed out. It does not emerge from the central peak until the temperature is well below the gapless region, where the theory does not hold. In Fig. (40) we show the dispersion relation for the finite frequency peak in $S(\omega,q)$ where we have only included the contribution to $S(\omega,q)$ from fluctuations in the imaginary part of the order parameter; i.e. we have neglected the first term on the right side of Eq. (89) in determining ω_p. By adjusting parameters such as $\xi(0)$ and $T_c(0)$ within the range of values consistent with the allowed experimental errors, we were not able to bring the theoretical curve into agreement with the experimental data. The dispersion relation does appear to be linear and to have a negative frequency intercept as is observed experimentally.

If we use $\rho = .074$ and compare the temperature dependence of the finite frequency peak in $S(\omega,q)$ determined from theory with experiment, we find that the theoretical frequencies fall well below the observed frequencies. For smaller ρ the disagreement becomes

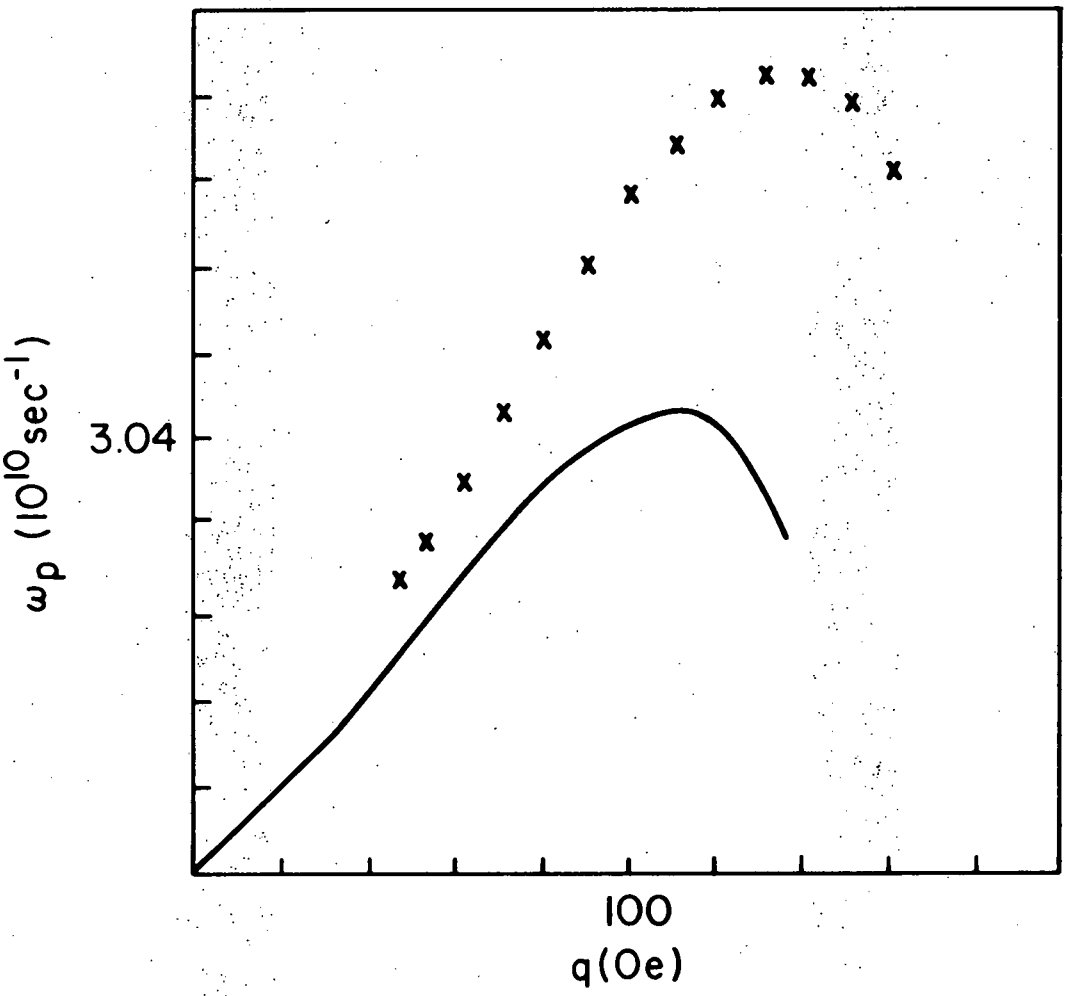

Fig. (40) Dispersion relation (solid line) determined from Eq. (89) with the first term in the brackets set equal to zero, compared to the data for Al2-64 at T = 1.77 K. A depairing parameter of ρ =.024 with D = 18.9 was used.

larger. The theoretical values of ω_p drawn in Fig. (3) of Ref. 10 as solid and dashed lines were determined by using the hydrodynamic limit for the velocity $\bar{c}$, Eq. (94), which only applies in the $\omega = q = 0$ limit. However, over the narrow gapless region (4-7 mK) the difference is small.

The fact that experimental frequencies are higher than the theoretical ones may be a consequence of the coupling of the collective mode to charge fluctuations which are not included in the Gor'kov-Eliashberg equations. A neutral theory would be expected to give a lower frequency than a theory including charge.

The following comments on the gapless theory seem to be noteworthy at this time:

(a) There is no strong evidence that the aluminum films are characterized by large depairing parameters. In fact, there seems to be strong indications that the only pair breaking mechanism involved is the applied magnetic field.

(b) The values of ρ listed in Table IV, rather than indicating a large pair breaking parameter are a reflection of the errors in determining the peak voltage.

(c) If (a) is the case, then the region of gaplessness is extremely small and no conclusions from this work can be drawn as to the validity of the theories of Brieskorn et al. and Maki and Sato.

(d) If (a) is not true and the mode seen is actually

a consequence of the superconductor being gapless, then Eqs. (87) and (88) which give the value of ρ from the peak voltage measurements above T_c are incorrect since they predict a value of ρ too small to explain the width of the gapless region. This would be a significant result since it implies that the theory which relates pair breaking mechanisms to the relaxation frequency shift is incorrect.[38]

(e) If (a) is not true and the values of ρ listed in Table IV are characteristic of the aluminum films, then although there is qualitative agreement between theory and experiment, there are still several serious discrepancies between the theory and the data in the temperature region where the superconductor would be gapless.

(f) Although it does not seem that the theories of Brieskorn et al. and Maki and Sato are applicable to this experiment, these theories do provide valuable insight into the physical processes occuring in the fluctuating films. From them we can infer that the finite frequency peak in the structure factor is associated with fluctuations in the imaginary part of the order parameter (phase fluctuations to the first order), while the central peak is associated with fluctuations is the real part of the order parameter (amplitude fluctuations).

(g) The possible existence of iron in some of the films is a complication whose implications to this work are

not well understood at this time. If as mentioned earlier the iron in aluminum is a pair weakening rather than a pair breaking mechanism, then the gapless theory is not an applicable and a theoretical calculation of the effect of pair weakening on the susceptibility should be carried out.

D.2.b Calculation of Šimánek In Section IV.D.1 it was stated that in charged superconductors, the Coulomb interaction prevents the occurence of an order parameter phonon-like mode, replacing it with a plasmon. After the calculations of Refs. 17 and 18 were published, Šimánek suggested that by including the coupling of longitudinal lattice phonons to the eletron-density fluctuations, a phonon-like mode in the order parameter would be obtained. Since the frequency of the collective mode is comparable with the frequencies of the longitudinal phonons, the ions follow the motion of the electrons and maintain charge neutrality.

Šimánek[21] has proposed the following set of equations to describe the coupling of lattice phonons to a wave-like motion of the superfluid where the normal fluid is fixed:

$$\frac{\partial Q}{\partial t^2}(k,T) + \Omega_L Q(k,t) = - V_k \rho(k,t)$$

$$j_s = - \frac{\rho}{t} \quad , \quad j_n = n v_n = 0$$

$$\frac{\partial v_s}{\partial t} = -\nabla \mu + \frac{e}{m} \vec{E} \qquad (96)$$

$$\vec{\nabla} \rightarrow = -4\pi \rho (\rho_L - \rho)$$

Here Q(k,t) is the k^{th} longitudinal lattice mode, Ω_L is the ionic plasma frequency, V_K is the electron ion coupling, μ is the electrochemical potential, and ρ_L is the ionic charge density. These equations can be reduced to two coupled wave equations whose solutions exhibit both optical and acoustical branches. The dispersion relation of the acoustical branch is

$$\omega^2 = \frac{\Omega_L^2}{\omega_p^2 X + \Omega_L^2} \left(\frac{v_f^2 X}{3} \right) q^2 . \qquad (97)$$

Here ω_p is the electronic plasma frequency and X is the superfluid fraction given near T_c by

$$\frac{\rho_s}{\rho} = \frac{n_s}{n} = \frac{7}{16} \frac{\zeta(3) \Delta^2(T)}{\pi^2 k_B^2 T_c^2(H)} \left(\frac{\xi^2(0)}{.55 \xi_o^2} \right) . \qquad (98)$$

Simanek also found the contribution to the structure factor due to fluctuation in the imaginary part of the order parameter to be proportional to

$$\left(1 + \frac{X \omega_p^2}{\Omega_L^2}\right)^{-1} . \qquad (99)$$

Using ρ_s given by Eq. (98) and $\Omega_L^2/\omega_p^2 = 5 \times 10^{-5}$ for aluminum, we have calculated ω as a function of temperature according to Eq. (97). These results are presented in Fig. (41) and compared to the data for sample A12-64 at H = 125 Oe. Although the behavior is

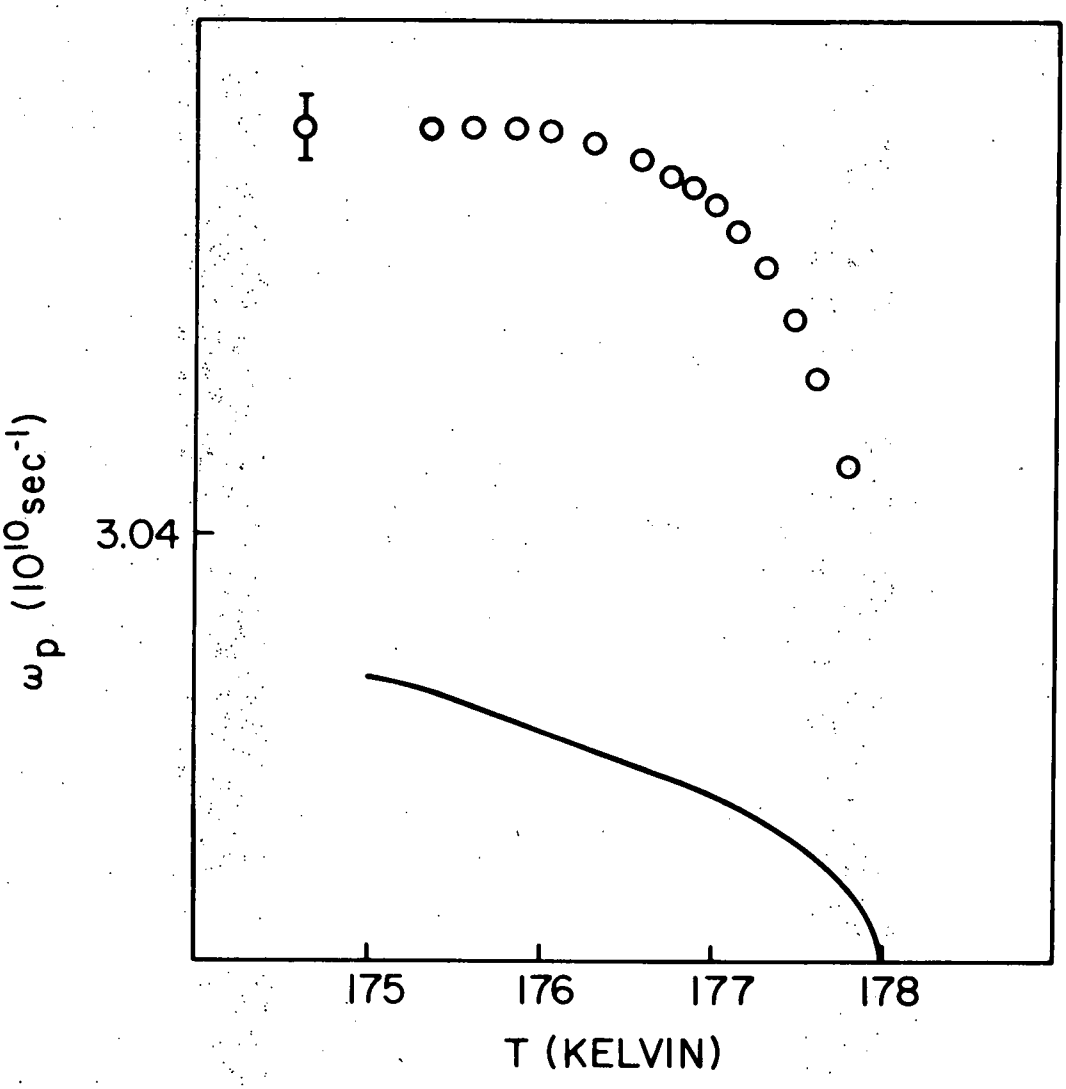

Fig. (41) Dependence of ω_p on temperature determined from Eq. (97) with D = 18.9 and H = 125 Oe compared to the data for A12-64.

qualitatively similar, the agreement between theory and experiment is not good. Also the dispersion relation determined using Eq. (97) will not predict the apparent negative frequency intercept observed in the data, since Eq. (98) is a linear function of wave vector with intercept at zero frequency.

It is suspected that the discrepancy between theory and experiment is due to the fact that the set of equations used to describe the oscillations is not complex enough to provide a valid description of the processes occuring in the experiment.

D.2.c The Calculation of Schmid and Schön The most recent theoretical explanation of the propagating order parameter mode has been given by Schmid and Schön,[20] who have carried out a microscopic calculation on a charged-dirty superconductor with a gap. They have found that near $T_c(H)$, wave-like motion of the superfluid is possible with little damping. The screening of the charge fluctuations is accomplished by the motion of the normal fluid. The calculation is based on a set of coupled linear equations for the changes in δf_E and $\delta\Delta$ which are the quasiparticle distribution function and the order parameter respectively. These equations have been derived from a generalization of the microscopic theories of Gor'kov, Eliashberg and Eilenberger.[70] Instead of determining the pair-field susceptibility,

only the oscillations in the imaginary part of the order parameter have been determined. In the limit of

$$\hbar\Gamma \ll \hbar\Omega \ll \Delta \ll k_B T , \tag{100}$$

and

$$Dq^2 \ll \omega ,$$

the following equations for the displacement fields X_s and X_n of the superfluid and the normal fluid respectively are found

$$\begin{aligned} \ddot{\vec{X}}_s &= c^2 \vec{\nabla}(\vec{\nabla} \vec{X}_s) + {}^e/_m \vec{E} \\ \dot{\vec{X}}_n &= \frac{e\tau}{m} \vec{E} , \end{aligned} \tag{101}$$

where τ is the collision time. The electric field is related to the charge density by Maxwell's equation.

$$\vec{\nabla}\cdot\vec{E} = -4\pi e \vec{\nabla}\cdot(\vec{X}_s n_s + \vec{X}_n n_n) . \tag{102}$$

With $n_n \approx n$ wave-like solutions to Eq. (101) of the from $\exp(i\vec{q}\vec{r} - \omega t)$ are possible with

(103)

$$\omega = \frac{i\pi\Delta^2(T)}{4\hbar k_B T} \pm \sqrt{\left(\frac{2\Delta(T)D}{\hbar}\right) q - \left(\frac{\pi\Delta^2(T)}{4\hbar k_B T}\right)^2} ,$$

where $\vec{E}$ is parallel to $\vec{q}$.

Physically this mode corresponds to relative motion of the normal and superfluid where neither the normal nor the superfluid are in local thermal equilibrium. The motion of the superfluid is wave-like. The resulting

charge separation induces a counterflow of normal fluid such that the total electric current is almost zero. The motion of the normal fluid is responsible for the damping, however near T_c the superfluid is a relatively small fraction of the total fluid so that the charge separation can be compensated by small oscillations of the normal fluid and the damping is subtantially reduced.

The characteristics of this mode are similar to what is observed experimentally. As shown in Fig. (32) the damping of the propagating mode seen experimentally increases as T is decreased from $T_c(H)$, while Eq. (103) also predicts that the damping, which is proportional to the imaginary part pf the dispersion relation, increases as T is lowered. Shown in Fig. (42) is the real part of Eq. (103), plotted as a function of temperature compared to data from sample A12-64. A value of $D = 16.9$ has been chosen to obtain the best agreement of theory to data. It is important to note that the theory is an extremely sensitive fucntion of D; if $D = 18.9$ is used, the agreement is not nearly as good.

The dispersion relation predicted by Eq. (103) is not phonon-like for small q, but rather it exhibits a cutoff wave vector below which the mode does not propagate. This behavior is plausible, since for large wave length oscillations of the superfluid, the normal fluid, which does not move freely, cannot move enough

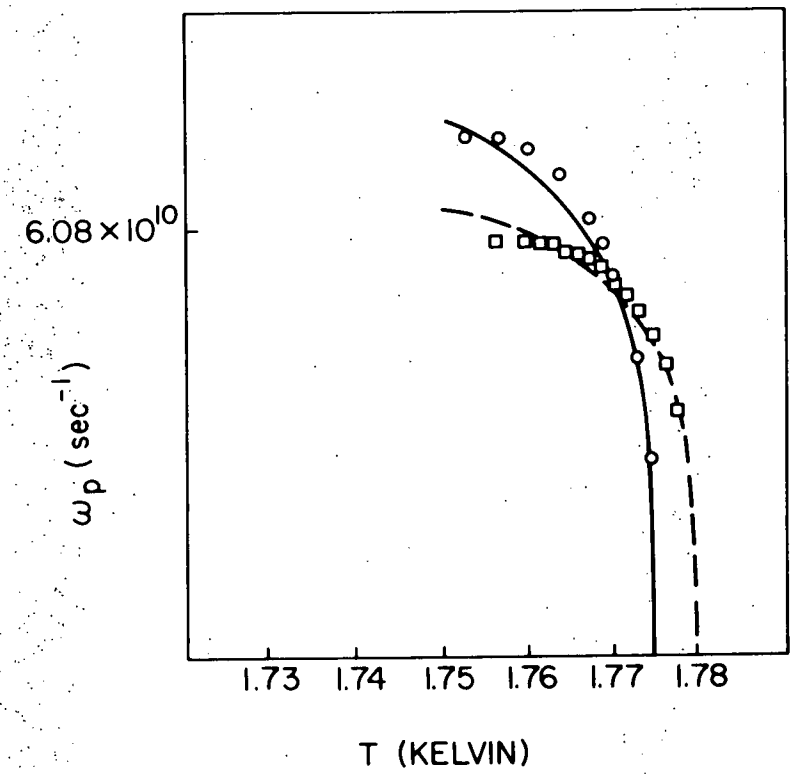

Fig. (42) Temperature dependence of ω_p calculated from Eq. (102) with D = 16.9 and H = 125 Oe (dashed line) and 150 Oe (solid line) compared with data for A12-64.

to maintain charge neutrality and thus the mode becomes highly damped. Shown in Fig. (43) is the dispersion relation predicted in Eq. (103) compared to the data for samples A12-64 and 79. As shown in Figs. (43.a) and (b) the agreement between theory and experiment is very good for temperatures close to $T_c(H)$. The shaded region of the plots indicates the range of ω_p versus q given by Eq. (103) consistent with the maximum allowable errors in the experimentally determined parameters. However, disagreement between theory and experiment becomes very evident at low temperatures because of a cutoff wave vector which is an increasing function of decreasing temperature. This is shown in Fig. (43.c) where we have determined the theoretical curve by using the parameters that gave the best agreement with the theory for the data of Fig. (43.a). The temperature dependence of the low q behavior is not evident in the data. The data shows that at a fixed q, ω_p is independent of temperature; that is, the velocity $(d\omega/dq)$ is temperature independent while theory predicts a temperature dependent velocity.

Also for the above reasons, Eq. (103) does not predict the apparent negative frequency intercept of the experimentally determined dispersion curve. It predicts a fall off from a linear relationship between q and ω where the high q values would extrapolate to zero. The data indicates the linear region extrapolates to a

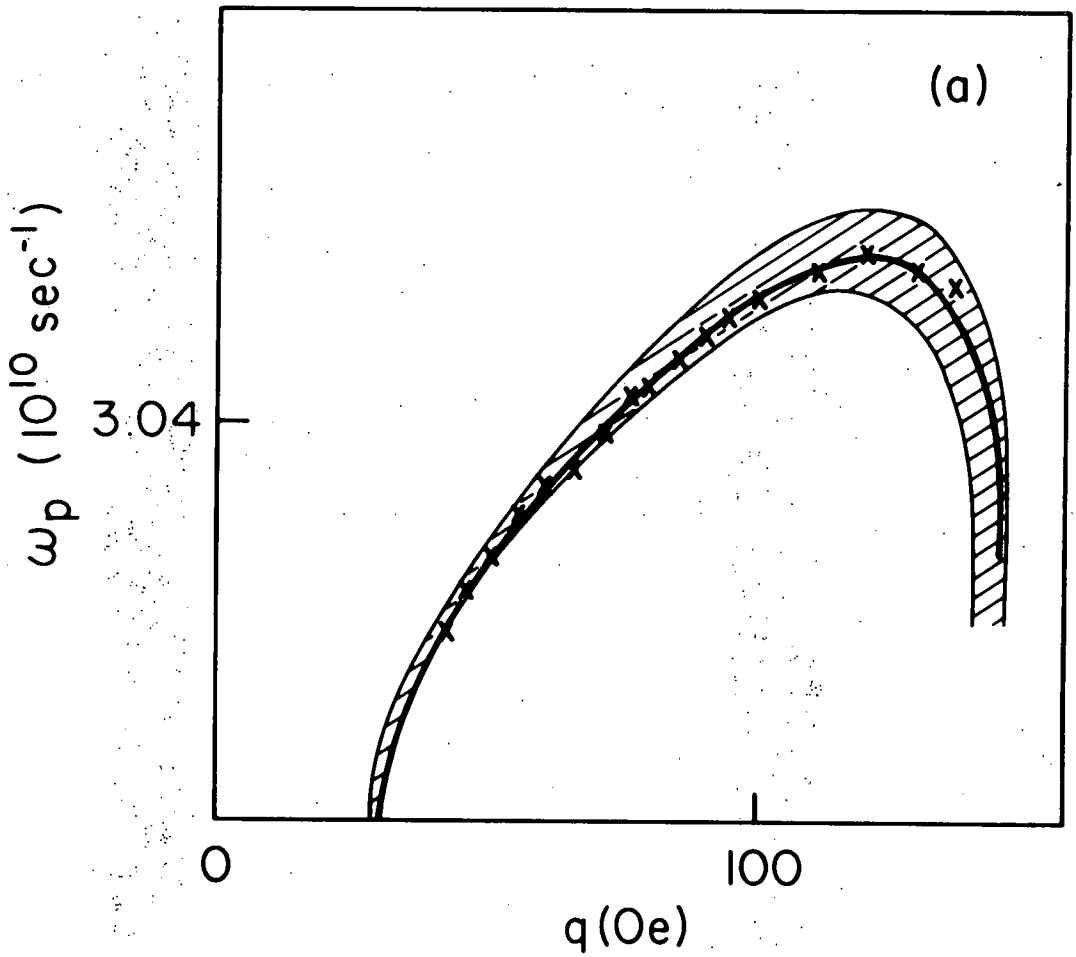

Fig. (43) a) Dispersion relation at T = 1.77104 K for A12-64 compared with the prediction of Eq. (102). The shaded region represents values of theory consistent with uncertainties in experimental parameters.

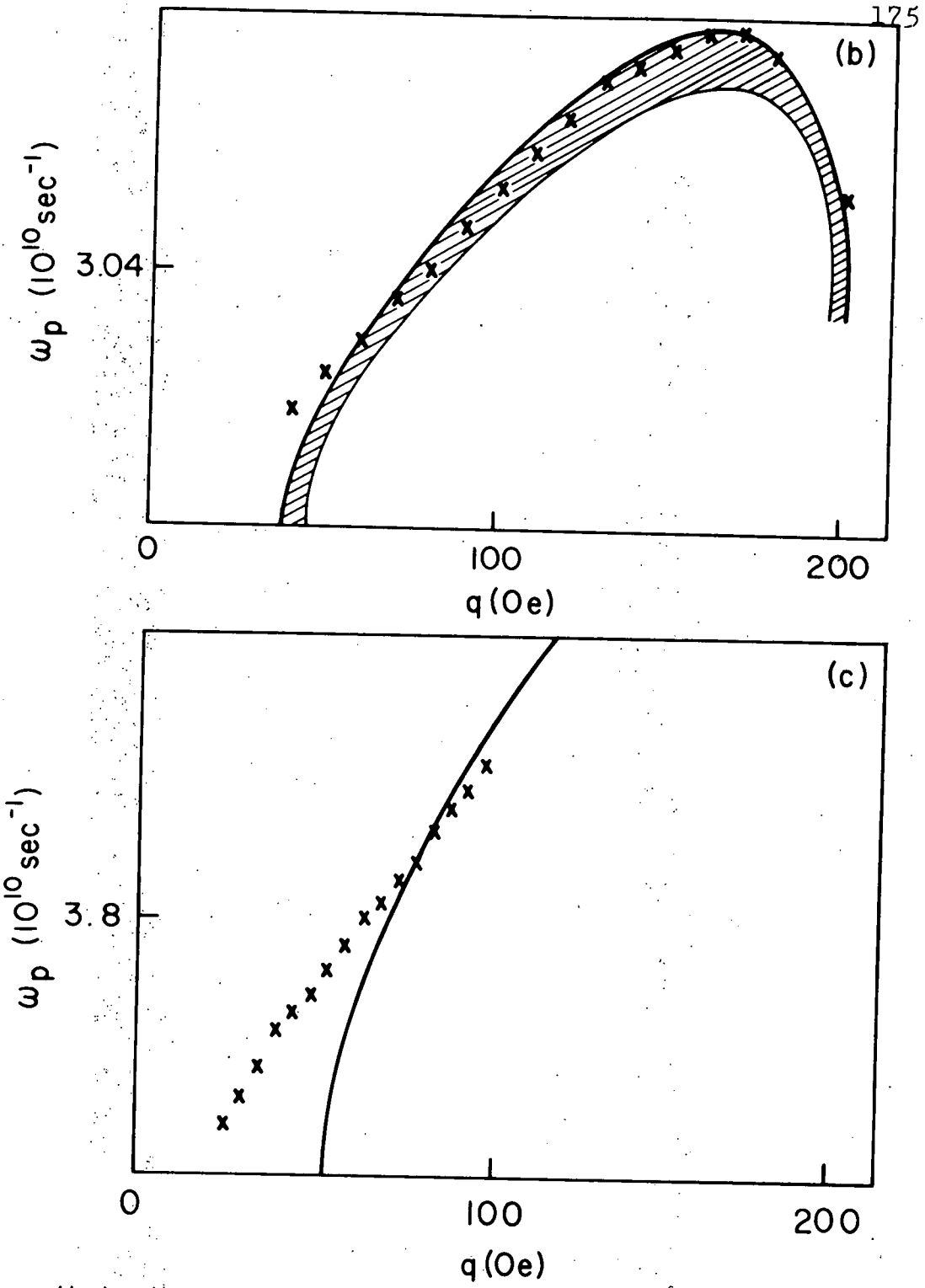

Fig. (43) b) Dispersion relation at T = 1.93341 K for Al2-79 compared with the predictions of Eq. (102). The shaded region represents the values of theory consistent with uncertainties in experimental parameters.
c) Dispersion relation at T = 1.75317 K for Al2-64 compared with the predictions of Eq. (102). The experimental parameters used in Eq. (102) are those which give the best fit to the data in Fig. (43.a).

negative intercept. One is thus forced to conclude that the behavior of the mode of Schmid and Schön is quantitatively different from what is seen experimentally for low q.

The disagreement between theory and experiment may be a consequence of the comparison being made outside the ranges of temperature and magnetic field over which the theory is valid. Eq. (103) sets a lower limit on T since at fixed q as the temperature is reduced, the mode first moves out from zero frequency, then turns around and moves back to the origin. At this temperature, the frequency is purely imaginary and the mode is nonpropagating. It is not clear whether the theory breaks down before this temperature is reached. There is no experimental evidence that the mode ever moves back to the origin.

The limits on the magnetic field are set by the condition $Dq^2 \ll \omega$. This is not generally valid for the fields used in this work. Schmid and Schön have found that for $Dq^2 \approx \omega$ the damping of the mode increases significantly, however they have not carried out a detailed calculation in this region. They have also assumed that $\hbar\Gamma \ll \hbar\omega$, that is, they are far outside the gapless region.

In conclusion we find that close to $T_c(H)$ and for relatively large q values the parameters of the theory can be adjusted to give good agreement between theory

and experiment, however for small q and large $(T_c(H) - T)$ the theory does not adequately describe the experimental data. A further critical comparison of the theory, with experiment cannot be made until the full pair-field susceptibility, including both fluctuations of the real and imaginary part of the order parameter is made available.

D.2.d Related Experiments Below $T_c(H)$ The theory and experimental measurements described in this dissertation offer a clear indication that dc tunneling measurements on Al-Al_2O_3-Pb Josephson junctions are a direct probe of the spectrum of order parameter fluctuations in the aluminum film near T_c. Above T_c the fluctuations diffuse with lifetime $\tau_{GL} \; {}^{1}/\Gamma_o$ where τ_{GL} is a characteristic time of the time-dependent Ginzburg-Landau theory. τ_{GL} sets the time scale for fluctuations of the superconducting order parameter. τ_{GL} is easily determined by measuring the frequency of the resonance of the pair-field susceptibility or equivalently, the halfwidth of the order parameter structure factor. Below T_c measurements of the structure factor indicate that there are significant changes in the dynamics of order parameter fluctuations from a simple diffusive behavior. The theoretical discussion of the last section has shown that it is possible to associate the finite frequency peak with fluctuations in the phase of the order para-

meter while the zero frequency peak is connected with amplitude fluctuations. The halfwidth of these peaks is a measure of the lifetimes associated with the particular fluctuating component of the order parameter.

Most nonequilibrium experiments involve creation of an excess quasiparticle density in the superconductor by applying a pulse of heat or light, or by injection of quasiparticles through a tunneling barrier or a normal metal-superconductor interface.[84] The characteristic times associated with these processes are: τ_T, a measure of the thermalization time for excited quasiparticles to come into equilibrium by photon or phonon emission or by pair breaking; τ_n, the characteristic time for recombination of quasiparticles to pairs or establishing equilibrium between pairs and quasiparticles and τ_Q, a measure of the relaxation time for equilibrium to be reached after a change in the relative density of quasiparticles in the two branches $k < k_f$ and $k > k_f$ of the quasiparticle excitation curve.

To understand the explicit relationship between the above relaxation times and the widths of the peaks in the structure factor, requires a detailed theoretical analysis of the relaxation processes involved in the present experiment. Such an analysis has not been carried out. We would expect however, that experiments which measure the relaxation of the Cooper pair density below T_c, such as those of Peters and Meissner,[85] to be

related to the relaxation of the central mode, while experiments which perturb the supercurrent should excite the phase mode and be related in some manner to the lifetime of the finite frequency peak.

V. CONCLUSIONS AND SUGGESTIONS FOR FURTHER EXPERIMENTS

We have demonstrated that the tunneling technique can be an extremely useful means of obtaining detailed information on superconducting order parameter fluctuations in the vicinity of the phase transition.

We have used this technique to determine the pair-field susceptibility and structure factor of "dirty" aluminum films. Measurements carried out above T_c are in excellent agreement with predictions based on a diffusive time-dependent generalization of the Ginzburg-Landau theory. In zero field, away from T_c, the pair relaxation frequency is quantitatively equal to the theoretical value. Deviations which occur are only in the magnitudes of coefficients which are dependent on parameters of the sample which are only imprecisely known. In finite fields above T_c, the low field results are in agreement with an extension of the zero field theory. High field results are in qualitative agreement with theory. The difficulties appearing in the immediate vicinity of T_c are not well understood and require further experimental and theoretical study.

Measurements carried out below T_c clearly demonstrate the existence of a low frequency propagating order parameter collective mode in "dirty" aluminum films. The mode is observed as a peak in the structure factor and has a linear dispersion relation over the range in which it is characterized. Theoretical calculations

have identified the mode with fluctuations in the phase of the order parameter, however at the present time, no theory adequately describes the experimental features of the mode over the ranges of temperature and magnetic field in which it has been investigated. Further experimental and theoretical study will be required for a complete understanding.

Several modifications of the experimental procedure should be considered. A better method of producing the electrodes of the junction than evaporation from resistively heated sources would improve the character of the films. An electron beam system would be extremely helpful as impurity contamination could be reduced to a minimum. The use of alumina covered boats provides a convenient method of producing granular films, however, control of the characteristics of such films is impossible. Analysis of films with a technique such as Auger spectroscopy is absolutely essential if firm conclusions are to be made from the results.

For the extension of this technique to study other superconducting systems, a method of producing a reliable insulating layer on the reference metal (lead) would be helpful. Several times during the course of this investigation, thermal oxidization of the lead electrode was attempted with no success. The barrier was too thin, either containing filamentary shorts or the junctions exhibited large ohmic conductivity, making excess current

measurements impossible. Reasonable oxidization times to obtain the required junction resistances were found to be prohibitively long. Techniques such as r.f. plasma discharge and glow discharge are known to give durable oxide layers and should be applied to these experiments. It also may be possible to use oxidized niobium films as the reference metal.

Further experimental work on the characterization of the width and peak frequencies of the mode as a function of temperature and magnetic field with a detailed fitting program would be a valuable aid in the understanding of the mode.

Extensions of this work to the investigation "clean" (long m.f.p.) aluminum systems would be interesting. Again this was attempted with no success because of large ohmic conduction through the junction, in the samples made.

Performing the experiment on voltage biased junctions would also be interesting. With careful selection of the load line, the full I-V characteristic, without the existence of negative resistance regions could be observed. In small magnetic fields the development of the Josephson current along with the propagating mode could be observed as the transition temperature was crossed.

It would also be interesting to directly observe the propagation of the collective mode. With a clever

arrangement of electrodes and the proper biasing scheme, the mode might be generated at one point and detected with a second junction further along the strip. However, as the mode is highly damped, it would propagate only a distance of the order of 10^{-4} cm, thus it would seem to be a difficult experiment to perform.

Two extensions of this work are suggested by the theoretical work of Schmidt.[17,38,39] It would be of considerable interest to introduce paramagnetic impurities into the fluctuating film and examine the pair-field susceptibility both above and below T_c. This would be an extremely valuable test of the theory discussed in Refs. 17, 38 and 39. The relationship between the apparent shift in the relaxation frequency and ρ given by Eq. (88), has never been checked.

The extension of the above work with the introduction of ferromagnetic impurities has also been suggested by A.M. Goldman. A calculation of the susceptibility with ferromagnetic impurities has been carried out by Entin-Wohlman and Orbach.[86] They suggest that the excess tunneling current can be used to study critical scattering of conduction electron spins in the vicinity of the magnetic ordering temperature. Such investigations require films which contain sufficiently high magnetic impurity concentrations that the magnetic ordering tmperature falls in the fluctuating regime just above the superconducting transition temperature. The peak in the excess current-voltage characteristic would then reflect the onset of magnetic ordering.

REFERENCES

1. P.C. Hohenberg, Proceedings of the XIIth International Conference on Low Temperature Physics, E. Kanda, ed. (Academic Press of Japan, 1971), p.211.

2. V.L. Ginzburg, Fiz. Tverd. Tela. 2, 2031 (1960) (English transl., Soviet Phys. - Solid State 2, 1824 (1960)).

3. V. Ambegaokar, Proceedings of the International Conference on the Science of Superconductivity, Palo Alto, Calif. 1969, published in Physica 55, 32 (1971).

4. R.A. Ferrell, J. Low Temp. Phys. 1, 423 (1969).

5. D.J. Scalapino, Phys. Rev. Lett. 24, 1052 (1970).

6. J.T. Anderson and A.M. Goldman, Phys. Rev. Lett. 25, 743 (1970).

7. J.T. Anderson, Doctoral Dissertation, University of Minnesota (1971), (unpublished).

8. J.T. Anderson, R.V. Carlson, and A.M. Goldman, J. Low Temp. Phys. 8, 29 (1972).

9. J.T. Anderson, R.V. Carlson, A.M. Goldman, and H.T. Tan, Proceedings of the XIIIth International Conference on Low Temperature Physics, Boulder, Colorado 1972, in Low Temperature Physics - LT 13, Vol. 3, K.D. Timmerhaus, W.J. O'Sullivan, and E.F. Hammel, eds. (Plenum Publishing Co. New York, 1974), p. 709.

10. R.V. Carlson and A.M. Goldman, Phys. Rev. Lett. 31, 880 (1973).

11. R.V. Carlson and A.M. Goldman, Phys. Rev. Lett. 34, 11 (1975).

12. R.A. Glover, in Progress in Low Temperature Physics, C.J. Carter, ed. (North-Holland, Amsterdam, 1970), Vol.6.

13. J.P. Gollub, M.R. Beasley, and M. Tinkham, Phys. Rev. Lett. 25, 1646 (1970).

14. A.W. Cohen, B. Abeles, and C.R. Fuselier, Phys. Rev. Lett. 23, 377 (1969).

15. S.R. Shenoy and P.A. Lee, Phys. Rev. B 10, 2744 (1974).

16. For a recent review of Ginzburg-Landau theory and time-dependent generalizations of this theory, see: M. Cryot, Rep. Progr. Phys. 36, 103 (1973).

17. G. Brieskorn, M. Dinter and H. Schmidt, Solid State Commun. 15, 757 (1974).

18. K. Maki and H. Sato, J. Low Temperature Phys. 16, 557 (1974).

19. L.P. Gor'kov and G.M. Eliashberg, J. Low Temp. Phys. 2, 161 (1970).

20. Albert Schmid and Gerd Schön, Phys. Rev. Lett. 34, 937 (1975).

21. E. Šimánek, preprint.

22. L.D. Landau, Phys. Z. Soviet Un. 11, 545 (1937) (translation: D. ter Haar, Men of Physics: L.D. Landau II (Pergamen, New York, 1969)).

23. L.P. Gor'kov, Z. Ekep Teor. Fiz. 36, 1918 (1959) (translation: Sov. Phys.- JETP 9, 1364, (1959)).

24. V. Ginzburg and L. Landau, Zh. Eksp. Teor. Fiz. 20, 1065 (1950) (translation: D. ter Haar, Men of Physics: L.D. Landau I (Pergamon, New York, 1965)).

25. A. Schmid, Phys. Kondens. Materie 5, 302 (1966).

26. E. Abrahams and T. Tsuneto, Phys. Rev. 152, 416 (1966).

27. H. Takayama, Progr. Theoret. Phys. (Kyoto) 46, 1 (1971).

28. P.W. Anderson, Lectures on the Many Body Problem, E.R. Caianiello, ed. (Academic Press, New York, 1964).

29. M. Weihnacht, Physica Status Solids 32, K169 (1969).

30. For a discussion of linear response theory, see: D.J. Amit in Quantum Fluids, Nathan Wiser and D.J. Amit, eds. (Gordon and Breach, New York, 1970), p. 141.

31. B.D. Josephson, Phys. Lett. 1, 251 (1963).

32. B.D. Josephson, Adv. Phys. 14, 419 (1965).

33. H. Schmidt, Z. Physik 216, 336, (1968).

34. I.O. Kulik, Zh. Eksp. Teor. 59, 937 (1970).

35. D. St. James, E.J. Thomas and G. Sarma, Type II Superconductivity, (Permagon, New York, 1969), and D. St. James and P.G. de Gennes, Phys. Lett. 7, (1963).

36. H.T. Tan, (unpublished).

37. For a discussion of gapless superconductivity, see: K. Maki, Superconductivity, Vol. 2, R.D. Parks, ed. (Marcel Dekker, New York 1969), Chapter 18.

38. H. Schmidt, Phys. Lett. 27A, 658 (1968).

39. H. Mikeska and H. Schmidt, Z. Physik 230, 239 (1970).

40. E. Šimánek and P. Walker, Phys. Lett. 44A, 419 (1973).

41. I.O. Kulik, Zh. Eksp. i. Teor. Fiz. 59, 937 (1970) (English transl: Soviet Phy. - JETP 32, 510 (1971).

42. Y. Ichikawa, Phys. Lett. 35A, 5 (1971).

43. K. Yoshihiro and Kajimura, Phys. Lett. 32A, 71 (1970).

44. S.G. Lipson, C.G. Kuper and A. Ron, in Proceedings of the International Conference on the Science of Superconductivity, Palo Alto, Calif. (1969), published in Physica 55, 269 (1971).

45. K. Yoshihiro, K. Yamaji and K. Kajimura, J. Phys. Soc. Japan 33, 100 (1972).

46. Metals were obtained from Johnson, Matthey and Company and United Mineral and Chemical Corp.

47. J. Matisoo, Phys. Lett. 29A, 473 (1969).

48. R.J. Peterson and F.L. Vernon, J. Appl. Phys. Lett. 10, 29 (1965).

49. These filters consisted of an Allen Bradley "pi-section" kit CK68-5N in series with a Lenox-Fugle 82 μh shielded inductor.

50. CryoCal, Inc., 1371 Avenue "E", Riviera Beach, Florida 33404.

51. Technical Report of CryoCal, Inc.

52. I. Giaever, in Tunneling Phenomena in Solids, E. Burstein and S. Lundquist, eds. (Plenum, New York, 1969), p. 260.

53. Some of the data has been previously published in Refs. 8-11.

54. D.D. Coon and M.D. Fiske, Phys. Rev. 138, A744 (1965).

55. J.J. Hauser, Phys. Rev. B 3, 1611 (1971).

56. S. Akselrod, M. Pasternak and S. Bukshpan, J. Low Temp. Phys. 17, 375 (1974).

57. B. Abeles, R.W. Cohn and W.R. Stowell, Phys. Rev. Lett. 18, 902 (1967).

58. G. Deutscher, H. Fenichel, M. Gershenson, E. Grunbaum and Z. Ovadiahu, J. Low Temp. Phys. 10, 231 (1973).

59. J.C. Solinsky, A.M. Goldman, and T. Magee, to be published in J. Low Temp. Phys.

60. D.J. Scalapino, Tunneling Phenomena in Solids, E. Burstein and S. Lundquist, eds. (Plenum, New York, 1959), Chapter 33.

61. R.A. Ferrell and D.J. Scalapino, (unpublished result).

62. G. Deutscher and P.G. de Gennes, Superconductivity, Vol. 2, R.D. Parks, ed. (Marcel Dekker, New York, 1969), Chapter 17.

63. Ref. 7 has a complete discussion of thermal fluctuation effects on the dc Josephson current.

64. E. Šimánek and J.C. Hayward, (to be published).

65. J.R. Schrieffer and J.W. Wilkens, Phys. Rev. Lett. 10, 17 (1963).

66. B.N. Taylor and E. Burstein, Phys. Rev. Lett. 10, 14 (1963).

67. Šimánek, preprint.

68. If modes of frequencies ω_1 and ω_2, where $\omega_1 \gg \omega_2$ are coupled together, then the dispersion relation can be of the form $\omega = \omega_2 - |V|^2/|\omega_1 - \omega_2|$, where V is the coupling parameter.

69. S.L. Lehoczky and C.V. Briscoe, Phys. Rev. Lett. 24, 880 (1970).

70. Albert Schmid and Gerd Schön, to be published in J. Low Temp. Phys.

71. J.C. Swihart, J. Appl. Phys. 32, 461 (1961).

72. D.V. Mason and R.W. Gould, J. Appl. Phys. 40, 2039 (1969).

73. R.E. Eck, D.J. Scalapino and B.N. Taylor, Phys. Rev. Lett. 13, 15 (1963).

74. P.W. Anderson, Phys. Rev. 112, 1900 (1958).

75. J. Bardeen, Phys. Rev. Lett. 1, 399 (1958).

76. V.L. Ginzburg, Zh. Eksp. Teor. Fiz. 41, 828 (1962). (Sov. Phys. JETP 14, 594 (1962)).

77. C.P. Enz, Rev. Mod. Phys. 46, 705 (1974).

78. N.W. Bogoliuvbov, V.V. Tolmachev and D.V. Shirkov, A New Method in the Theory of Superconductivity, Academy of Science, Moscow, 1958, Consultants Bureau, New York, 1959.

79. For a discussion of collective modes in super conductors, see: P.C. Martin, Superconductivity, Vol. 1, R.D. Parks, ed. (Marcel Dekker, New York, 1969), Chapter 7.

80. A discussion of the application of the Goldstone Theorem to general phase transitions is given by: H. Wagner, Z. Physik 195, 273 (1966).

81. For a discussion of localized moments and quenched moments in metals and a list of references, see: A.J. Heeger in Solid State Physics, Vol. 23, P. 283, F. Seitz, D. Turnbull and H. Ehrenreich, eds. (Academic Press, New York, 1969).

82. M. Brian Maple in Magnetism, Vol. 5, G.T. Rado, ed. (Academic Press, New York, 1973).

83. E. Šimánek and Hayward, private communication.

84. For a recent review of nonequilibrium processes in superconductor, see: P.N. Langenberg, in Festkorperprobleme/ Advances in Solid State Physics, Vol. XIV, H.J. Queisser, ed. (Permagon, New York, 1974), p. 67.

85. R. Peters and H. Meissner, Phys. Rev. Lett. 30, 965 (1973).

86. O. Entin-Wohlman and R. Orbach, (submitted to Phys. Rev.).

ACKNOWLEDGEMENTS

It is with great pleasure that the author expresses his appreciation to the thesis advisor, Professor Allen M. Goldman. His enthusiasm was a constant source of encouragement.

The author gratefully acknowledges the theoretical support provided during the progress of this experiment. Discussions and correspondences with the following were especially helpful: Professor Charles Campbell, Professor J. Woods Halley, Professor Douglas Scalapino, Professor H. Schmidt, Professor A. Schmid, Professor K. Maki, Professor E. Šimánek and Dr. Patrick Lee.

The author acknowledges the support for this research by the Materials Division of ERDA on Contract AT(11-1)-1569. The author also thanks the Office of Naval Research for providing the He gas used in this experiment and the National Science Foundation for financial support during part of his tenure as a graduate student.

The author also thanks his fellow graduate students who helped during the experiment.

Finally the author would like to thank his wife, Susan, without whose love, understanding and patience this work would have been extremely arduous.